Factors Contributing to T Cell Persistence in a Tolerizing Tumor Environment

by

Mobolaji O. Olurinde

B.S. Chemical Engineering (Highest Honors)
B.S. Agricultural & Biological Engineering (Honors)
University of Florida, 2002

M.S. Biological Engineering, Massachusetts Institute of Technology, 2007

SUBMITTED TO THE DIVISION OF HEALTH SCIENCES AND TECHNOLOGY IN PARTIAL FULFILLMENT OF THE REQUIREMENTS FOR THE DEGREE OF

DOCTOR OF PHILOSOPHY IN MEDICAL ENGINEERING
AT THE
MASSACHUSETTS INSTITUTE OF TECHNOLOGY

FEBRUARY 2010

Signature of Author.....
Division of Health Sciences & Technology
September 22, 2009

Certified by.....
Jianzhu Chen, PhD
Thesis Supervisor
Cottrell Professor of Immunology and Biology

Accepted by.....
Ram Sasisekharan, PhD
Director, Harvard-MIT Division of Health Sciences & Technology
Edward Hood Taplin Professor of Health Sciences & Technology and Biological Engineering

Factors Contributing to T Cell Persistence in a Tolerizing Tumor Environment

by

Mobolaji O. Olurinde

Submitted to the Division of Health Sciences & Technology
on September 22, 2009 in Partial Fulfillment of the
Requirements for the Degree of Doctor of Philosophy in
Medical Engineering

ABSTRACT

Cancer is a leading cause of death worldwide, accounting for at least 10% of all deaths globally. Current therapies for cancer include surgical excision, chemotherapy and immunotherapy. $CD8^+$ T cells are adaptive immune cells responsible for eradicating tumor cells. However, these T cells can be rendered ineffective through tolerance. Yet in various mouse models and human patients, tolerant T cells persist. The aim of this project is to identify factors that support T cell persistence in a tolerizing tumor environment. Using a spontaneous prostate cancer model, we study antigen-specific T cells that have been shown to be locally tolerant in the prostate tumor environment. In this thesis, I compare the immune response in normal, antigen-bearing, tumor transgenic and tumor-antigen transgenic mouse models. Results show that T cell infiltration and persistence in the tolerizing prostate environment is dependent on the presence of antigen and tumorigenic/tumor-related factors. Although antigen-specific T cells are locally tolerant in the prostate of tumor-antigen transgenic mice, they generally persist in the prostates of tumor transgenic mice regardless of whether antigen is present or not. Further analyses revealed that T cells infiltrate the prostate and can proliferate extensively in the tolerizing tumor environment due to the presence of antigen. Interestingly, antigen-specific T cells are depleted from the spleens of mice that express antigen in their prostates. This depletion from the spleen is correlated with low levels of IL-7Rα expression and the presence of antigen in the prostate. Tumorigenic or tumor-related factors in the prostate also appear to be supporting $CD8^+$ T cell persistence. This thesis shows that persistence of antigen-specific T cells in the tumor environment is not dependent on IL-15 and IL-7; cytokines known to support proliferation and maintenance of persisting functional $CD8^+$ T cells. Some potential candidates are also discussed. More investigative work needs to be done to identify the role of these factors on T cell infiltration and persistence. In combination with tolerance-breaking strategies, persisting T cells may be excellent vehicles for delivering site-specific cancer immunotherapy.

Thesis Supervisor: Jianzhu Chen
Title: Cottrell Professor of Immunology and Biology

ACKNOWLEDGMENTS

First, I would like to thank my Lord and Savior, Jesus Christ, for the opportunity to realize a dream. Thank you God for the inspiration, wisdom and strength to complete this Ph.D. It has always been about you. I would also like to thank the chemist who shared her biography and coined the phrase, "Praising Him (God) Daily". Taking things one day at a time with that phrase in mind make the good times glorious and the difficult times quite bearable.

I would like to thank my advisor Jianzhu Chen for his continued support as I developed and worked on this project. You taught me how to think about "interesting and feasible" science. Also, my gratitude goes to my thesis committee members, Lee Gehrke, Darrell Irvine and Sangeeta Bhatia. I really appreciated your input at critical points of this research, and the encouraging words offered that helped to push me in making progress in this work. Special thanks to all former and current members of the Chen lab. Your patience in teaching me techniques, generosity in sharing reagents, and honesty in providing constructive criticism will always be remembered fondly. Thank you. In particular, I am grateful to advice from Ching-Hung Shen, Adam Drake and Ailin Bai as I developed and executed experiments. Thanks to Eileen Higham, the best colleague one could ask for, who served as great resource in answering my questions about this prostate cancer model, as well as ensured that we always had mice to work with! I appreciate Maria (Mimi) Fragoso's, Kristyn Ferber's and Carol McKinley's technical assistance in maintaining the mouse colonies splendidly. Thanks Ilya for sharing your biotinylated 1B2 antibody. And what would I have done without Kristyn's, Camille's and Oezcan's extra pairs of hands at critical times? Thank you all. You made working in Chen lab fun.

I also had a lot of help from faculty and staff. Special thanks to Paul Matsudaira (my former co-advisor), Dr. Herman Eisen, Rick Mitchell, Julie Greenberg, Alan Grodzinsky, Bruce Tidor, Mehmet Toner, Dan Shannon, and many more. You gave me advice and encouragement when I wanted to give up. I am eternally grateful to you. Thanks to the staff at the Koch Institute headquarters and core facilities, particularly those in the Flow Cytometry, Histology and Microscopy facilities. Your assistance was invaluable. Also worthy of mention is the DCM staff who kept a close eye on our mice and assisted me in caring for them properly. Thank you to the administrative staff from the HST, Harvard MD-PhD program, and MIT Graduate Student offices. My deepest appreciation to Cathy Modica, Patty Cunningham, Linda O'Mahony, Linda Burnley, Julianna Braun, Irene Huang, Laurie Ward, Traci Anderson, Brima Wurie, and Domingo Altarejos for making the administrative aspects (course registration, funding, etc.) of my time here easier. This research was funded by the NIH Individual NRSA predoctoral NIH-F31-AI080286, UNCF-Merck Graduate Research, and National Science Foundation Graduate Research fellowships (to M.O.), HST-MEMP funding, as well as the Singapore-MIT Alliance (SMA-2) Advanced Tissue Systems Biology grant to Jianzhu Chen.

A feat like this is impossible without support from mentors, family and friends. I had wonderful mentors who made sure I was still staying on track. Thanks to Susan Shih for discussing project ideas with me and following my progress to make sure I would finish in a timely manner. Kalpit Vora suggested reading articles by John Wherry which triggered ideas and some of the experiments in this thesis. Thanks Kalpit. I really appreciated the lead. Also thank you to Felicia B. Johnson for prompting me to write my dissertation. I will not forget your text messages inquiring about the number of pages I have written! Thank you. Thanks to Drs. Richard B. Dickinson, Leslie Z. Benet, Wayne A. Marasco, Jean Andino and Joel Sheets for

encouraging me through my undergraduate and pre-clinical medical school years even until now. I also appreciate your letters of recommendation that helped me to secure graduate admission and funding. The external fellowships helped to make the graduate years more enjoyable. I am grateful to many friends from Nigeria and across the United States --Florida, Harvard, MIT and the greater Boston area -- who supported me throughout this program even though sometimes it meant missing out on activities together! Alisha Kithcart and LeSette Wright, you will always be close to my heart. Thank you for listening to my research woes, sharing a kind word when I needed one, and for celebrating my victories with me. I could not have completed this program without you. Finally, I am grateful for and to my family, both nuclear and extended members. Your calls, emails and visits from all parts of the world warmed my heart and kept me going. May God bless you immensely. Thank you to my grandmother, Granny Ikoyi, for fueling a joy for reading. I probably would not have applied to graduate school if I had not read broadly and gotten intrigued about viral infectious diseases, the other aspect of Chen lab that was part of my Master's thesis. This Ph.D. is dedicated to my parents, Babatunde and Yetunde Olurinde. You have always supported my education even when you did not understand my career path choices! I am indebted to your love and prayers. Thank you to all!

TABLE OF CONTENTS

CHAPTER 1

INTRODUCTION

1.1. Background & Significance

Cancer is a leading cause of death worldwide, accounting for at least 10% of all deaths globally [1]. Almost twenty-five percent of the 2.4 million deaths in the United States (U.S.) are due to cancer [2, 3]. About 1.5 million new cases are expected to be diagnosed in 2009 [2]. The current therapies for cancer include surgical excision of the affected tissue, chemotherapy, radiation therapy, hormone therapy and immunotherapy [4-6]. Immunotherapeutic regimens so far have involved transfer of dendritic cells (DC) [6-8] and/or $CD8^+$ T cells [9-11], depletion of T regulatory cells [12], and administration of cytokines that enhance T cell survival such as IL-2 and IL-15 [9-11, 13-16]. Refractory cases, particularly when the diagnosis is made in the late stages of cancer, are often fatal. Even with the armamentarium of current treatment options, when cancers from all sites are combined, a patient's 5-year survival is estimated at about only 66% [2]. Thus, developing new treatment strategies and optimizing current therapies is essential in the fight against cancer.

One of the difficulties of current immunotherapy for cancer is the development of tolerance [17]. $CD8^+$ T cells are the main adaptive immune cell type responsible for destroying tumor cells [18, 19], as well as cells infected with intracellular pathogens such as viruses [20]. Naïve $CD8^+$ T cells recognize antigen (a peptide sequence foreign to the host), and are activated to eliminate the cells that bear this antigen. Tumor cells have tumor antigens that can be processed and presented by professional antigen-presenting cells such as DC to $CD8^+$ T cells. Then, activated $CD8^+$ T cells eliminate tumor cells. However, the host's $CD8^+$ T cells may not be completely effective in combating tumor cells, and cancer develops. Adoptively transferred $CD8^+$ T cells targeting specific tumor antigens also develop this problem. Different mechanisms have been proposed to explain why $CD8^+$ T cells become ineffective against tumor cells [6, 21-23].

In some cases, tumor cells down-regulate molecules like major histocompatibility complex (MHC) class I that would allow them to be recognized by $CD8^+$ T cells [22]. They may also up-regulate Fas ligand and other molecules to induce apoptosis in $CD8^+$ T cells [21-25]. Sometimes, secretion of cytokines such as interleukin (IL)-4, IL-10, and transforming growth factor-β (TGF-β) by the tumor cells, or other cell types in the tumor environment, suppress cytolytic function of $CD8^+$ T cells [21-23, 26, 27]. Host $CD8^+$ T cells may also just be "ignorant" of the presence of tumor cells [18, 23]. This state in which host or adoptively transferred $CD8^+$ T cells used in immunotherapy are unable to perform their effector functions despite antigen stimulation is called tolerance.

Tolerant (non-functional) T cells have been identified in animal models for cancer, as well as human patients, but no one has reported how or why tolerant T cells persist in the tumor environment. In addition to identifying the mechanisms for tolerance, published research have focused mainly on characterizing the phenotype of tolerant T cells and developing strategies to restore T cell function. In most cancer models available, non-functional T cells are depleted from the host [28-30]. Such models do not mimic the phenomenon of tolerant but persisting T cells observed in certain cancers, and their use is limited to studies that develop strategies for enhancing survival and maintenance of cytolytic T cells. In other studies where tolerant $CD8^+$ T cells are generated, the cells are characterized as having impaired proliferative ability, defective T cell receptor (TCR) signaling, and increased sensitivity to cell death [28, 31, 32]. For example, in a study by Dubois *et al.* (1998), F5 $CD8^+$ T cells became tolerant after continued exposure to cognate influenza virus $NP_{366-374}$ peptide. The peptide antigen was delivered via multiple intraperitoneal injections [28], instead of being constitutively expressed in the mice like our tumor model. The tolerant T cells displayed the hallmarks described above. Antigen-specific T cells

with impaired proliferation, IL-2 secretion, and Calcium ion release in response to peptide stimulation, have also been reported to persist in the TCRxgag mice which have the tumor antigen expressed in the liver [32]. Most of these experiments, however, evaluate cell proliferation and cytolytic activity *in vitro* and may not accurately reflect tolerant T cell response in the tolerizing environment *in vivo*.

In the cases where tolerant T cells are maintained, the reports focus on how to reverse the cells to a functional state [8, 11, 33]. Some of these efforts have resulted in only a transient break in T cell tolerance [8]. Overwijk *et al.* (2003) performed studies with B16 transplant melanoma mouse model. Without exogenous administration of IL-2, tumor-specific $CD8^+$ T cells were maintained in the solid transplant tumor for up to 30 days but were not fully activated [11]. Boosting with peptide vaccination and IL-2 on day 30 increased the number of tumor-specific $CD8^+$ T cells by 34-fold and increased interferon (IFN)-γ production, suggesting reversal of the transferred T cells into functional state [11]. Anderson *et al.* (2007) showed that tumor Ag-specific $CD8^+$ T cells adoptively transferred into TRAMP mice failed to degranulate and secrete IFN-γ and granzyme B [8]. Again, this group focused on how to restore the effector function of these cells by using *ex vivo*-matured DC vaccinations. Although they observed increased proliferation and IFN-γ production initially, despite DC vaccination, the tumor-specific T cells in the TRAMP prostate became tolerant by week 5 [8]. These studies alert us to the fact that in order to develop effective immunotherapy against cancer, it is imperative that we understand the mechanism for persistence of T cells in a tolerizing or immunosuppressive environment. Recently, Thomas *et al.* (2009) showed that mice with MC57-SIY-Lo brain tumors developed recurring brain tumors even though 2C T cells persist for up to 35 days in this tissue [33]. After the initial tumor regression, the MC57-SIY-Lo mice developed tumor cell variants that did not express the SIY

peptide and presumably could no longer be recognized by the persisting 2C T cells [33]. The authors do not expound on the phenotype of these persisting 2C T cells or the mechanism by which they persist.

1.2. Description of the TRAMP-SIY Experimental System

Our model system is based on the transgenic adenocarcinoma of the mouse prostate (TRAMP) model developed by the Greenberg lab in the 1990s and resembles prostate cancer progression in humans [34, 35]. In this mouse model, the prostate-specific rat probasin promoter drives expression of the oncoprotein simian virus 40 (SV40) large tumor T antigen-coding region in the prostate epithelium [35]. This oncoprotein inhibits the regulatory function of the p53 and retinoblastoma (Rb) tumor suppressor genes [35]. After puberty, the male mice develop intraepithelial hyperplasia within 2-4 months of age [35]. Then, the disease progresses to neoplasia by 4 months of age, and invasive (metastatic) adenocarcinoma is evident from as early as 5 months old [35]. Ultimately, the mice develop fatal androgen-independent prostate cancer as is seen in humans [34]

In the Chen laboratory, former postdoctoral fellow, Dr. Ailin Bai, created a T cell antigen-specific model by modifying the TRAMP model such that its prostate epithelial cells express the SIYRYYGL (SIY) peptide. This model is called the TRAMP-SIY model. Dr. Bai engineered a β-galactosidase-SIY (β-gal-SIY) fusion protein under the control of the prostate-specific promoter such that the prostate epithelial cells in mice of C57BL/6 background express SIY peptide (B6-SIY). TRAMP mice and B6-SIY mice were crossed to create double transgenic TRAMP-SIY mice. To date, both the TRAMP and TRAMP-SIY mice models show similar disease progression.

Antigen-specific immune response to cells expressing SIY peptide is studied using the 2C TCR system. 2C TCR cells recognize SIY-K^b complexes presented on target cells [36]. In our lab, 2C T cells are isolated from transgenic mice on a recombination activating gene-1 deficient background (2C $RAG1^{-/-}$), and are adoptively transferred into recipient mice by retroorbital

injection. A monoclonal antibody 1B2 specific for the 2C TCR makes it possible for us to identify and track these T cells in different tissues. In addition, our group also has congenic 2C Thy1.1^{+} RAG1$^{-/-}$ transgenic mice that allow us to detect 2C TCR CD8^{+} T lymphocytes using a Thy1.1 antibody, particularly in cases where one may not want to perturb the TCR-MHC interaction.

In vivo activation of 2C T cells is achieved by vaccinating recipient mice with the Influenza A/WSN-SIY influenza virus. This virus, developed in collaboration with Dr. Astrid Flandorfer (Mount Sinai School of Medicine), is a mouse-specific recombinant H1N1 strain where the SIY peptide has been engineered onto the neuraminidase stalk. Naïve 2C T cells are adoptively transferred into mice post-puberty that also receive low dose WSN-SIY virus infection intranasally. Antigen-presenting cells presenting the SIY peptide to T cells having the 2C TCR eventually lead to activation of 2C T cells in the mediastinal lymph nodes (draining lymph nodes of the lung, the site of infection). These activated 2C T cells exit the lymph nodes, infiltrating different peripheral tissues including the prostate (Fig. 1).

This combination of the TRAMP/TRAMP-SIY prostate cancer models, the 2C TCR system, and the WSN-SIY engineered virus constitute our experimental system. Our studies show that 2C T cells that infiltrate the prostate of the TRAMP-SIY mice rapidly lose their ability to secrete IFN-γ, TNF-α and lyse tumor cells [37]. These 2C T cells exhibit the phenotype of exhausted effector T cells; they express high levels of PD-1 (Fig. 2). This immunosuppression occurs locally in the prostate [37]; 2C T cells from other tissues, for example, the lungs of TRAMP-SIY mice are able to secrete IFN-γ upon antigen stimulation. 2C T cells from the TRAMP prostate retain more functionality [37]. These results confirm that we have developed a prostate cancer model that mirrors the disease progression observed in humans [34, 35] and allows

us to track $CD8^+$ T cell response to a specific antigen at the tumor tissue site. In addition, this model is unique because it allows us to study local immunosuppression in the prostate; a phenomenon that has also been observed in human patients with esophageal squamous cancer [31].

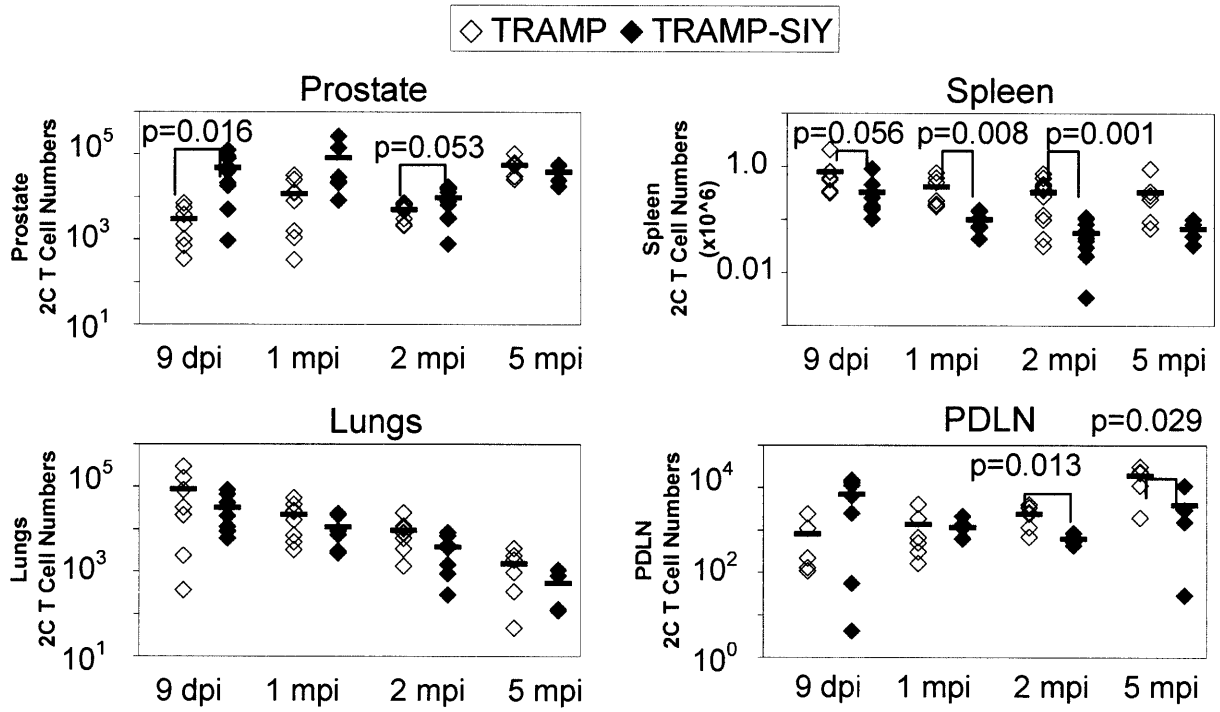

Figure 1. Tolerant antigen-specific T cells persist in the tumor environment but are depleted from other tissues.

Prostates, lungs, spleens and prostate draining lymph nodes (PDLN) from TRAMP-SIY (solid diamond) and TRAMP (open diamond) mice were harvested nine days, one-, two-, and five-months after 2C T cell transfer and WSN-SIY influenza infection as described in the methods section. Cells were stained with 1B2 and CD8α antibodies, as well as DAPI or PI to exclude dead cells, followed by flow cytometry analysis. After gating on live $1B2^+$ $CD8^+$ cells, total cell numbers were calculated by multiplying the ratio of $1B2^+$ $CD8^+$ cells from FlowJo analysis and the total cell numbers counted by hemacytometer and tryphan blue exclusion before antibody staining. The plot shown is generated using Microsoft Excel. Each shape represents one mouse. Solid black bars indicate the average of the data for each mouse model ($n \geq 4$ per group). The p-values for cell numbers from student t-tests comparing TRAMP to TRAMP-SIY are given for $p \leq 0.05$.

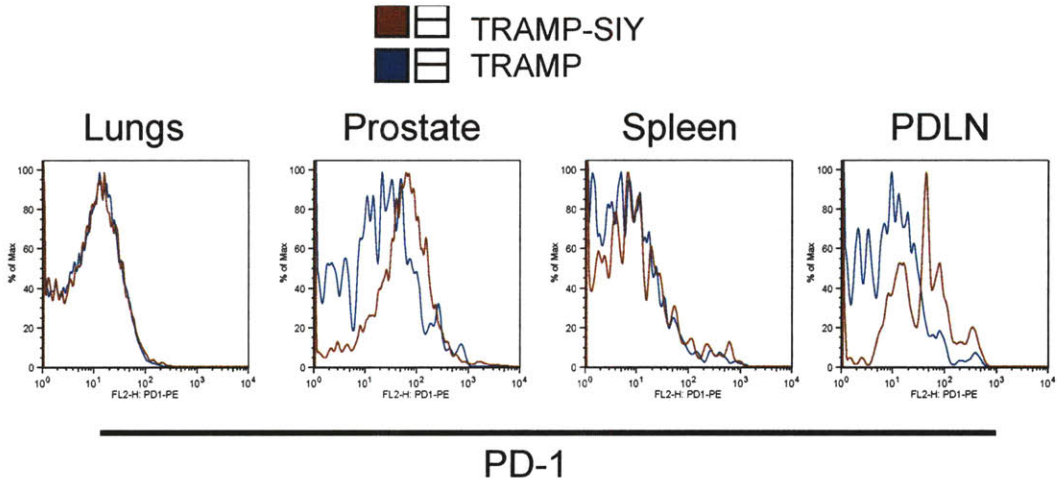

Figure 2. Tolerant 2C T cells express higher levels of PD-1.
Tissues from TRAMP (red) and TRAMP-SIY (blue) mice were harvested 45 dpi and stained with Biotinylated 1B2, Streptavidin-APC, CD8α-FITC, and PD-1-PE (clone J43) antibodies, as well as PI for analysis by flow cytometry. FlowJo software was used to generate PD-1 expression histograms.

1.3. Persistence of Tolerant T Cells in TRAMP-SIY Prostate

By analyzing the number of 2C T cells using the flow cytometry technique, we observe that tolerant 2C T cells persist in both TRAMP and TRAMP-SIY prostates for at least five months post-transfer and infection (mpi) (Fig. 1). Initially there is a marked increase in the number of 2C T cells in TRAMP-SIY prostate until 1 mpi. Then long-term, there is a population of 2C T cells that are maintained in TRAMP-SIY prostate (Fig. 1) although these cells are tolerant. We define this population of T cells that are maintained in the tissues as persisting T cells. The mice analyzed in these studies are between the ages of 4 – 8 months old that have not developed visible palpable masses. As time goes by, the number of T cells again increases in the prostate tumor environment of 5 mpi recipient mice i.e. mice that are approximately 8 months old at the time of analysis (Fig. 1).

Interestingly, antigen-specific 2C T cells are preferentially depleted from other tissues of TRAMP-SIY mice over the course of time. For instance at 2 mpi, 2C T cell numbers in TRAMP-SIY spleens (Fig. 1) and prostate draining lymph nodes (PDLN, Fig. 1), are lower than that of TRAMP. In the lungs, both TRAMP and TRAMP-SIY mice show declining numbers of 2C T cells (Fig. 1). This data suggests that tolerant antigen-specific T cells persist in the tolerizing TRAMP-SIY prostate, but antigen-specific T cells are depleted from other tissues.

1.4. Summary of Thesis

This thesis reveals that the presence of persistent antigen and tumorigenic/tumor-related factors contribute to persistence of tolerant antigen-specific T cells by inducing proliferation. By comparing the $CD8^+$ T cell response in normal, antigen-bearing, tumor transgenic, and mouse models having both the tumor and antigen transgenes, this report shows that antigen-specific T cells generally persist in the prostates of tumor transgenic mice regardless of whether antigen is present or not. This persistence occurs even though antigen-specific T cells in the tumor transgenic TRAMP and TRAMP-SIY prostates are functionally different. Interestingly, the presence of antigen in the prostate leads to depletion of antigen-specific T cells from other peripheral tissues such as the spleen. This depletion correlates with low levels of IL-7Rα (CD127) expression. Previous reports classically characterize tolerant T cells as having defective TCR signaling, impaired proliferation and increased sensitivity to cell death [28, 31, 32]. Our data shows that T cells persist *in vivo* by proliferating extensively in the tolerizing tumor environment. These results are in contrast to *in vitro* studies concluding that tolerant $CD8^+$ T cells are characterized by impaired proliferation. Furthermore, in addition to antigen, it appears that tolerant T cells *in vivo* depend on tumor-related factors in the tolerizing environment for their persistence. These studies show that these tumor-related factors do not include IL-15 and IL-7 cytokines known to support functional memory T cell maintenance. This revelation about a dominant role for tumor-related factors opens up new areas of investigation to identify molecules that support T cell infiltration and persistence. This knowledge used in combination with tolerance-breaking methods might provide novel strategies in the treatment of cancer. Understanding the molecular mechanisms for persistence of tolerant T cells may also prove

beneficial by providing new ways to induce T cell suppression, for example, in organ transplantation and treatment of autoimmune diseases.

1.5. Materials and Methods

Mice & Viruses: 2C TCR transgenic mice on RAG1$^{-/-}$ and B6 backgrounds were maintained at the Massachusetts Institute of Technology (MIT) Animal Care Facility. Congenic 2C TCR Thy1.1 mice were also bred in our facility. Recipient mouse strains (TRAMP and TRAMP-SIY) ages 3-8 months old, were also maintained in the MIT facility. Recombinant WSN (H1N1) influenza virus with SIYRYYGL peptide engineered onto the neuraminidase stalk originally constructed by plasmid-based reverse genetics [38] was grown on Madine-Darby Canine Kidney (MDCK) cells.

Antibodies & Reagents: Biotinylated 1B2 monoclonal antibody was produced in-house. 1B2 is a monoclonal antibody specific for the 2C TCR. Other anti-mouse monoclonal antibodies, CD16/32 (Fc blocker), Streptavidin-APC, CD8α-PerCP-Cy5.5 clone 53-6.7, CD8α-APC, CD8α-PE, CD8α-FITC, CD90.1(Thy1.1)-APC, CD90.1(Thy1.1)-FITC, and PD-1-PE clone J43 for flow cytometry studies were purchased from BioLegend (San Diego, CA), BD Biosciences (San Jose, CA) or eBioscience (San Diego, CA). Pierce Chemical 4',6-diamidino-2-phenylindole hydrochloride (DAPI) PI46190 was purchased from VWR (USA). Propidium iodide P4170 (PI) was purchased from Sigma-Aldrich (USA).

Lymphocyte Isolation (Lymph Nodes and Spleen): Lymph nodes (LN) and spleens from 2C RAG1$^{-/-}$ mice were extracted, one mouse at a time, after carbon dioxide (CO_2) inhalation. The sacrificed animal's fur was sterilized with 70% ethanol. Dissected LN and spleens were stored on ice in 4 ml of RPMI 1640 media supplemented with 5% fetal bovine serum and 10 mM HEPES buffer solution (RPMI complete). After dissection, the LN were gently mashed between

rough surfaces of two microscope slides immersed in RPMI complete to release lymphocytes. Cell suspensions were filtered through an 80-μm nylon mesh (Sefar) and transferred into 15-ml BD Falcon tubes kept on ice. A similar procedure was followed for cell isolation from the spleen. Splenocytes used for flow cytometry analysis were further purified by a red blood cell (RBC) lysis step after grinding.

Cell Transfer & Influenza Infection: Cells isolated from 2C lymph nodes and spleens as described above were resuspended in Hank's Balanced Salt Solution (HBSS, serum-free media), filtered and kept on ice. Following approved animal care facility protocol, recipient mice were anesthetized with 2.5% Avertin and intranasally infected with 100 pfu of WSN-SIY or 100 pfu WSN-SIIN Influenza virus suspended in 50 μl. Still under anesthesia, infected mice were immediately injected retroorbitally with 1-2 x 10^6 total live cells suspended in 100 μl HBSS.

Lymphocyte Extraction (Prostate and Lungs): Prostate lobes were extracted by microdissection following procedures in Current Protocols in Immunology [34]. Briefly, the urogenital system from each mouse was extracted after CO_2 inhalation, and transferred into 15-ml of RPMI complete on ice. A dissecting microscope was used to identify prostate lobes in the urogenital system placed on cold 1x PBS. The prostate lobes were subsequently removed using tweezers and transferred into 2-ml of 1 mg/ml Collagenase A (from Roche) in RPMI complete solution. The tissue was digested for about 45 min in a 37°C water bath, vortexing at 15-20 min intervals. Then, digested tissues were gently mashed between rough surfaces of two microscope slides immersed in RPMI complete to release lymphocytes. Cell suspensions were filtered through an 80-μm nylon mesh (Sefar) and transferred into 15-ml Falcon tubes kept on ice.

To extract cells from the lungs, each specimen was ground through a cell strainer in 10 ml of RPMI complete. Then the suspension was centrifuged and resuspended in 2 ml of 2 mg/ml Collagenase A (from Roche) in RPMI complete solution. The tissue was digested for 1 hr in a 37°C water bath, vortexing at 15-20 min intervals. An equal volume of 70% Percoll was added to the digest followed by centrifugation at ~2000 rpm for 20 min. Tissue debris and supernatant from lungs were gently aspirated, followed by RBC lysis.

Red Blood Cell (RBC) Lysis: Two milliliters of red blood cell lysis buffer (144 mM ammonium chloride and 17 mM Tris-HCl pH7.4 in distilled deionized water) was added to pellets from spleen and lungs specimens and kept on ice for 2-4 min, vortexing at 2 min intervals. Ten millimeters of RPMI complete was added to stop the lysis. Cell suspensions were centrifuged at ~1200 rpm, resuspended in an appropriate buffer for further analysis, and filtered through a nylon mesh (Sefar) into appropriately labeled tubes kept on ice.

Cell Counting: The total number of viable cells for each tissue specimen was counted using a hemacytometer and tryphan blue exclusion.

Flow Cytometry: Appropriate numbers of counted cells in suspension were transferred into labeled Falcon® round-bottom tubes (FACS tubes), and centrifuged at ~1200 rpm for 5 min. All procedures were performed on ice. Antibodies in FACS buffer (1% BSA and 0.1% sodium azide in 1x PBS) were used for staining following the manufacturer's recommended range. Purified anti-mouse CD16/32 (BioLegend), the Fc blocker, was added for 10 min prior to adding the primary antibody. Cells were incubated with the primary biotinylated antibody on ice for 30-45

min, washed and then incubated with the secondary and fluorophore-conjugated antibodies for 15-20 min while covered with foil paper. The cells were washed again, and resuspended in 50-μl of DAPI or 1 μg/ml propidium iodide solution except where indicated. Samples were sorted using a BD™ LSRII or BD FACSCalibur™ flow cytometer (BD Biosciences). Further data analysis was carried out using FlowJo software (Tree Star, Inc., Ashland, OR).

Statistical Analyses: All p-values are from unpaired two-tailed equal variance Student's t-Tests.

1.6. References

(1) WHO World Health Organization WHO Cancer. http://www.who.int/mediacentre/factsheets/fs297/en/index.html (accessed August/21, 2009).

(2) American Cancer Society Cancer Facts & Figures 2009. **2009**.

(3) Centers for Disease Control and Prevention CDC NVSS Mortality Data. http://www.cdc.gov/nchs/deaths.htm (accessed August, 21, 2009).

(4) Kupelian, P.; Klein, E. A. Overview of treatment for early prostate cancer. *www.uptodate.com* (accessed August/2, 2007).

(5) Savarese, D. M. F. Overview of treatment for advanced prostate cancer. *www.uptodate.com* (accessed August/2, 2007).

(6) Totterman, T. H.; Loskog, A.; Essand, M. The Immunotherapy of Prostate and Bladder Cancer. *BJU Int.* **2005**, *96*, 728-735.

(7) Waeckerle-Men, Y.; Uetz-von Allmen, E.; Fopp, M.; von Moos, R.; Bohme, C.; Schmid, H. P.; Ackermann, D.; Cerny, T.; Ludewig, B.; Groettrup, M.; Gillessen, S. Dendritic Cell-Based Multi-Epitope Immunotherapy of Hormone-Refractory Prostate Carcinoma. *Cancer Immunol. Immunother.* **2006**, *55*, 1524-1533.

(8) Anderson, M. J.; Shafer-Weaver, K.; Greenberg, N. M.; Hurwitz, A. A. Tolerization of Tumor-Specific T Cells Despite Efficient Initial Priming in a Primary Murine Model of Prostate Cancer. *J. Immunol.* **2007**, *178*, 1268-1276.

(9) Rosenberg, S. A.; Spiess, P.; Lafreniere, R. A New Approach to the Adoptive Immunotherapy of Cancer with Tumor-Infiltrating Lymphocytes. *Science* **1986**, *233*, 1318-1321.

(10) Yee, C.; Thompson, J. A.; Roche, P.; Byrd, D. R.; Lee, P. P.; Piepkorn, M.; Kenyon, K.; Davis, M. M.; Riddell, S. R.; Greenberg, P. D. Melanocyte Destruction After Antigen-Specific Immunotherapy of Melanoma: Direct Evidence of t Cell-Mediated Vitiligo. *J. Exp. Med.* **2000**, *192*, 1637-1644.

(11) Overwijk, W. W., et al Tumor Regression and Autoimmunity After Reversal of a Functionally Tolerant State of Self-Reactive CD8+ T Cells. *J. Exp. Med.* **2003**, *198*, 569-580.

(12) Shimizu, J.; Yamazaki, S.; Sakaguchi, S. Induction of Tumor Immunity by Removing CD25+CD4+ T Cells: A Common Basis between Tumor Immunity and Autoimmunity. *J. Immunol.* **1999**, *163*, 5211-5218.

(13) Dudley, M. E., et al Cancer Regression and Autoimmunity in Patients After Clonal Repopulation with Antitumor Lymphocytes. *Science* **2002**, *298*, 850-854.

(14) Klebanoff, C. A.; Finkelstein, S. E.; Surman, D. R.; Lichtman, M. K.; Gattinoni, L.; Theoret, M. R.; Grewal, N.; Spiess, P. J.; Antony, P. A.; Palmer, D. C.; Tagaya, Y.; Rosenberg, S. A.; Waldmann, T. A.; Restifo, N. P. IL-15 Enhances the in Vivo Antitumor Activity of Tumor-Reactive CD8+ T Cells. *Proc. Natl. Acad. Sci. U. S. A.* **2004**, *101*, 1969-1974.

(15) Roychowdhury, S.; May, K. F.,Jr; Tzou, K. S.; Lin, T.; Bhatt, D.; Freud, A. G.; Guimond, M.; Ferketich, A. K.; Liu, Y.; Caligiuri, M. A. Failed Adoptive Immunotherapy with Tumor-Specific T Cells: Reversal with Low-Dose Interleukin 15 but Not Low-Dose Interleukin 2. *Cancer Res.* **2004**, *64*, 8062-8067.

(16) Teague, R. M.; Sather, B. D.; Sacks, J. A.; Huang, M. Z.; Dossett, M. L.; Morimoto, J.; Tan, X.; Sutton, S. E.; Cooke, M. P.; Ohlen, C.; Greenberg, P. D. Interleukin-15 Rescues Tolerant

CD8+ T Cells for use in Adoptive Immunotherapy of Established Tumors. *Nat. Med.* **2006**, *12*, 335-341.

(17) Staveley-O'Carroll, K.; Sotomayor, E.; Montgomery, J.; Borrello, I.; Hwang, L.; Fein, S.; Pardoll, D.; Levitsky, H. Induction of Antigen-Specific T Cell Anergy: An Early Event in the Course of Tumor Progression. *Proc. Natl. Acad. Sci. U. S. A.* **1998**, *95*, 1178-1183.

(18) Ochsenbein, A. F.; Klenerman, P.; Karrer, U.; Ludewig, B.; Pericin, M.; Hengartner, H.; Zinkernagel, R. M. Immune Surveillance Against a Solid Tumor Fails because of Immunological Ignorance. *Proc. Natl. Acad. Sci. U. S. A.* **1999**, *96*, 2233-2238.

(19) Ali, S.; Ahmad, M.; Lynam, J.; Rees, R. C.; Brown, N. Trafficking of Tumor Peptide-Specific Cytotoxic T Lymphocytes into the Tumor Microcirculation. *Int. J. Cancer* **2004**, *110*, 239-244.

(20) Abbas, A. K.; Lichtman, A. H.; Pober, J. S. In *Cellular and molecular immunology;* W.B. Saunders: Philadelphia, 2000; , pp 553.

(21) Rabinovich, G. A.; Gabrilovich, D.; Sotomayor, E. M. Immunosuppressive Strategies that are Mediated by Tumor Cells. *Annu. Rev. Immunol.* **2007**, *25*, 267-296.

(22) Croci, D. O.; Zacarias Fluck, M. F.; Rico, M. J.; Matar, P.; Rabinovich, G. A.; Scharovsky, O. G. Dynamic Cross-Talk between Tumor and Immune Cells in Orchestrating the Immunosuppressive Network at the Tumor Microenvironment. *Cancer Immunol. Immunother.* **2007**.

(23) Mapara, M. Y.; Sykes, M. Tolerance and Cancer: Mechanisms of Tumor Evasion and Strategies for Breaking Tolerance. *J. Clin. Oncol.* **2004**, *22*, 1136-1151.

(24) Gastman, B. R.; Atarshi, Y.; Reichert, T. E.; Saito, T.; Balkir, L.; Rabinowich, H.; Whiteside, T. L. Fas Ligand is Expressed on Human Squamous Cell Carcinomas of the

Head and Neck, and it Promotes Apoptosis of T Lymphocytes. *Cancer Res.* **1999**, *59*, 5356-5364.

(25) Chappell, D. B.; Restifo, N. P. T Cell-Tumor Cell: A Fatal Interaction? *Cancer Immunol. Immunother.* **1998**, *47*, 65-71.

(26) Steinman, R. M.; Nussenzweig, M. C. Avoiding Horror Autotoxicus: The Importance of Dendritic Cells in Peripheral T Cell Tolerance. *Proc. Natl. Acad. Sci. U. S. A.* **2002**, *99*, 351-358.

(27) Nakamura, K.; Kitani, A.; Strober, W. Cell Contact-Dependent Immunosuppression by CD4(+)CD25(+) Regulatory T Cells is Mediated by Cell Surface-Bound Transforming Growth Factor Beta. *J. Exp. Med.* **2001**, *194*, 629-644.

(28) Dubois, P. M.; Pihlgren, M.; Tomkowiak, M.; Van Mechelen, M.; Marvel, J. Tolerant CD8 T Cells Induced by Multiple Injections of Peptide Antigen show Impaired TCR Signaling and Altered Proliferative Responses in Vitro and in Vivo. *J. Immunol.* **1998**, *161*, 5260-5267.

(29) Zhang, Q.; Yang, X.; Pins, M.; Javonovic, B.; Kuzel, T.; Kim, S. J.; Parijs, L. V.; Greenberg, N. M.; Liu, V.; Guo, Y.; Lee, C. Adoptive Transfer of Tumor-Reactive Transforming Growth Factor-Beta-Insensitive CD8+ T Cells: Eradication of Autologous Mouse Prostate Cancer. *Cancer Res.* **2005**, *65*, 1761-1769.

(30) Otahal, P.; Schell, T. D.; Hutchinson, S. C.; Knowles, B. B.; Tevethia, S. S. Early Immunization Induces Persistent Tumor-Infiltrating CD8+ T Cells Against an Immunodominant Epitope and Promotes Lifelong Control of Pancreatic Tumor Progression in SV40 Tumor Antigen Transgenic Mice. *J. Immunol.* **2006**, *177*, 3089-3099.

(31) O'Sullivan, G. C.; Corbett, A. R.; Shanahan, F.; Collins, J. K. Regional Immunosuppression in Esophageal Squamous Cancer: Evidence from Functional Studies with Matched Lymph Nodes. *J. Immunol.* **1996**, *157*, 4717-4720.

(32) Ohlen, C.; Kalos, M.; Cheng, L. E.; Shur, A. C.; Hong, D. J.; Carson, B. D.; Kokot, N. C.; Lerner, C. G.; Sather, B. D.; Huseby, E. S.; Greenberg, P. D. CD8(+) T Cell Tolerance to a Tumor-Associated Antigen is Maintained at the Level of Expansion rather than Effector Function. *J. Exp. Med.* **2002**, *195*, 1407-1418.

(33) Thomas, D. L.; Kim, M.; Bowerman, N. A.; Narayanan, S.; Kranz, D. M.; Schreiber, H.; Roy, E. J. Recurrence of Intracranial Tumors Following Adoptive T Cell Therapy can be Prevented by Direct and Indirect Killing Aided by High Levels of Tumor Antigen Cross-Presented on Stromal Cells. *J. Immunol.* **2009**, *183*, 1828-1837.

(34) Hurwitz, A. A.; Foster, B. A.; Allison, J. P.; Greenberg, N. M.; Kwon, E. D. In *The TRAMP Mouse as a Model for Prostate Cancer;* Current Protocols in Immunology; John Wiley & Sons, Inc.: 2001; pp 20.5.1-20.5.23.

(35) Greenberg, N. M.; DeMayo, F.; Finegold, M. J.; Medina, D.; Tilley, W. D.; Aspinall, J. O.; Cunha, G. R.; Donjacour, A. A.; Matusik, R. J.; Rosen, J. M. Prostate Cancer in a Transgenic Mouse. *Proc. Natl. Acad. Sci. U. S. A.* **1995**, *92*, 3439-3443.

(36) Chen, J.; Eisen, H. N.; Kranz, D. M. A Model T-Cell Receptor System for Studying Memory T-Cell Development. *Microbes Infect.* **2003**, 5, 233-240.

(37) Bai, A.; Higham, E.; Eisen, H. N.; Wittrup, K. D.; Chen, J. Rapid Tolerization of Virus-Activated Tumor-Specific CD8+ T Cells in Prostate Tumors of TRAMP Mice. *Proc. Natl. Acad. Sci. U. S. A.* **2008**, *105*, 13003-13008.

(38) Fodor, E.; Devenish, L.; Engelhardt, O. G.; Palese, P.; Brownlee, G. G.; Garcia-Sastre, A. Rescue of Influenza A Virus from Recombinant DNA. *J. Virol.* **199***9, 7*3, 9679-9682.

CHAPTER 2

MASS BALANCE ANALOGY APPROACH TO IDENTIFY FACTORS CONTRIBUTING TO T CELL PERSISTENCE

2.1. Summary

This chapter explores various mechanisms by which T cells may be persisting in the TRAMP-SIY prostate. First, we investigated the role that cell trafficking may have on the persistence of T cells in the prostate. Depletion of cells from lymphoid tissues such as the spleen and PDLN, and persistence of antigen-specific T cells in the prostate suggested that cells may be trafficking from the other tissues into the prostate. Memory cell transfer experiments into donor TRAMP and TRAMP-SIY indicated that 2C T cells do not preferentially migrate into the TRAMP-SIY prostate. Other experiments evaluating cell migration markers such as CCR7 and CD62L also did not show any appreciable difference between 2C T cells from TRAMP and TRAMP-SIY mice. Our analysis of IL-7Rα expression indicated that deletion rather than cell trafficking may explain the markedly reduced cell numbers in spleens and PDLN of SIY-expressing mice. All these results strongly suggest that cell trafficking is not one of the main mechanisms by which T cells persist in a tolerizing tumor environment.

Another mechanism that may contribute to T cell persistence is proliferation. Accumulation of transferred memory 2C T cells preferentially in recipient naïve TRAMP-SIY mice indicated that persistence may be due to T cell proliferation. A series of experiments which include (1) dilution of CFSE in CFSE-labeled memory 2C T cells, (2) incorporation of BrdU in persisting T cells and (3) identification of S-phase cells in freshly isolated 7-AAD labeled T cells confirmed that this is the case. These results are in stark contrast to previous literature about tolerant T cells but agree with reports about persisting 'exhausted' non-functional T cells in chronic infection models. This chapter reveals that the main mechanism by which T cells persist in the tolerizing tumor environment is through proliferation.

Also, we investigated the effect of changes in cell death or survival on T cell persistence. Previous publications showed that tolerant T cells are more sensitive to death. We chose to analyze markers that might suggest a change in tolerant T cell death. We analyzed expression of Fas, Caspase-3, and Annexin V in the apoptosis cell death pathway. Only our RNA analysis of Fas expression and intracellular staining for cleaved Caspase-3 indicate an increase in cell death among tolerant T cells. No significant difference could be found in the analysis for Fas protein expression or Annexin V/7-AAD staining of tolerant versus non-tolerant T cells. One of the reasons for these mixed results may be the different timepoints of the analyses and poor sensitivity of the assays. However, the lack of correlation between cell number trends and proliferation patterns still makes us infer that tolerant T cells are more prone to death. Thus, although tolerant T cells persist by proliferating extensively, it appears their persistence is limited by their increased sensitivity to cell death.

2.2. Introduction

This phenomenon of cell persistence can be likened to the mass and material balance problems solved in engineering systems. For a given system, there are input, output, and internal processes that help to determine the overall state of the system. By defining our system of interest as the prostate, we can identify the analogous input, output and internal processes that might contribute to T cell persistence in the prostate. Cell trafficking and migration are input and output processes that can alter the number of T cells one may observe in the prostate at any given time. Within the prostate, cell proliferation and death could also be occurring. Figure 3 is a schematic of this mass balance analogy. Using the TRAMP-SIY model, we have observed that 2C T cells persist in the prostate but are depleted from other tissues. Therefore, these T cells may persist by (1) cell trafficking from other tissues into the prostate tumor environment, (2) cell proliferation in the prostate, and/or (3) increased T cell survival or a decrease in the death rate of T cells in the tolerizing environment. This chapter investigates the role of each of these factors in persistence of tolerant T cells.

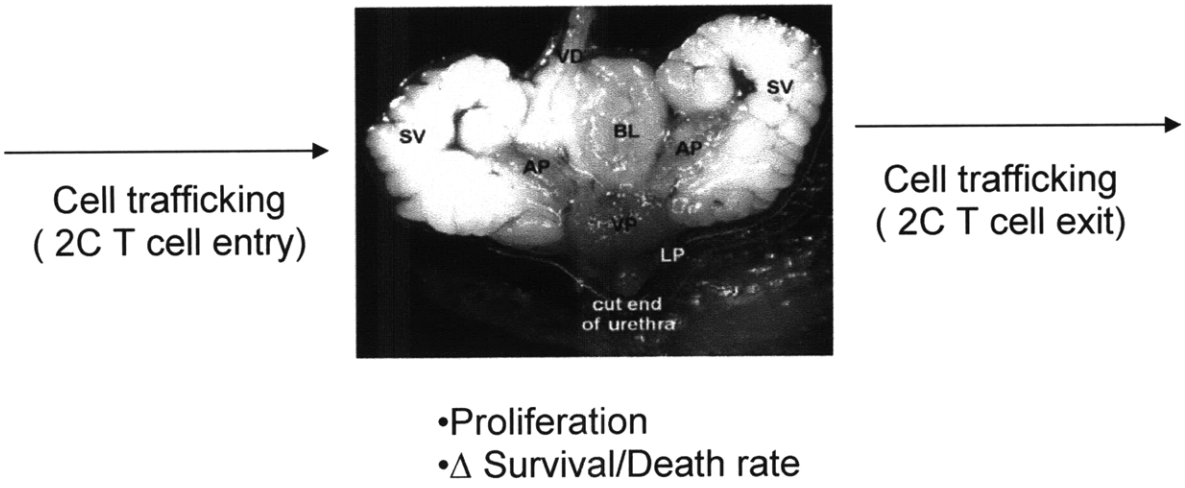

Figure 3. Schematic of processes that may contribute to T cell persistence ("Mass Balance" Analogy).
Image of prostate tissue is from Hurwitz A.A. *et al.* (2001) [1].

2.3. Role of Cell Trafficking in T Cell Persistence

2.3.1. Results

Depletion of T cells from the spleens is antigen-specific

Using flow cytometry, we analyzed the number of 2C T cells in B6 (non-tumor, non-antigen) and B6-SIY (non-tumor) tissues, and recognized that depletion of antigen-specific 2C T cells in B6-SIY spleens is similar to that seen in TRAMP-SIY spleens (Fig. 4). The total number of $CD8^+$ T cells is similar in all mouse models (Fig. 5). These trends suggested an effect of expression of SIY antigen in the prostate on depletion of antigen-specific T cells in the spleens.

To determine whether this depletion effect is antigen-specific, we adoptively transferred $CD8^+$ T cells with another TCR, OT-I T cells, which would not recognize SIY antigen presented on the MHC-I complex. Mice that received naïve OT-I T cells were also infected with low dose WSN-SIINFEKL (abbreviated WSN-SIIN) virus so that the OT-I T cells would be activated *in vivo* and would be able to infiltrate all tissues. Then, tissues from these mice were analyzed 2 mpi. OT-I T cells infiltrate and are maintained for at least 2 mpi in B6, B6-SIY, TRAMP and TRAMP-SIY mice (Fig. 6). Interestingly, in the spleen, unlike the depletion pattern observed for 2C T cells (Fig. 4), B6-SIY and TRAMP-SIY mice maintain OT-I T cells in their spleens (Fig. 6). Again the total number of $CD8^+$ T cells is similar for all mouse models (Fig. 7). These data suggests that the presence of SIY antigen in the prostate may be contributing to depletion of antigen-specific 2C T cells from the spleens and other tissues.

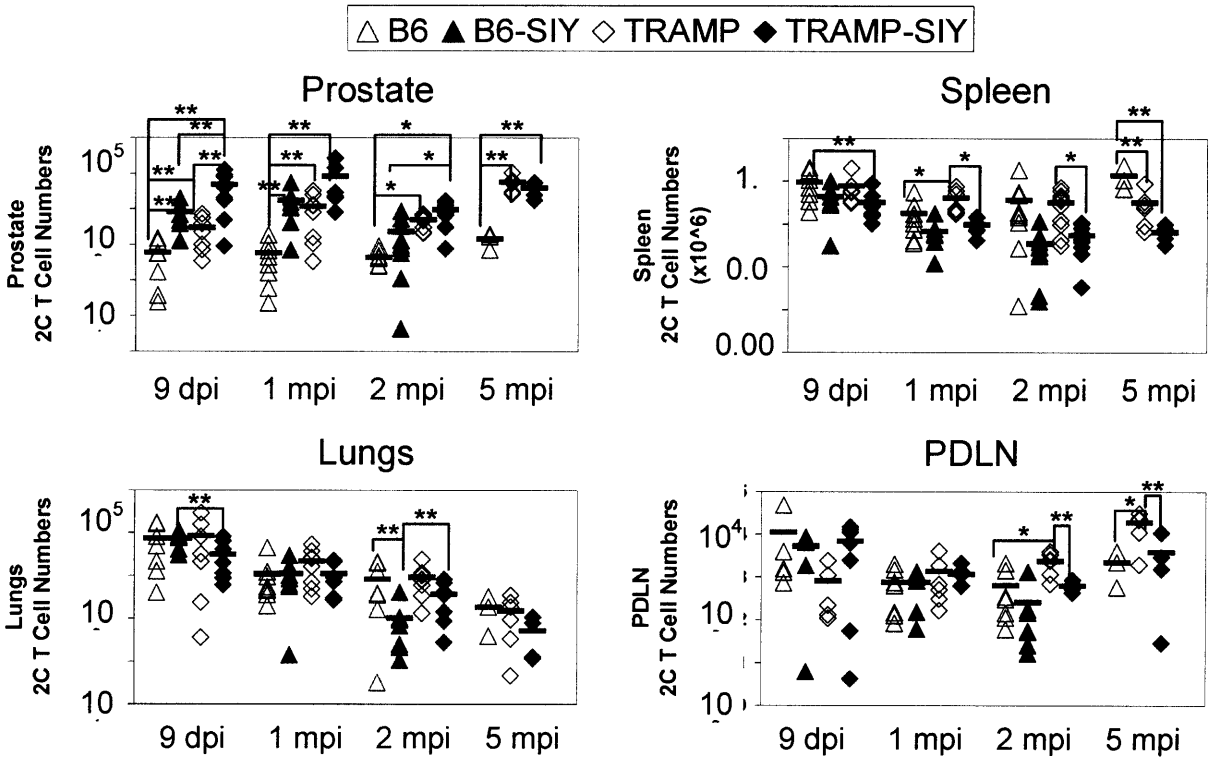

Figure 4. Tolerant antigen-specific T cells persist in the tumor environment but are depleted from other tissues.

Prostates, lungs, spleens and PDLN from TRAMP-SIY (solid diamond), TRAMP (open diamond), B6-SIY (solid triangle) and B6 (open triangle) mice were harvested nine days, one- and two- months after 2C T cell transfer and WSN-SIY influenza infection as described in the methods section. Cells were analyzed as described in Fig. 1. Each shape represents one mouse. Solid black bars indicate the average of the data for each mouse model ($n \geq 5$ per group). The p-values for cell numbers from student t-tests comparing B6 to TRAMP, B6-SIY to TRAMP-SIY, B6 to B6-SIY and TRAMP to TRAMP-SIY are given for $p \leq 0.05$. Values $p < 0.01$ are represented with an asterisk (*) and $p < 0.05$ are represented with a double asterisk (**).

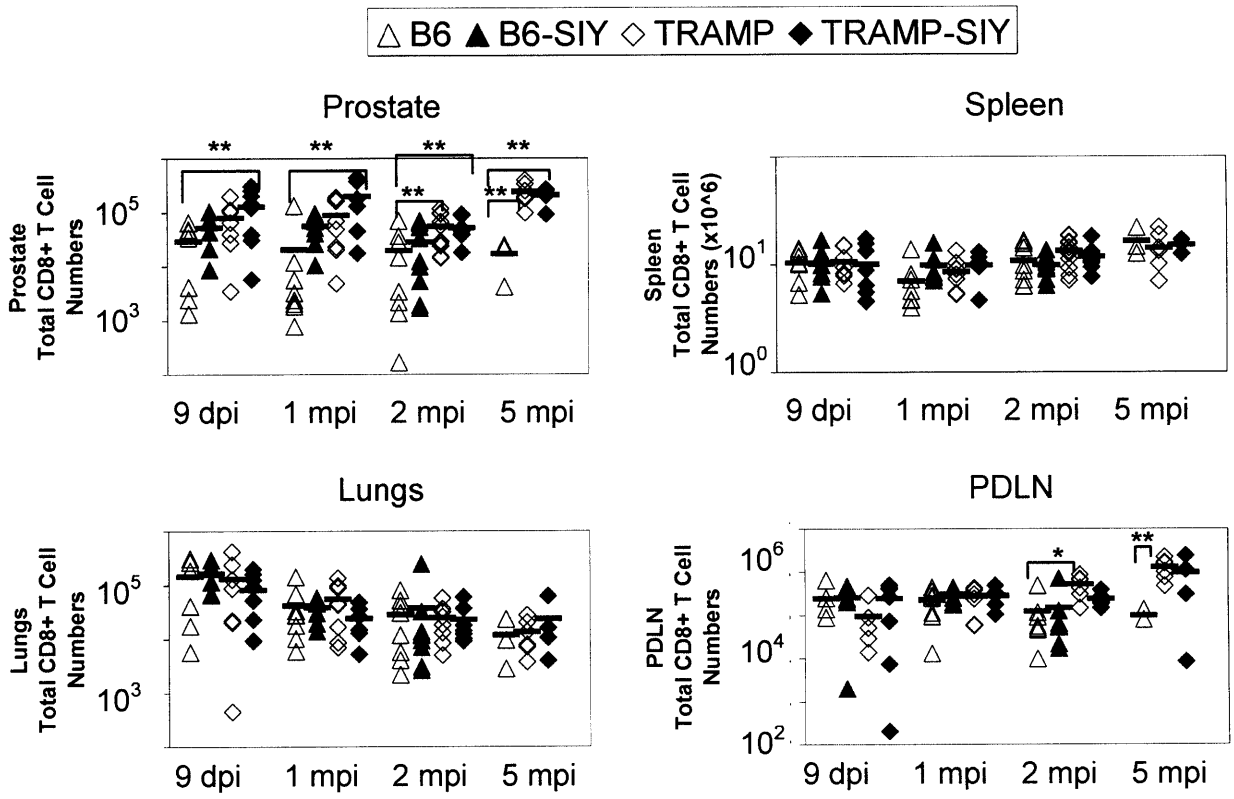

Figure 5. Total CD8$^+$ T cell numbers in 2C recipient mice.
Tissues from TRAMP-SIY (solid diamond), TRAMP (open diamond), B6-SIY (solid triangle) and B6 (open triangle) mice were harvested at the times indicated after 2C T cell transfer and WSN-SIY influenza infection as described in the methods section. Total numbers of CD8$^+$ T cells were determined from flow cytometry analysis as previously described. Each shape represents one mouse ($n \geq 5$ per group). Solid black bars indicate the average of the data for each mouse model. The p-values for cell numbers from student t-tests comparing B6 to TRAMP, B6-SIY to TRAMP-SIY, B6 to B6-SIY and TRAMP to TRAMP-SIY are given for $p<0.05$. Values $p<0.01$ are represented with an asterisk (*) and $p<0.05$ are represented with a double asterisk (**).

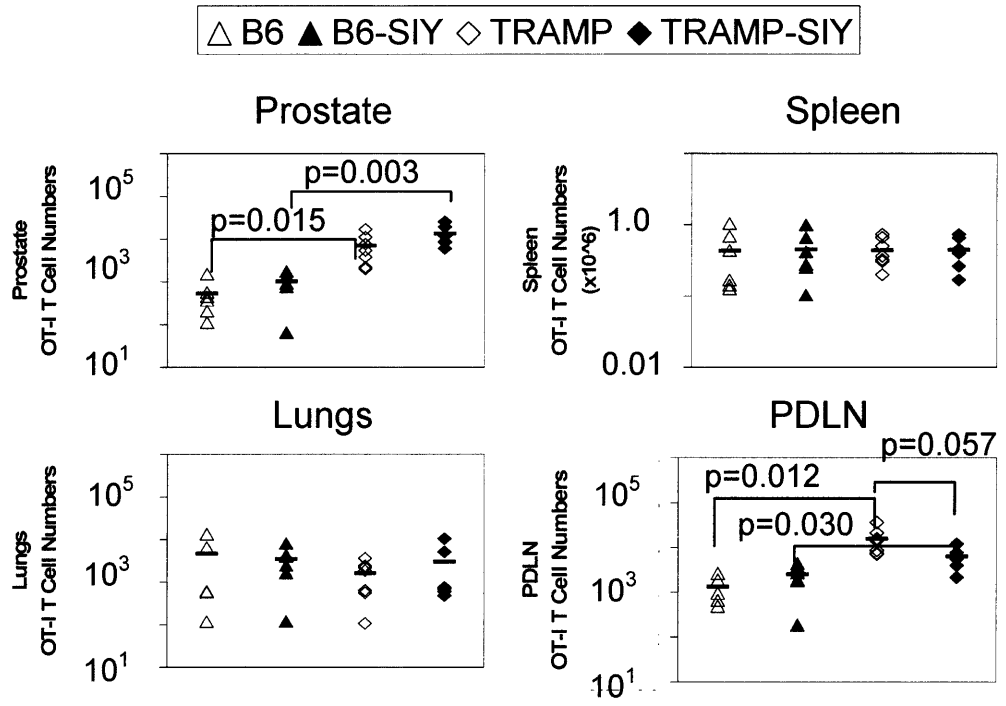

Figure 6. Non-antigen-specific OT-I T cells are not preferentially depleted from lymphoid tissues of SIY-expressing mice.

Prostates, lungs, spleens and PDLN were harvested two-months after OT-I T cell transfer and WSN-SIIN influenza infection from TRAMP-SIY (solid diamond), TRAMP (open diamond), B6-SIY (solid triangle) and B6 (open triangle). Cells were stained with vα2, vβ5, and CD8α antibodies, as well as PI to exclude dead cells, followed by flow cytometry analysis. After gating on all live $CD8^+$ cells using the FlowJo software, OT-I cells were identified by gating on $v\alpha2^+$ and $v\beta5^+$ cells. Total cell numbers were calculated by multiplying ratio of $v\alpha2^+$ $v\beta5^+$ $CD8^+$ cells from FlowJo analysis and the total cell numbers counted by hemacytometer and tryphan blue exclusion before antibody staining. The cell number calculations and plot generation were performed using Microsoft Excel. Each shape represents data for one mouse ($n \geq 5$ per group). Solid black bars indicate the average of the data for each mouse model. The p-values for cell numbers from student t-tests comparing B6 to TRAMP, B6-SIY to TRAMP-SIY, B6 to B6-SIY and TRAMP to TRAMP-SIY are given for $p \leq 0.05$.

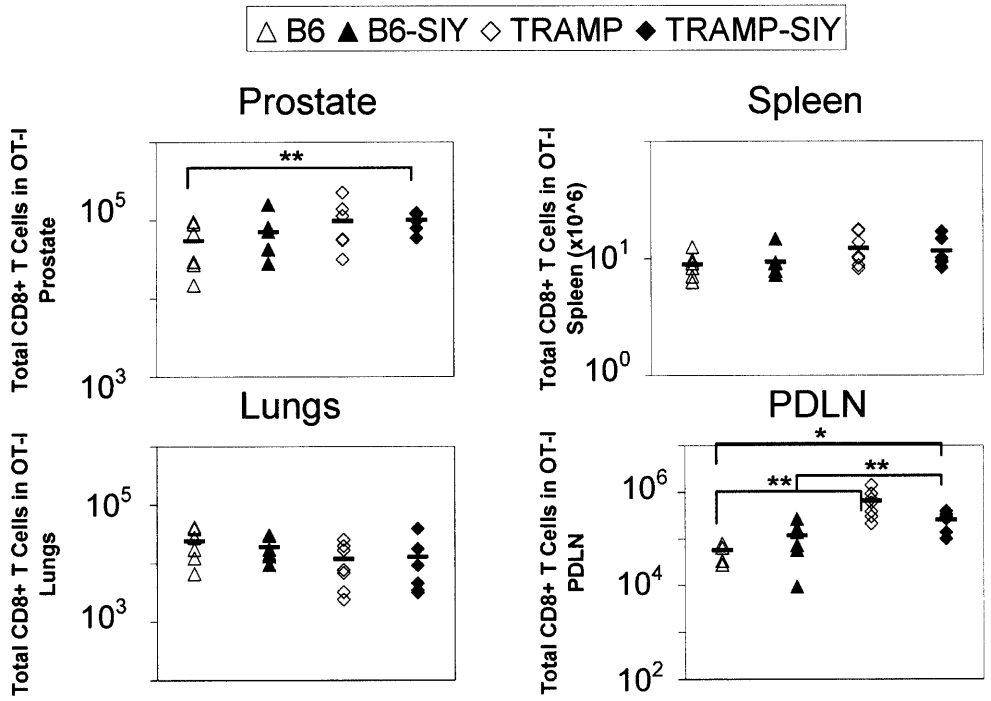

Figure 7. Total CD8$^+$ T cell numbers in OT-I recipient mice.
Tissues from TRAMP-SIY (solid diamond), TRAMP (open diamond), B6-SIY (solid triangle) and B6 (open triangle) mice were harvested at the times indicated after OT-I and WSN-SIIN infection as described in the methods section. Total numbers of CD8$^+$ T cells were determined from flow cytometry analysis as previously described. Each shape represents one mouse ($n \geq 5$ per group). Solid black bars indicate the average of the data for each mouse model. The p-values for cell numbers from student t-tests comparing B6 to TRAMP, B6-SIY to TRAMP-SIY, B6 to B6-SIY and TRAMP to TRAMP-SIY are given for $p<0.05$. Values $p<0.01$ are represented with an asterisk (*) and $p<0.05$ are represented with a double asterisk (**).

Depletion of T cells from the spleens correlates with low IL-7Rα levels

Previous studies have shown that gradual loss of IL-15Rβ (CD122) and IL-7Rα (CD127) in memory 2C T cells of WSN-SIY virus infected B6 mice corresponds to decline in 2C T cell numbers in the lungs of these mice [2]. 2C T cells in B6 spleens that maintain high levels of IL-7Rα persist [2]. Flow cytometry experiments were performed to determine the protein expression levels IL-7Rα in 2C T cells from spleens of SIY-expressing and non-SIY mice. Analysis of IL-7Rα expression in 2C T cells from the spleen revealed a correlation between IL-7Rα levels and the presence of SIY antigen in the prostate (Fig. 8). As early as 1 mpi, 2C T cells from B6-SIY and TRAMP-SIY spleens have lower levels of IL-7Rα expression compared to cells from B6 and TRAMP spleens. This difference remains evident at 2 mpi (Fig. 8). This lower level of IL-7Rα correlates with depletion of 2C T cells from spleens of mice expressing SIY antigen in their prostates.

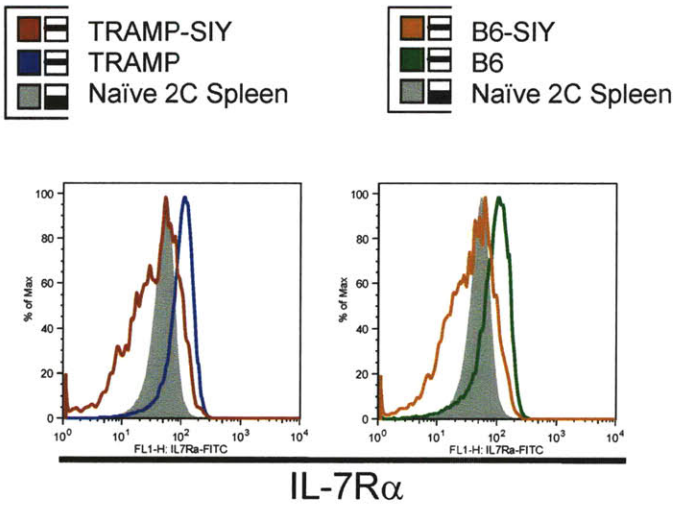

Figure 8. Depletion of antigen-specific T cells from the spleens correlates with low IL-7Rα levels.

Spleens from TRAMP-SIY (red), TRAMP (blue), B6-SIY (orange) and B6 (green) mice were harvested 2 months after 2C T cell transfer and WSN-SIY influenza infection. Cells were stained with 1B2, CD8α, and IL-7Rα antibodies, as well as PI to exclude dead cells. Using the FlowJo software, IL-7Rα expression histograms were generated by gating on PI^{Neg} $CD8^{+}$ cells followed by FSC versus SSC lymphocyte gating, selecting $1B2^{+}$ $CD8^{+}$ cells, and finally, overlaying histogram plots. Freshly isolated naïve 2C T cells analyzed at the same time were used to determine baseline level comparisons (gray shadow).

Cell trafficking does not seem to be a major contributor to T cell persistence

An additional explanation for the depletion observed in the spleens is that T cells may be preferentially trafficking from other tissues into the TRAMP-SIY prostate where they persist. To investigate the effect of cell trafficking from the spleens, we developed an adoptive transfer system of memory 2C T cells. Previous work has shown that 2C T cells in the spleen are more functional than cells from TRAMP-SIY prostate [3]. We deduced that if cell trafficking is occurring, then upon transfer of functional persisting 2C T cells into each mouse, one would observe preferential entry of 2C T cells into TRAMP-SIY prostate. We generated functional persisting memory 2C T cells in normal B6 mice. These B6 (Thy1.2) mice received naïve 2C Thy1.1$^+$ CD8$^+$ T cells and were infected with low-dose WSN-SIY influenza virus. After 1 mpi when activated 2C T cells have transitioned into memory T cells [2], 2C Thy1.1$^+$ CD8$^+$ T cells were isolated and magnetically sorted from the spleens. Further details about the procedure are given in the methods section. Approximately 0.5 x 10^6 memory 2C Thy1.1$^+$ CD8$^+$ T cells were retroorbitally injected into TRAMP and TRAMP-SIY mice. None of the recipient mice have ever been infected with WSN-SIY virus or previously received 2C T cells. Since TRAMP and TRAMP-SIY mice are from a Thy1.2 background, this system allowed us to recognize the presence of 2C T cells in any of the tissues by using Thy1.1 and CD8α antibodies. After 36 hr post-transfer (h36), the numbers of 2C T cells from different tissues were analyzed. The 2C T cell numbers in the prostate, lungs, spleens, and PDLN are similar for both groups (Fig. 9). Each mouse had approximately twenty 2C T cells in its prostate (Fig. 9). This h36 data suggests that there are no differences in the ability of 2C T cells to migrate into the prostate of tumor transgenic mice.

Further analyses of tissues from recipient mice kept at longer time points, nine, twenty and sixty days after transfer, show that 2C T cells become tolerant (Fig. 10 and Table 1) and accumulate (Fig. 9) in TRAMP-SIY prostate compared to TRAMP prostate. The 2C T cell numbers in the spleens, PDLN and non-draining lymph nodes (NDLN) of TRAMP and TRAMP-SIY mice are not statistically significantly different (Fig. 7). However, significantly lower numbers of 2C T cells are found in the mesenteric lymph nodes (MesLN), another type of non-draining LN, of TRAMP-SIY mice compared to TRAMP MesLN on day 60 (Fig. 7). Upon analysis of the 2C T cells for PD-1 expression, a marker to show the functional state of cells, the cells accumulating in TRAMP-SIY prostate are predominantly PD-1^{high} i.e. tolerant 2C T cells (Fig. 10 and Table 1). When these memory 2C T cells are labeled with carboxyfluorescein diacetate succinimidyl ester (CFSE) before transfer, the accumulation can be attributed to extensive proliferation (Figs. 14 to 16) and not cell trafficking. Therefore, it appears that cell trafficking is not one of the main mechanisms for T cell persistence in the tolerizing tumor environment.

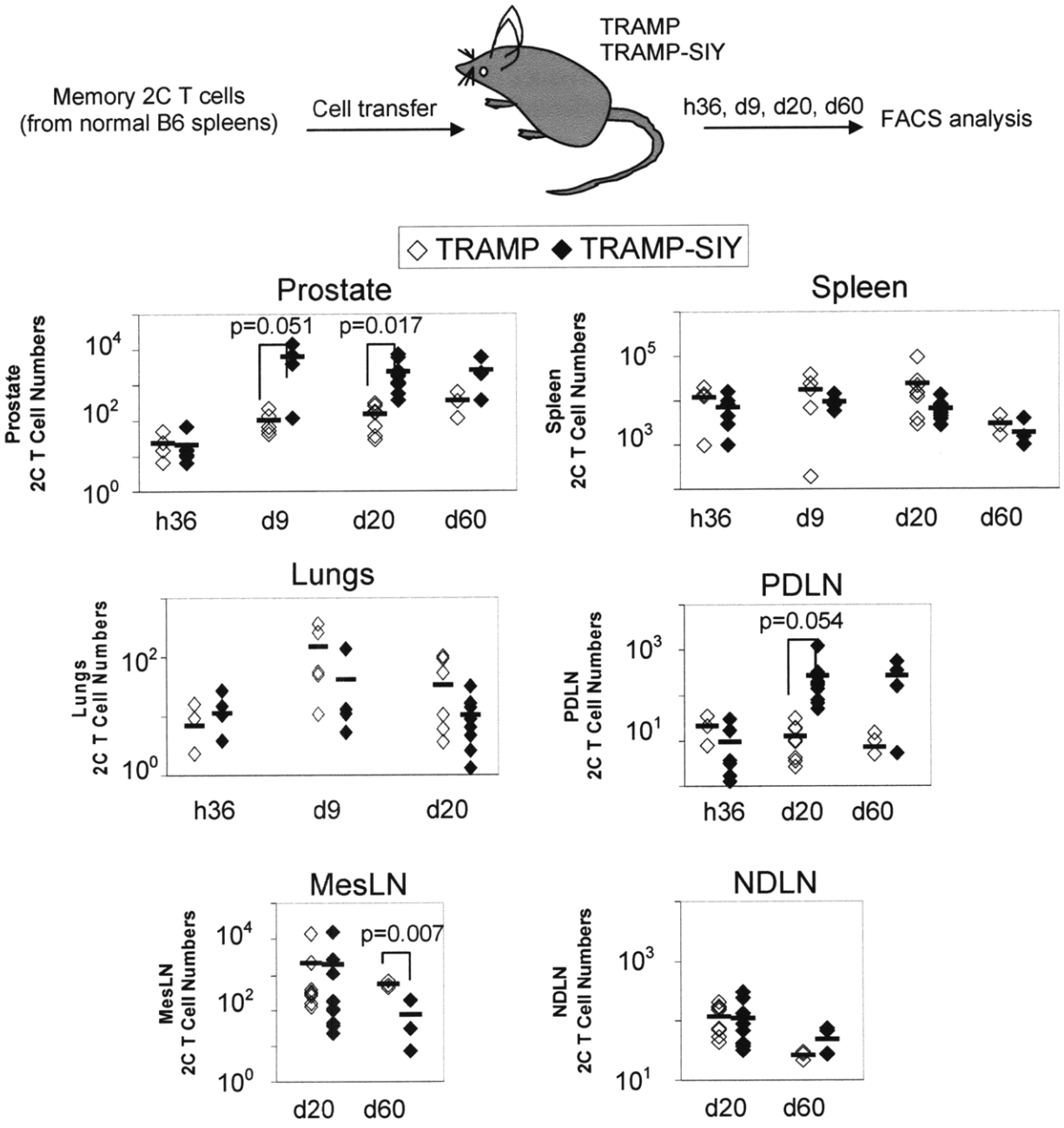
TRAMP
TRAMP-SIY
Memory 2C T cells
(from normal B6 spleens)
Cell transfer
h36, d9, d20, d60
FACS analysis
◇ TRAMP ◆ TRAMP-SIY
Prostate
Prostate
2C T Cell Numbers
p=0.051
p=0.017
h36
d9
d20
d60
Spleen
Spleen
2C T Cell Numbers
Lungs
Lungs
2C T Cell Numbers
PDLN
PDLN
2C T Cell Numbers
p=0.054
MesLN
MesLN
2C T Cell Numbers
p=0.007
NDLN
NDLN
2C T Cell Numbers

Figure 9. Functional memory T cells become tolerant and preferentially accumulate in TRAMP-SIY prostate. Memory 2C (Thy1.1$^+$) T cells were generated and sorted from B6 (Thy1.2) spleens as described in the methods section. After CD8$^+$ T cell enrichment, ~0.5 x 10^6 memory 2C Thy1.1$^+$ CD8$^+$ T cells were transferred into each TRAMP (open) and TRAMP-SIY (solid) mouse by retroorbital injection. Tissues from recipient mice were analyzed for the presence of Thy1.1$^+$ and CD8$^+$ cells at different time points indicated after 2C T cell transfer. MesLN stands for mesenteric lymph nodes and NDLN is a pooled sample of axial, brachial and inguinal lymph nodes. Total cell numbers were calculated by multiplying ratio of Thy1.1$^+$ CD8$^+$ cells from FlowJo analysis and the total cell numbers counted by hemacytometer and tryphan blue exclusion before antibody staining. Each point represents one mouse ($n \geq 3$ per group). Solid black bars indicate the average of the data for each mouse model. The p-values from student t-tests comparing cell numbers from TRAMP to TRAMP-SIY are given for $p \leq 0.05$.

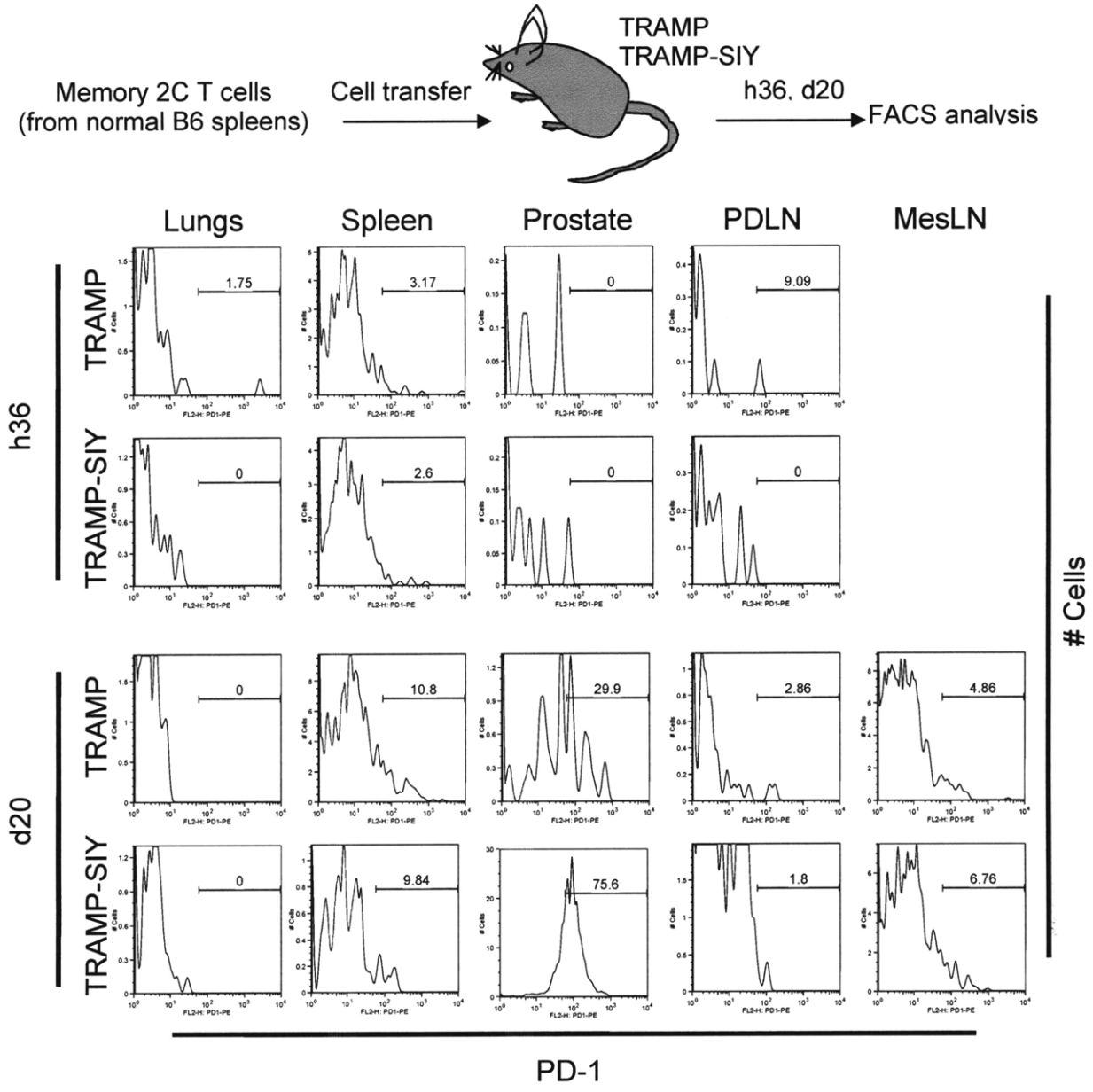

Figure 10. Functional memory T cells become tolerant in TRAMP-SIY prostate.
Memory 2C (Thy1.1$^+$) T cells were generated in B6 (Thy1.2) mice, and 0.5 x 10^6 memory 2C Thy1.1$^+$ CD8$^+$ T cells were transferred into TRAMP and TRAMP-SIY (as described in Fig. 9). Cells from recipients were stained with PD-1 on 36 hr and day 20 after transfer to assess their functional state. Using FlowJo software, histograms showing PD-1 expression were generated and the percentage of Thy1.1$^+$ CD8$^+$ cells that are PD-1^{high} was determined. The gating was determined using 2C T cells on day 0 (before transfer) and cells from the lung at d-20.

Table 1. Antigen-specific T cells accumulating in TRAMP-SIY prostate are tolerant. Memory 2C (Thy1.1$^+$) T cells were generated in B6 (Thy1.2) mice, and 0.5 x 10^6 memory 2C Thy1.1$^+$ CD8$^+$ T cells were transferred into TRAMP and TRAMP-SIY (as described in Fig. 10). Cells from recipients were stained with PD-1 on day 20 after transfer to assess their functional state. Using FlowJo software, histograms showing PD-1 expression were generated and the percentage of Thy1.1$^+$ CD8$^+$ cells that are PD-1^{high} was determined. The gating was determined using 2C T cells on day 0 (before transfer) and cells from the lung at d-20. This table shows the average and standard deviation values for two TRAMP and three TRAMP-SIY mice analyzed. This experiment was performed twice.

	TRAMP (%)	TRAMP-SIY (%)	p-value
Lungs	0.0 ± 0.0	1.15 ± 2.0	0.495
Spleen	15.05 ± 6.0	23.01 ± 13.6	0.508
Prostate	**30.75 ± 1.2**	**79.67 ± 4.6**	**0.001**
PDLN	1.43 ± 2.0	20.97 ± 17.5	0.232
MesLN	37.88 ± 46.7	35.19 ± 27.3	0.938

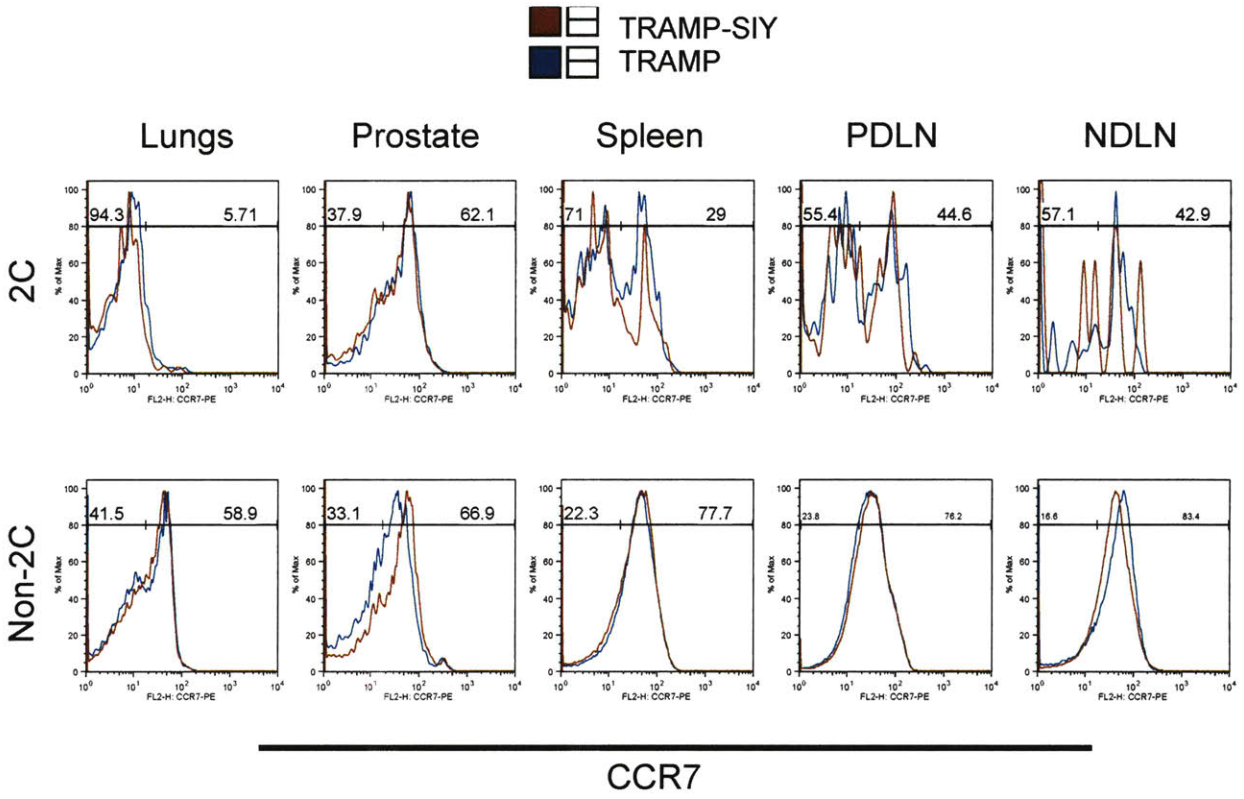

Figure 11. Similar CCR7 expression in TRAMP and TRAMP-SIY mice.
Tissues from TRAMP (red) and TRAMP-SIY (blue) mice were harvested 2 mpi and stained with Thy1.1-APC, CD8α-FITC, and CCR7-PE antibodies, as well as PI for analysis by flow cytometry. Note that CCR7 (eBioscience) was incubated at 37°C following optimized conditions recommended by the manufacturer. FlowJo software was used to generate CCR7 histograms. "Non-2C" histograms are CCR7 expression levels in Thy1.1^{Neg} CD8^{+} T cells. This is a representative plot of a pair of mice analyzed on the same day.

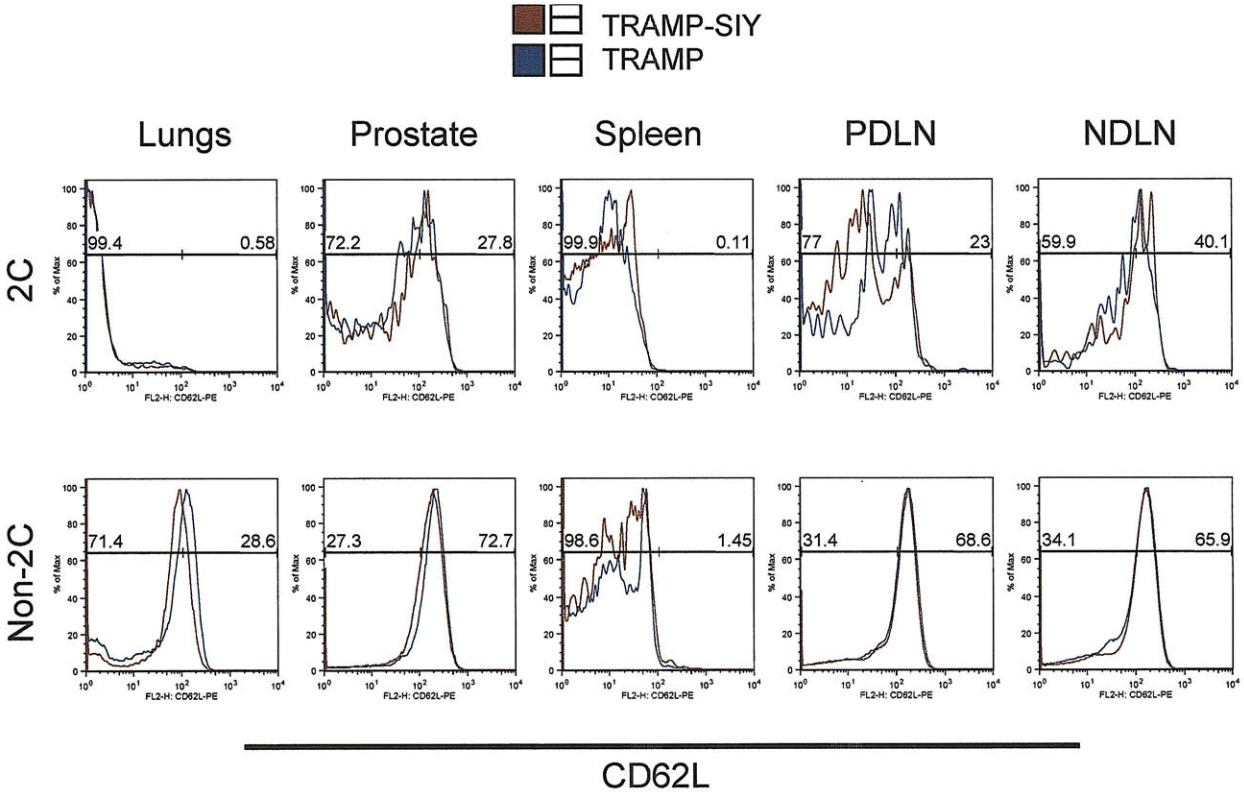

Figure 12. Similar CD62L expression in TRAMP and TRAMP-SIY mice.
Tissues from TRAMP (red) and TRAMP-SIY (blue) mice were harvested 2 mpi and stained with Thy1.1-APC, CD8α-FITC, and CD62L-PE antibodies, as well as PI for analysis by flow cytometry. FlowJo software was used to generate CD62L histograms. "Non-2C" histograms are CD62L expression levels in Thy1.1^{Neg} CD8^{+} T cells. This is a representative plot of a pair of mice analyzed on the same day.

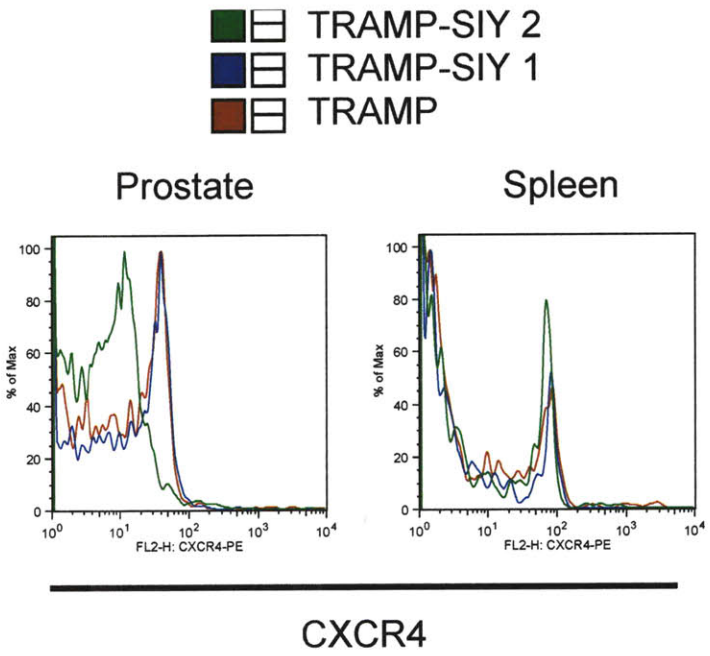

Figure 13. TRAMP-SIY has similar or lower level of CXCR4 expression compared to TRAMP tissues.
Tissues from TRAMP (red) and TRAMP-SIY (blue) mice were harvested 2 mpi and stained with Thy1.1-APC, CD8α-FITC, and CXCR4-PE antibodies, as well as PI for analysis by flow cytometry. FlowJo software was used to generate CXCR4 histograms.

2.3.2. Discussion

One mechanism that could explain the depletion trend observed in spleens might be preferential cell trafficking of antigen-specific 2C T cells from other tissues into the prostate and retention in the prostate due to the presence of SIY antigen. Our results suggest that this is probably not the case. Close examination of the 2C T cell numbers show that the decline in T cell numbers in TRAMP-SIY spleen (~100 000 less than TRAMP spleen) is not reflective of the number of cells increase in TRAMP-SIY prostate (~5 000 more than TRAMP prostate) (Fig. 4). $CCR7^{high}$ T cells are reported to preferentially exit peripheral tissues while $CCR7^{low}$ T cells accumulate in the tissue [4]. CD62L has been shown to be necessary for migration of circulating mature T cells into lymph nodes [5]. Our analyses of CCR7 and CD62L expression do not indicate any significant differences between 2C T cells from TRAMP and TRAMP-SIY tissues (Figs. 11 and 12). Also, 2C T cells from TRAMP-SIY tissues have similar or lower levels of CXCR4 compared to TRAMP (Fig. 13). Therefore, expression levels of these markers of cell migration cannot explain the preferential depletion of 2C T cells observed in TRAMP-SIY spleens but not in TRAMP spleens. Furthermore, because antigen-specific T cells are being depleted from other tissues, it seems unlikely that they are leaving the prostate. Our use of a common approach of transferring T cells from a donor to a recipient (Fig. 9) to evaluate cell trafficking indicated that preferential proliferation in the presence of antigen rather than preferential cell trafficking contribute to tolerant T cell persistence.

A more probable explanation for the depletion trend is an active process of deletion of antigen-specific T cells from the spleen. The presence of persistent antigen in the prostate creates a situation of persistent antigen-presentation, possibly by DC, in SIY antigen-expressing spleens. As a result, 2C T cells are trapped in an "effector" T cell state. In accordance with this

state, 2C T cells from the spleens of SIY-expressing mice express low levels of IL-7Rα (Fig. 8). Only mice that lack persistent antigen are able to progress to a memory phenotype of high IL-7Rα levels (Fig. 6) needed for maintaining antigen-specific T cells in the spleen [2]. Kaech *et al.* (2003) showed that antigen-specific T cells with low IL-7Rα levels were more prone to apoptosis [6]. As a result, these cells did not persist [6]. Our Annexin V and Caspase-3 cell death assays have not been able to detect significant differences in apoptotic rates between 2C T cells from TRAMP and TRAMP-SIY spleens (Figs. 20 and 21). However, it appears that depletion of antigen-specific T cells from the spleen is correlated with low levels of IL-7Rα that could make them more apoptotic. This deletion process contributes to the observation that tolerant antigen-specific T cells preferentially persist locally in the tolerizing tumor and antigen transgenic prostate.

2.4. Effect of Proliferation on T Cell Persistence

2.4.1. Results

Tolerant antigen-specific T cells proliferate extensively

To assess whether tolerant T cells could persist by proliferation, we adapted the memory 2C T cell transfer system. After T cell isolation and magnetic sorting, cells were labeled with CFSE, and then transferred into TRAMP and TRAMP-SIY recipient mice (Figs. 14 to 16). CFSE is a fluorescent dye that dilutes by one-half for every cell division that occurs. When the cells are run through a fluorescence-based flow cytometer, multiple fluorescence intensity peaks are observed. The number of cell divisions, and hence proliferation rate, can be determined from the number of fluorescence intensity peaks present. We analyzed tissues from these recipient mice on days 6 (Fig. 14), 9 (Fig. 15) and 20 (Fig. 16) after the cell transfer. By day 20, 2C T cells in TRAMP-SIY prostate and PDLN appear to have completely diluted CFSE (Fig. 16), whereas only about 40% of the 2C T cells in TRAMP prostate have undergone more than four rounds of cell division (Fig. 16). This extensive cell division in TRAMP-SIY prostate is in agreement with the >10-fold more 2C T cells in TRAMP-SIY prostate compared to TRAMP prostate at day 20 post-transfer (Fig. 9) even though both mice received the same number of 2C T cells initially. On day 9, about five-fold more 2C T cells from TRAMP-SIY spleen have undergone more than four rounds of cell division compared to cells in TRAMP spleen (Fig. 15). By day 20, there is no statistical difference in CFSE dilution in the spleens (Fig. 16). This proliferation data based on CFSE dilution suggests that one of the mechanisms by which tolerant 2C T cells may be persisting in TRAMP-SIY prostate may be through extensive proliferation in the presence of SIY antigen.

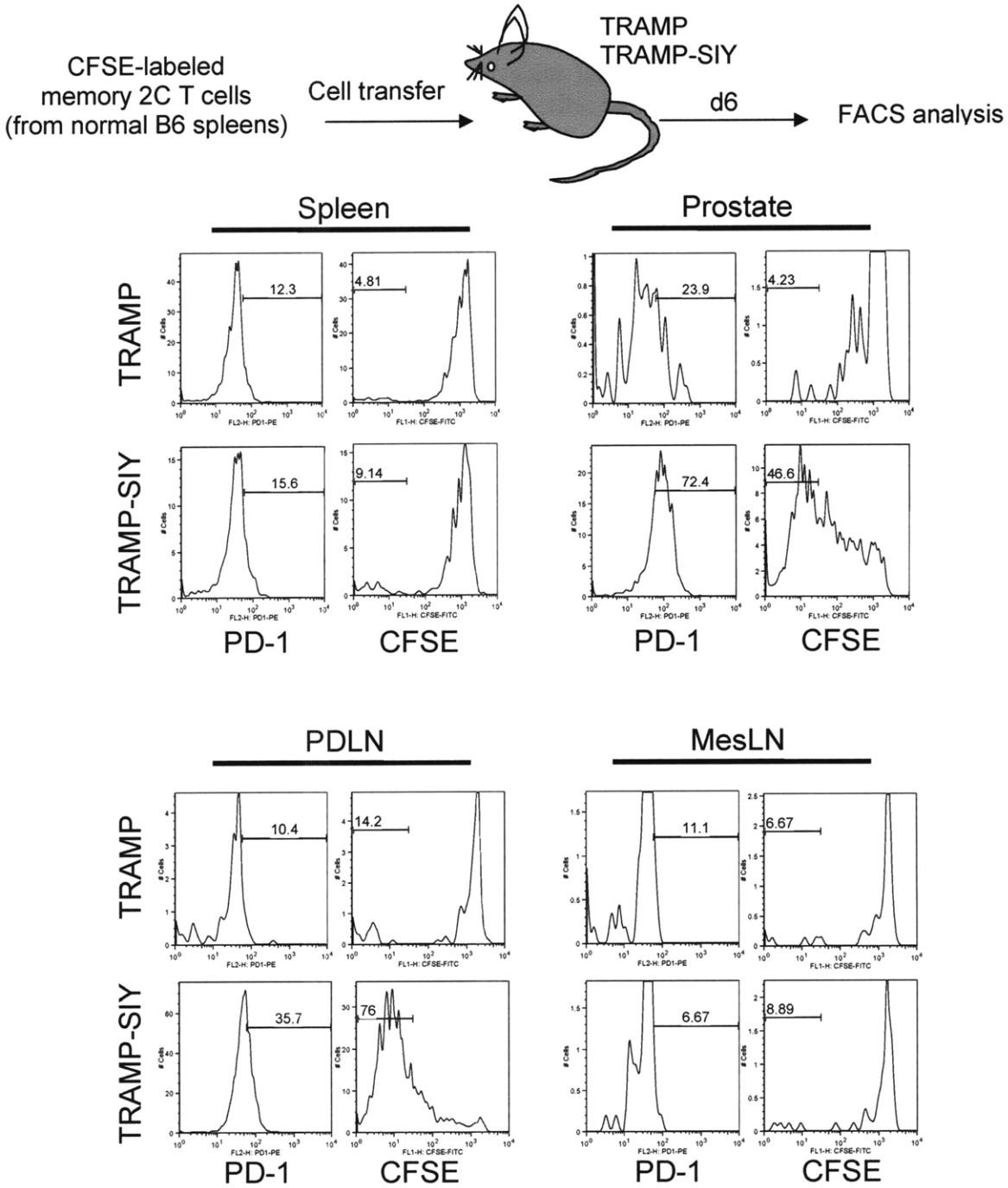
CFSE-labeled
memory 2C T cells
(from normal B6 spleens)
Cell transfer
TRAMP
TRAMP-SIY
d6
FACS analysis
Spleen
Prostate
PDLN
MesLN
TRAMP
TRAMP-SIY
12.3
4.81
23.9
4.23
15.6
9.14
72.4
46.6
10.4
14.2
11.1
6.67
35.7
76
6.67
8.89
PD-1
CFSE
PD-1
CFSE
PD-1
CFSE
PD-1
CFSE

Figure 14. Antigen-specific T cells become tolerant and proliferate in the presence of antigen.

About 0.5 x 10^6 CFSE-labeled memory 2C Thy1.1$^+$ CD8$^+$ T cells were transferred into TRAMP and TRAMP-SIY mice by retroorbital injection. Details are given in the methods section. Six days after transfer, tissues from recipient mice were stained with Thy1.1-APC and PD-1-PE antibodies, as well as PI to exclude dead cells, and analyzed by flow cytometry. Each diagram is data from pooling four mice per group. PD-1 and CFSE histogram plots are shown for cells gated on PI^{Neg} and Thy1.1$^+$ lymphocytes. The numbers in the PD-1 histograms indicate the percentage of PD-1^{high} cells determined using naïve 2C Thy1.1$^+$ RAG1$^{-/-}$ splenocytes as a negative control. The numbers in the CFSE histograms are Thy1.1$^+$ CD8$^+$ cells that have undergone $\geq$4 rounds of CFSE dilution.

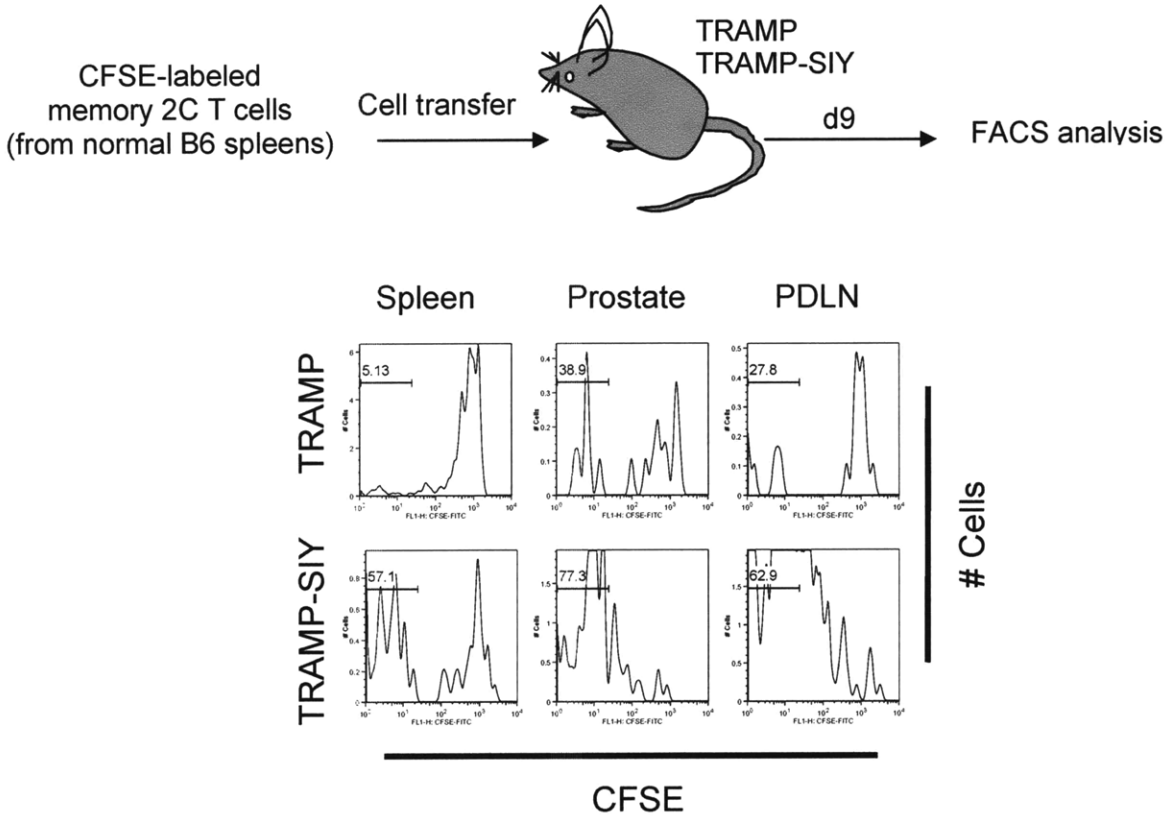

Figure 15. T cells accumulate in TRAMP-SIY prostate because they are proliferating. Memory 2C (Thy1.1$^+$) T cells were generated and enriched for CD8$^+$ T cells by magnetic negative selection. After enrichment, memory 2C (Thy1.1$^+$) T cells as described in the methods section, were labeled with 5 μM CFSE. About 0.5 x 10^6 memory 2C Thy1.1$^+$ CD8$^+$ T cells were transferred into TRAMP and TRAMP-SIY mice by retroorbital injection. On day 9, tissues from recipient mice were analyzed by flow cytometry. CFSE histogram plots are shown for cells gated on PI^{Neg}, Thy1.1$^+$ and CD8$^+$ lymphocytes. The numbers in the histograms indicate the percentage of Thy1.1$^+$ CD8$^+$ cells that have undergone ≥4 rounds of CFSE dilution. This is a representative plot for two mice per group.

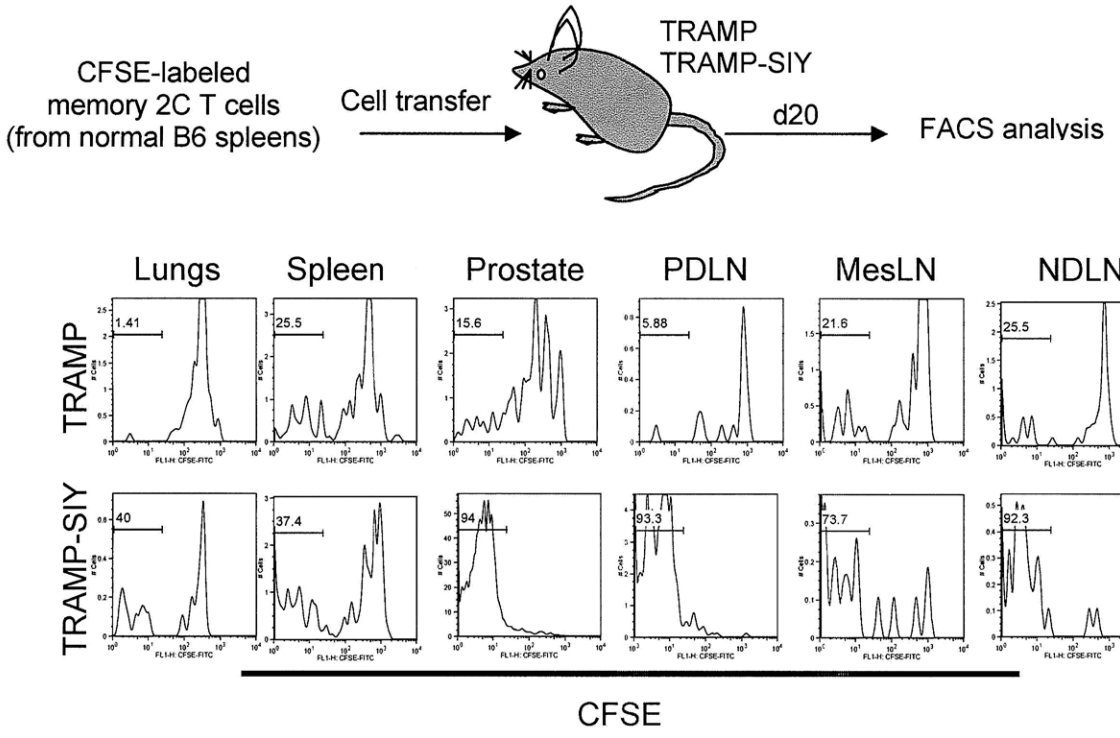
CFSE-labeled
memory 2C T cells
(from normal B6 spleens)
Cell transfer
TRAMP
TRAMP-SIY
d20
FACS analysis
Lungs
Spleen
Prostate
PDLN
MesLN
NDLN
TRAMP
TRAMP-SIY
1.41
25.5
15.6
5.88
21.6
25.5
40
37.4
94
93.3
73.7
92.3
Cells
CFSE

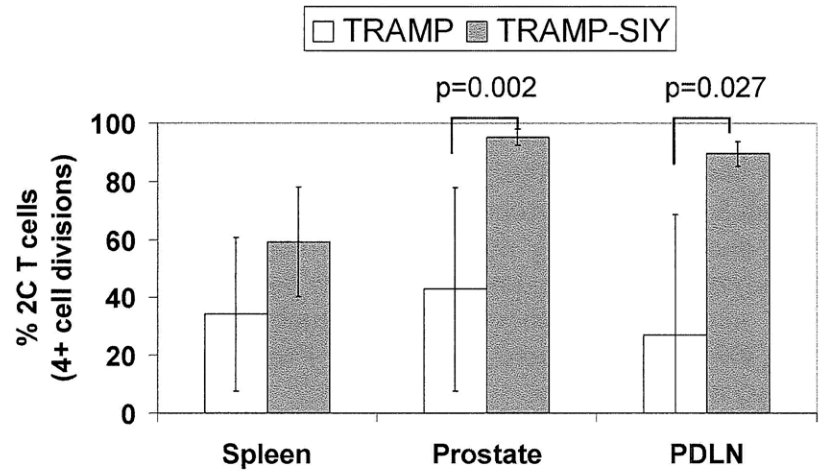
TRAMP
TRAMP-SIY
p=0.002
p=0.027
% 2C T cells
(4+ cell divisions)
100
80
60
40
20
0
Spleen
Prostate
PDLN

Figure 16. Tolerant T cells proliferate extensively in the presence of antigen. Memory 2C (Thy1.1$^+$) T cells were generated and enriched for CD8$^+$ T cells by magnetic negative selection. After enrichment, memory 2C (Thy1.1$^+$) T cells as described in the methods section, were labeled with 5 μM CFSE. About 0.5 x 10^6 memory 2C Thy1.1$^+$ CD8$^+$ T cells were transferred into TRAMP and TRAMP-SIY mice by retroorbital injection. On day 20, tissues from recipient mice were analyzed by flow cytometry. CFSE histogram plots are shown for cells gated on PI negative, Thy1.1$^+$ and CD8$^+$ lymphocytes. The numbers in the histograms indicate the percentage of Thy1.1$^+$ CD8$^+$ cells that have undergone ≥4 rounds of CFSE dilution determined using the FlowJo software proliferation algorithm on TRAMP prostate and applying it to other tissues. The bar chart shows the average and standard deviation of all mice analyzed (n≥6 per group). The p-values p≤0.05 from student t-tests comparing TRAMP to TRAMP-SIY are also shown. Each experiment was performed at least thrice.

To determine the cellular turnover rate of persisting 2C T cells in TRAMP and TRAMP-SIY mice, we also performed 5'-bromo-2'-deoxyruridine (BrdU) incorporation experiments. This method has been used by several groups including Tough and Sprent (1994) to determine the turnover of memory T cells [7, 8]. We reasoned that persisting T cells would have been formed by 30 days post-infection (dpi). Therefore, mice received BrdU starting at 30 dpi. For short pulse experiments, mice were injected intraperitoneally once with 2 mg BrdU and analyzed 36 hr later i.e. 32 dpi. Alternatively, for longer pulse-chase experiments, TRAMP and TRAMP-SIY mice received 0.8 mg/ml BrdU in drinking water for 16-days i.e. 46 dpi (Fig. 17), and then resumed regular drinking water (without BrdU) for another two weeks (60 dpi). BrdU is a thymidine analog incorporated into the DNA of proliferating cells and is detected by intracellular staining using a BrdU antibody [7]. BrdU was administered in an opaque water bottle and the water was changed daily because of reported BrdU sensitivity to light [7]. At 32 dpi, 39 dpi, 46 dpi and 60 dpi, tissues from TRAMP and TRAMP-SIY mice were analyzed for 2C Thy1.1$^+$ CD8$^+$ T cells that had incorporated BrdU. In agreement with the CFSE results, the proliferation rate of 2C T cells from TRAMP and TRAMP-SIY spleens assessed by BrdU incorporation are similar (Figs. 17 and 18). A short-term pulse (32 dpi analysis) did not show any significant difference in BrdU incorporation for 2C T cells in the prostates of either mouse group (Fig. 18). Using the benchmark from Tough and Sprent (2004) [7, 8], tolerant TRAMP-SIY and non-tolerant TRAMP 2C T cells in the prostate undergo rapid turnover (with 40 to 80% incorporating BrdU) between 39 dpi to 60 dpi (Fig. 18). In the PDLN, TRAMP-SIY 2C T cells proliferate at consistently higher levels than TRAMP 2C T cells (Fig. 18). This BrdU results from the PDLN (Fig. 18) are in agreement with the analyses performed using CFSE-labeled cells transferred into TRAMP-SIY recipients and processed on day-20 after the transfer (Fig. 16). These results

suggest that tolerant 2C T cells persist by extensive proliferation due to the presence of antigen in the prostate.

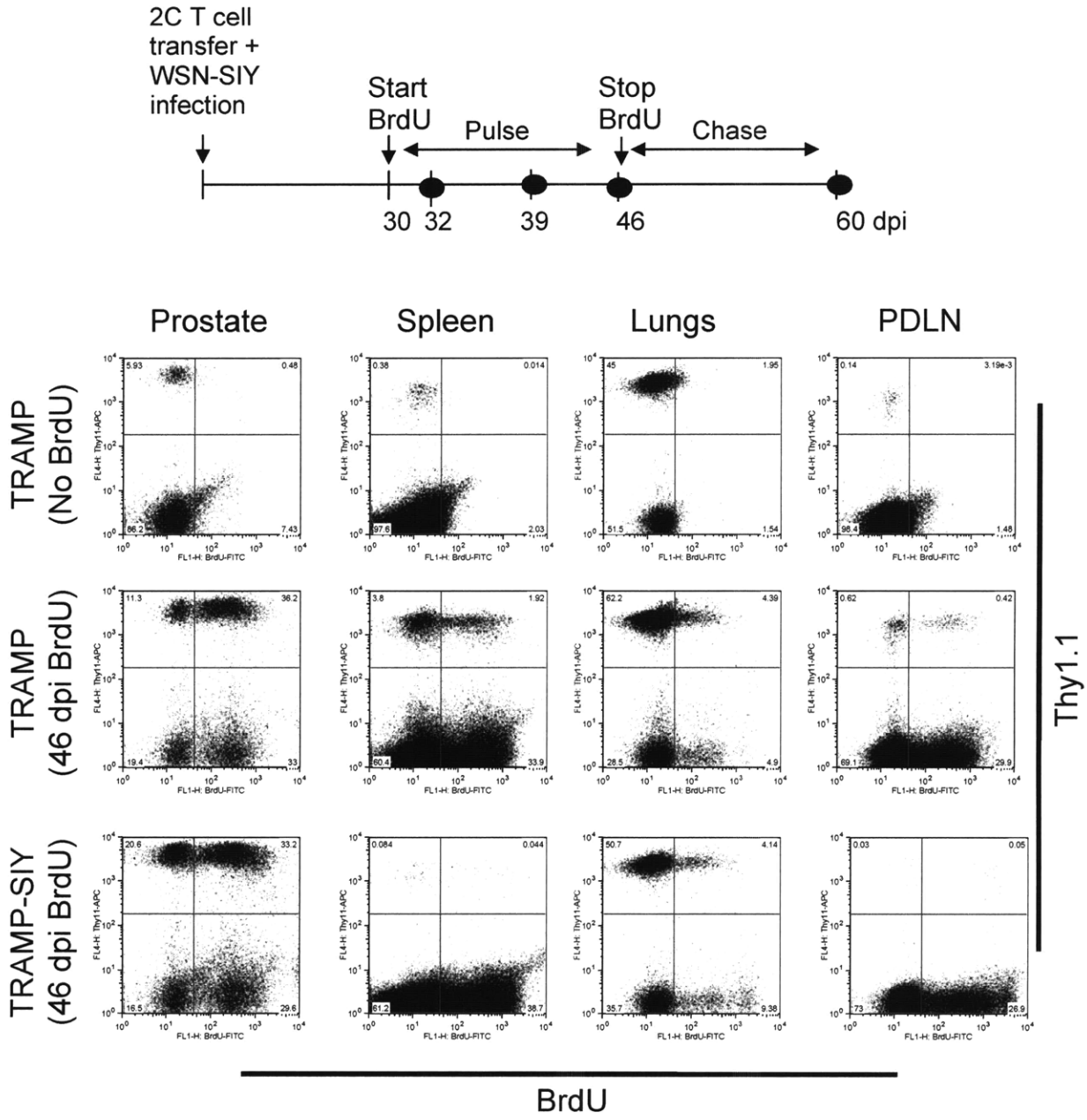
2C T cell transfer + WSN-SIY infection
Start BrdU
Pulse
Stop BrdU
Chase
30
32
39
46
60 dpi
Prostate
Spleen
Lungs
PDLN
TRAMP (No BrdU)
TRAMP (46 dpi BrdU)
TRAMP-SIY (46 dpi BrdU)
Thy1.1
BrdU

Figure 17. Persisting tolerant T cells incorporate BrdU.
TRAMP and TRAMP-SIY mice were infected and received 2C Thy1.1^{+} cells as previously described in other experiments. At 30 dpi, mice were either injected with 2 mg BrdU i.p. (from BD Biosciences BrdU Flow kit) for analysis 36-hr later i.e. the 32 dpi data points. For longer time points (46 and 60 dpi), mice received 0.8 mg/ml BrdU in drinking water that was changed daily for 16-days. On the day of analyses, tissues from TRAMP and TRAMP-SIY mice were processed and stained with Thy1.1-APC, CD8α-PE, and BrdU-FITC antibodies following the manufacturer's protocol (BD Biosciences BrdU Flow kit Cat. #559619). Flow cytometry analysis involved gating on CD8^{+} lymphocytes followed by placing quadrants for Thy1.1 versus BrdU^{+} cells. A 2C recipient TRAMP mouse that did not receive BrdU was also analyzed on the day of staining as a negative control. The FACS plots shows an example of a FlowJo analysis at 46 dpi.

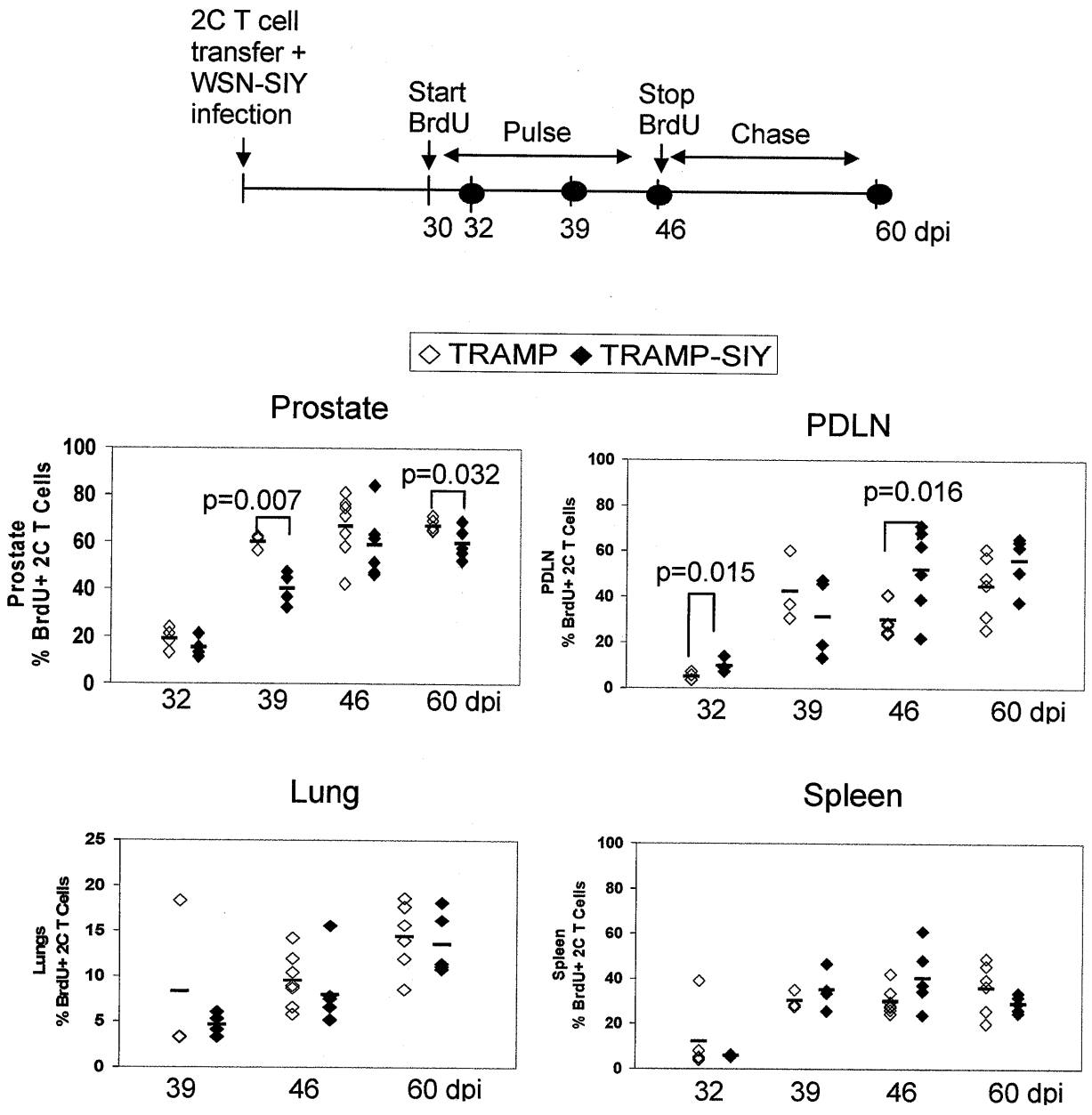
2C T cell transfer + WSN-SIY infection
Start BrdU
Pulse
Stop BrdU
Chase
30 32 39 46 60 dpi
◇ TRAMP ◆ TRAMP-SIY
Prostate
% BrdU+ 2C T Cells
p=0.007
p=0.032
32 39 46 60 dpi
PDLN
% BrdU+ 2C T Cells
p=0.015
p=0.016
32 39 46 60 dpi
Lung
Lungs
% BrdU+ 2C T Cells
39 46 60 dpi
Spleen
Spleen
% BrdU+ 2C T Cells
32 39 46 60 dpi

Figure 18. Persisting tolerant T cells proliferate extensively *in vivo*.
TRAMP and TRAMP-SIY mice were infected and received 2C Thy1.1$^+$ cells as described in the methods section. At 30 dpi, mice were either injected with 2 mg BrdU i.p. for analysis 36-hr later i.e. the 32 dpi data points. For longer time points (39, 46 and 60 dpi), mice received 0.8 mg/ml BrdU in drinking water that was changed daily. On the day of analyses, tissues from TRAMP and TRAMP-SIY mice were processed and stained with Thy1.1-APC, CD8α-PE, and BrdU-FITC antibodies for analysis by flow cytometry. The analysis involved gating on CD8$^+$ lymphocytes followed by placing quadrants for Thy1.1 versus BrdU$^+$ cells. A 2C recipient TRAMP mouse that did not receive BrdU was also analyzed on the day of staining as a negative control. The percentage of Thy1.1$^+$ CD8$^+$ cells that are BrdU$^+$ was determined using the equation % BrdU$^+$ 2C T cells = (BrdU$^+$ Thy1.1$^+$ CD8$^+$ cells/ Total Thy1.1$^+$ CD8$^+$ cells) x 100%. Each shape represents one mouse. Solid black bars indicate the average of the data for each mouse model ($n \geq 4$ per group). The p-values for cell numbers from student t-tests comparing TRAMP to TRAMP-SIY $p<0.05$ are shown.

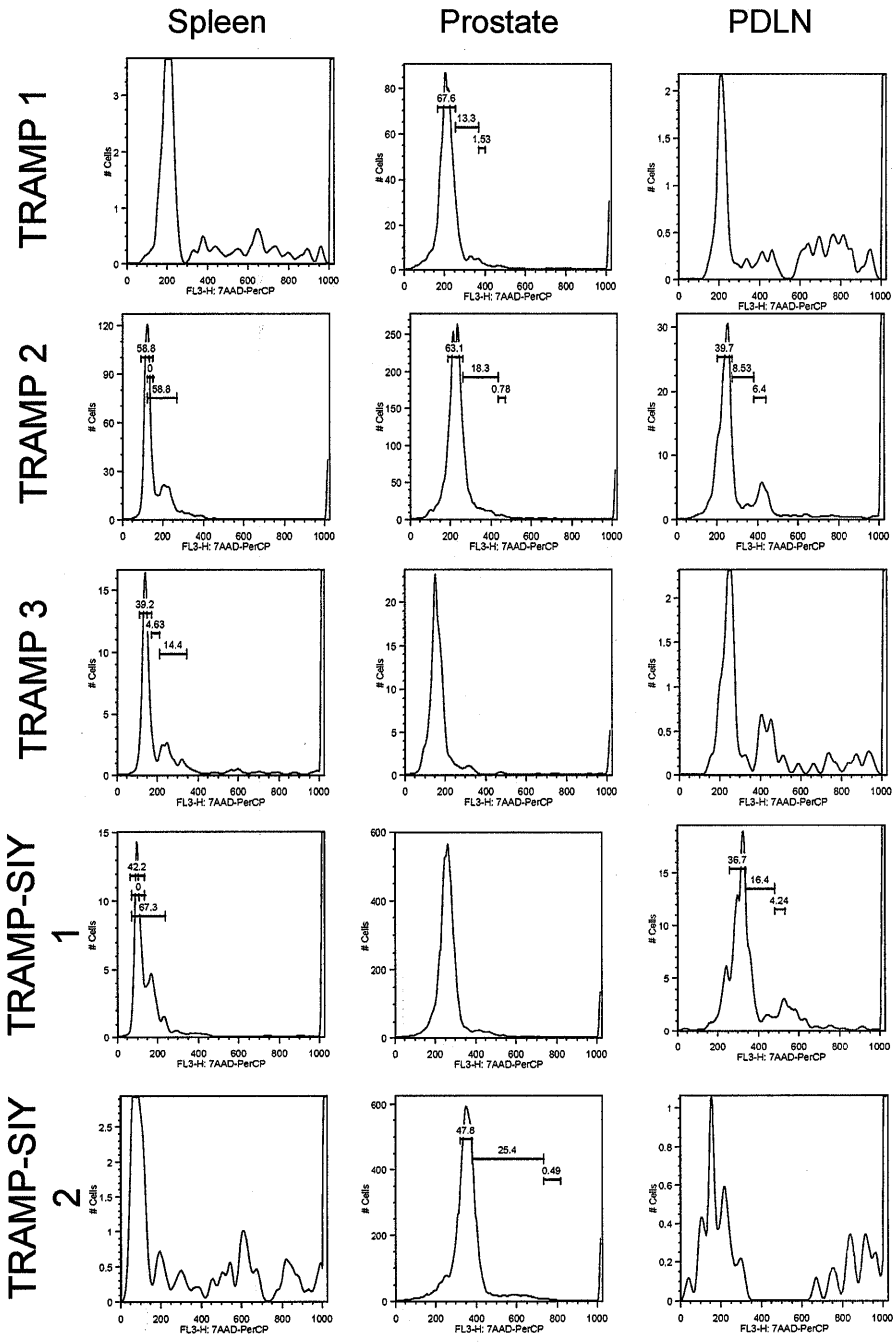
Spleen
Prostate
PDLN
TRAMP 1
TRAMP 2
TRAMP 3
TRAMP-SIY 1
TRAMP-SIY 2
Cells
FL3-H: 7AAD-PerCP
67.6
13.3
1.53
58.8
0
58.8
63.1
18.3
0.78
39.7
8.53
6.4
38.2
4.63
14.4
42.2
0
67.3
36.7
16.4
4.24
47.8
25.4
0.49

Figure 19. Tolerant T cells proliferate *in situ*.
TRAMP and TRAMP-SIY mice were infected and received 2C Thy1.1^{+} cells as described in the methods section. At 85 dpi, tissues from TRAMP and TRAMP-SIY mice were processed and stained with Thy1.1-FITC and CD8α-APC antibodies followed by the protocol for 7-AAD staining given in the BD Biosciences BrdU Flow kit. Details are given in the methods section. The flow cytometry analysis involved gating on Thy1.1 $^{+}$ CD8^{+} lymphocytes followed by generating 7-AAD histograms. Gates for G0/G1, S, and G2/M indicated in some histograms was obtained by applying the Dean-Jett-Fox cell cycle model in the FlowJo software to each histogram. The program would not generate gates for the others.

2.4.2. Discussion

Cell proliferation is one of the main mechanisms contributing to persistence of T cells in the tolerizing TRAMP-SIY prostate. Analysis of CFSE-labeled T cells show that tolerant 2C T cells proliferate extensively in the presence of antigen (Figs. 14 to 16). BrdU pulse-chase experiments analyzing persisting 2C T cells in the prostate showed rapid turnover of both tolerant and non-tolerant 2C T cells (Fig. 18). Staining of cells from the prostate and PDLN with 7-aminoactinomycin D (7-AAD) showed some tolerant T cells in the S and G2/M phase of the cell cycle (Fig. 19). This data further supports the fact that tolerant T cells can persist by proliferating *in vivo*. This is contrast to reports that tolerant T cells are characterized by impaired proliferation. Local immunosuppression has been observed in human patients with esophageal squamous cancer [9]. Even when systemic immunity was preserved, only lymphocytes extracted from the tumor-draining lymph nodes of esophageal squamous cancer patients exhibited impaired proliferation and cytolytic function *in vitro* [9]. However, lymphocytes from draining lymph nodes of some patients with esophagogastric adenocarcinoma in the same report actually showed increased proliferative capacity after stimulation with phytohemaglutinin (PHA) compared to cells from the reference (non-draining) lymph nodes [9]. The authors do not show whether these extensively proliferating cells from a different form of cancer also had impaired cytolytic function. Studies evaluating proliferation and cytolytic activity are often carried out *in vitro* [9, 10] and may not accurately reflect tolerant T cell response to antigen in the tolerizing environment *in vivo*. The use of a mouse model that tolerizes antigen-specific T cells locally in the tumor environment has allowed use to investigate and reveal the proliferative ability of tolerant T cells *in vivo*.

2.5. Effect of Change in Survival/Death Rate on T Cell Persistence

2.5.1. Results

One of the other reported characteristics of tolerant $CD8^+$ T cells is increased sensitivity to cell death [10]. To assess cell death by apoptosis, Annexin-V, Caspase-3 and Fas (CD95) expression in 2C T cells were examined. The Annexin V assay showed no difference in the percentages of apoptotic or dead cells in 2C T cells from TRAMP and TRAMP-SIY mice (Fig. 20). It is possible that this assay is not sensitive enough to detect slight differences in apoptotic rates. As a result, I decided to investigate expression of upstream molecules, Caspase-3 and Fas, in the apoptotic pathway. Intracellular staining for caspase-3 expression only showed a borderline difference ($p=0.05$); TRAMP-SIY prostate had a higher percentage of Caspase-3^+ 2C T cells than TRAMP prostate (Fig. 21). Fas is an upstream inductor of apoptosis which had been identified as one of the differentially expressed genes in a PCR Superarray screen. The Fas transcript levels were about 15-fold greater in 2C T cells from TRAMP-SIY compared to those from TRAMP prostate 30 dpi (Fig. 22). Using flow cytometry, there is no difference in the percentages of 2C T cells expressing Fas protein (Fig. 23) between TRAMP and TRAMP-SIY mice.

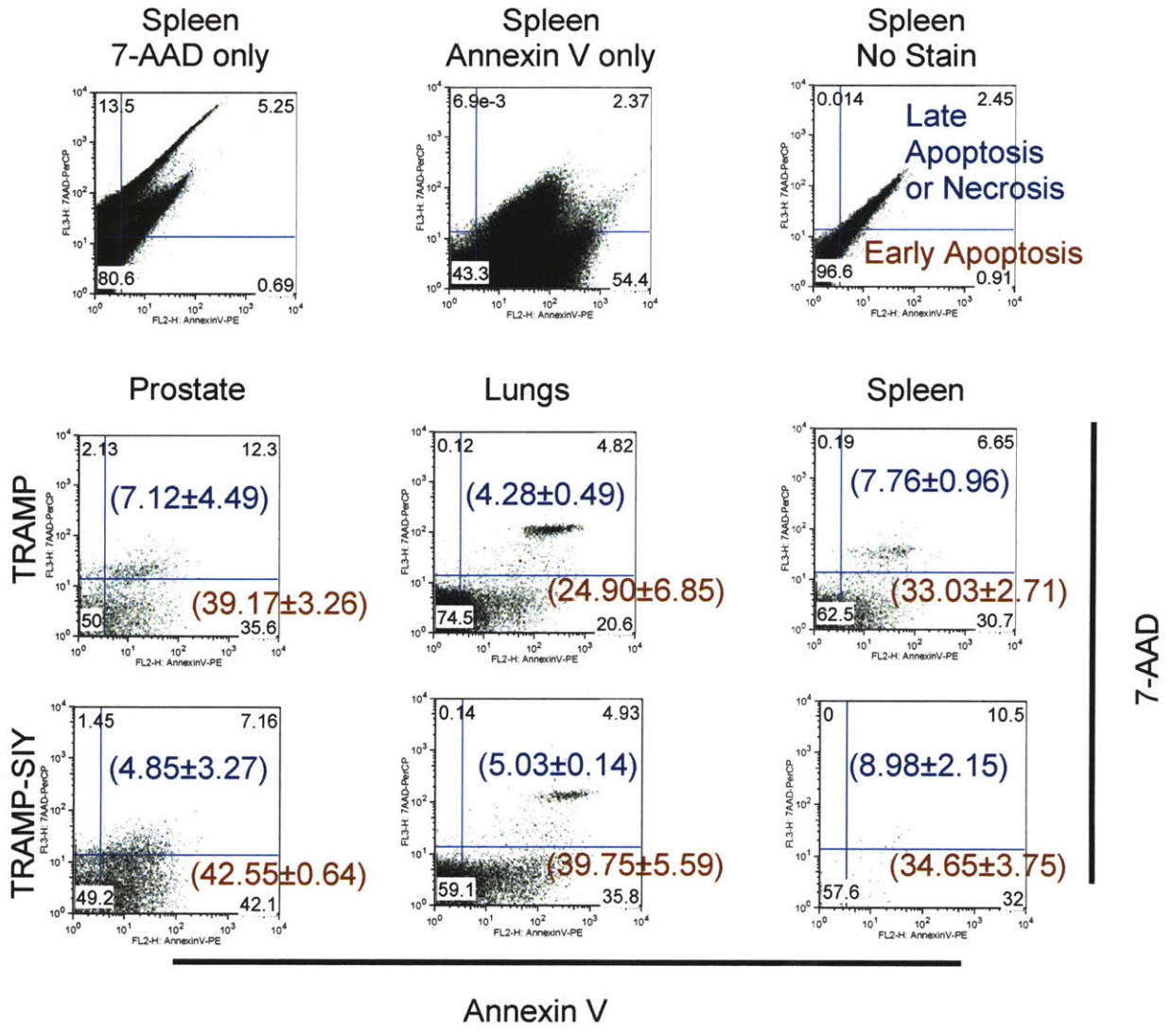

Figure 20. No significant difference in Annexin V/7-AAD expression between 2C T cells from TRAMP and TRAMP-SIY.

Tissues from TRAMP and TRAMP-SIY mice 46 dpi were processed as previously described. (See Methods section for details.) Cells were stained with Thy1.1, CD8α, Annexin-V and 7-AAD. Then the stained cells were analyzed by flow cytometry. The FlowJo analysis involved gating on 2C Thy1.1^{+} CD8^{+} cells, and then drawing quadrants for Annexin V versus 7-AAD cells. TRAMP spleen samples that were not stained or singly stained with either Annexin-V or 7-AAD were used to determine quadrant gates. The percentage (average ± standard deviation) of 2C T cells that are Annexin-V^{Pos} 7-AAD^{Neg} cells (right lower quadrant) and Annexin-V^{Pos} 7-AAD^{Pos} (right upper quadrant) are given. Statistical values are from analysis of two TRAMP-SIY and three TRAMP mice.

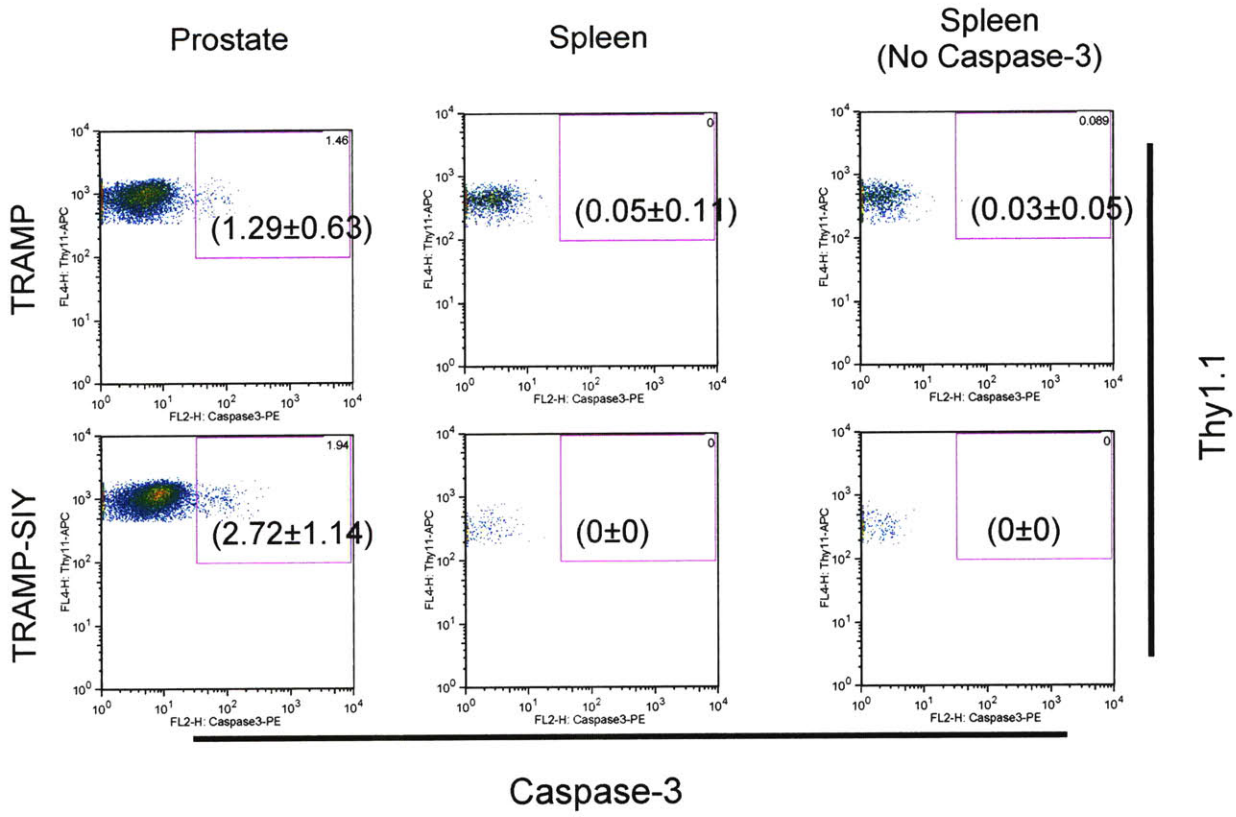

Figure 21. Borderline difference in Caspase-3 expression between 2C T cells from TRAMP and TRAMP-SIY prostate.

Tissues from TRAMP and TRAMP-SIY mice 85 dpi were processed and stained for Caspase-3 expression as described in the Methods section. The FlowJo analysis involved gating on Thy1.1$^+$ CD8$^+$ cells, followed by FSC versus SSC gating to select lymphocytes, and finally plotting Thy1.1 versus Caspase-3. Spleens and prostate samples that were not stained with Caspase-3 were used to determine Thy1.1 versus Caspase-3 gate shown. The percentage (average ± standard deviation) of Thy1.1$^+$ Capase-3$^+$ are given for n = 3 -5 mice per group. The p-value from student t-tests comparing five TRAMP-SIY and four TRAMP prostates is p=0.05. P-values for other tissues are >0.2.

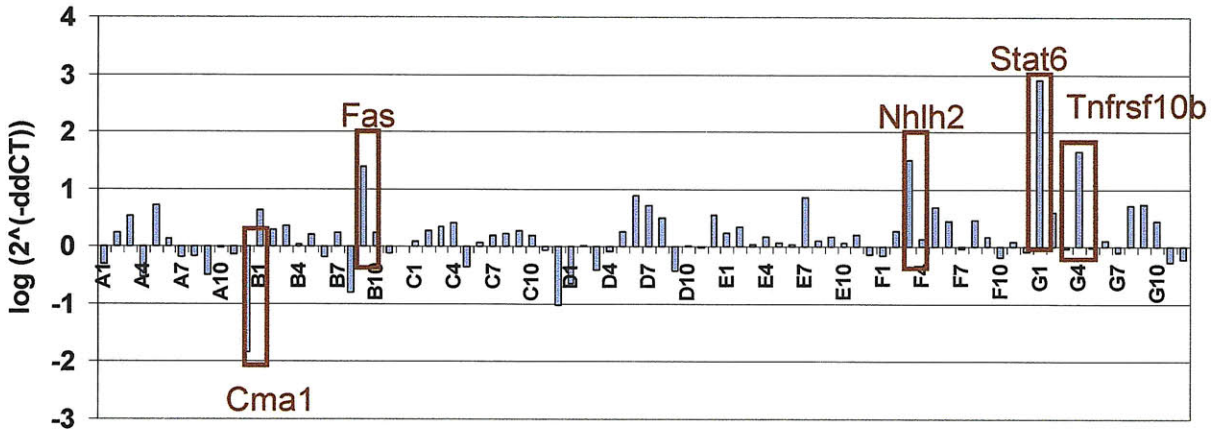

Figure 22. Fas is among the genes differentially expressed between 2C T cells from TRAMP and TRAMP-SIY prostate.

Fas is among genes differentially expressed (> 10-fold) in 2C T cells sorted from TRAMP and TRAMP-SIY prostates 30 dpi in a PCR superarray screen for genes involved in tolerance. Results show relative RNA levels of TRAMP-SIY to the same gene in TRAMP. All were normalized to internal controls given in the Superarray. Experiments were performed by Eileen Higham and Ching-Hung Shen (Chen Lab).

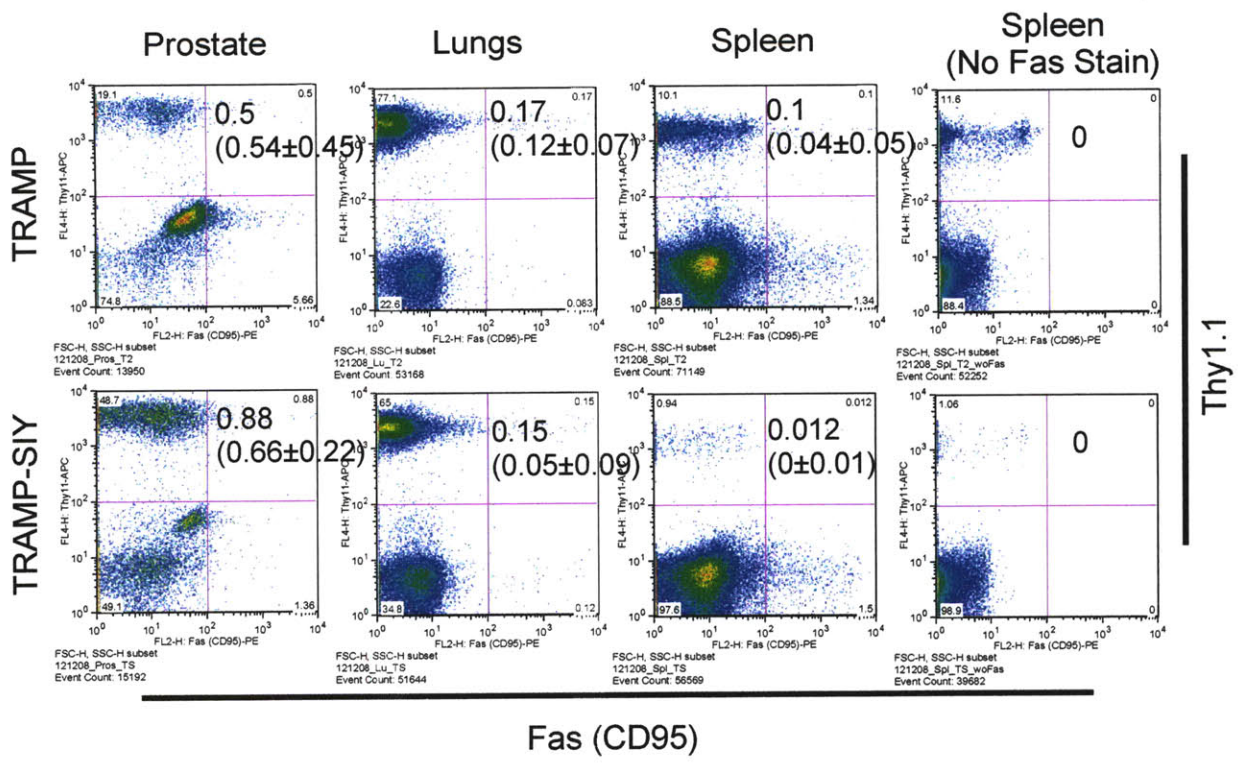

Figure 23. No difference in Fas protein expression between 2C T cells from TRAMP and TRAMP-SIY.

Tissues from TRAMP and TRAMP-SIY mice 39 dpi were processed as previously described. (See Methods section for details.) Cells were stained with Thy1.1, CD8α, and Fas (CD95) antibodies, as well as PI to exclude dead cells. Flow cytometry analysis involved gating on PI^{Neg} $CD8^{+}$ lymphocytes followed by placing quadrants for Thy1.1 versus Fas cells. Spleen samples that were not stained with Fas were used to determine quadrant gates. The percentage (average ± standard deviation) of 2C $Thy1.1^{+}$ $CD8^{+}$ T cells that are Fas^{+} cells (right upper quadrant) are given. Statistical values are from analysis of three TRAMP-SIY and four TRAMP mice.

2.5.2. Discussion

Thus far, our cell death assays have not been sensitive enough to detect slight significant differences in apoptotic rates between freshly isolated tolerant and non-tolerant T cells (Figs. 20, 21 and 23). Annexin V is a protein that binds to phosphatidyl serine. When cells are dying by apoptosis, they invert their inner membranes, thereby exposing phosphatidyl serine. 7-AAD is a nucleic acid dye that is taken up by dying and dead cells. Combining fluorescently labeled Annexin V and 7-AAD staining, one can identify cells in the early stages of apoptosis which are Annexin V positive and 7-AAD negative, and cells that are in the late stages of apoptosis or dead via necrosis (Annexin V positive and 7-AAD positive). Our assay showed low percentages of apoptotic cells but no statistically significant difference between tolerant cells from TRAMP-SIY compared to non-tolerant cells from TRAMP prostate (Fig. 20). Caspase-3 is one the molecules activated in the cell apoptosis cascade, upstream of the membrane inversion stage detected by Annexin V. By identifying Caspase-3^{+} cells, one might identify cells that are more prone to apoptosis. This assay showed a borderline difference (Fig. 21) indicating that tolerant T cells from the prostate are probably more apoptotic than non-tolerant TRAMP T cells. Fas is an upstream inductor of apoptosis. T cells expressing Fas can engage other cells including other T cells that have the Fas ligand (FasL) which leads to a cascade of pro-apoptotic events that result in death by apoptosis of the Fas-expressing cell [11]. However, there was no difference in Fas protein expression (Fig. 23) even though RNA expression levels had indicated about a 15-fold difference (Fig. 22) that suggested that tolerant T cells are more susceptible to Fas-induced apoptosis. The inconsistencies in results from the different cell death assays may be due to the varying timepoints when the assays were performed, as well as the tissue's efficient means for clearing apoptotic cells. Our assays are performed at specific timepoints that may not

correspond to the optimal period for detecting apoptotic cells. Apoptotic cells are cleared rapidly from tissues within 24 hr [12]. It is possible that macrophages responsible for engulfing apoptotic cells are performing this process efficiently [12] and the current assays cannot be used to detect slight differences in apoptotic cell numbers.

However, we can still deduce that tolerant T cells in the TRAMP-SIY model seem to have an increased sensitivity to cell death in the presence of antigen. This conclusion is drawn from observing that the proliferation trend (Figs. 16 and 18) does not correlate with the cell number trends (Fig. 4). Figure 4 shows that the number of 2C T cells in the TRAMP-SIY PDLN at 2 mpi are about three-fold less than that in TRAMP PDLN. Yet, both CFSE and BrdU methods reveal extensive proliferation (Figs. 16 and 18) in TRAMP-SIY PDLN. This deduction is in agreement with other reports about the characteristics of tolerant $CD8^+$ T cells [10] in the presence of antigen. In the InsHA transgenic mouse model, Hernandez *et al.* (2001) showed that tolerant Clone 4 $CD8^+$ T cells proliferate locally in the draining lymph nodes and are eventually deleted without any apparent cell trafficking occurring [13]. These results are similar to our observations in the PDLN of the TRAMP-SIY transgenic mouse model. In chronic infection models, fully exhausted T cells exposed to high antigen load are deleted [14] because they are more sensitive to death. Antigen-specific T cells in the TRAMP-SIY model are continuously exposed to SIY antigen [15] which would induce exhaustive proliferation and deletion. An increased sensitivity to cell death in the presence of persistent antigen might therefore be able to explain the perceived impaired proliferation reported about tolerant T cells. This is because tolerant T cells that proliferate extensively, that is incorporate BrdU or ^{3}H-thymidine (a common analog used *in vitro* proliferation assay), could die off more quickly, thereby leaving behind a lower proportion of $BrdU^+$ or $^3H^+$ tolerant T cells. Our results suggest that persistence of tolerant T

cells is driven by extensive proliferation but it is also limited by increased sensitivity of tolerant T cells to cell death in the presence of persistent antigen.

2.6. Materials and Methods

Mice & Viruses: 2C TCR and OT-I TCR transgenic mice on $RAG1^{-/-}$ and B6 backgrounds were maintained at the Massachusetts Institute of Technology (MIT) Animal Care Facility. Congenic 2C TCR Thy1.1 mice were also bred in our facility. OT-I TCR CD45.1 transgenic mice on a $RAG2^{-/-}$ background were a kind donation from Tyler Jacks lab at MIT. Recipient mouse strains (TRAMP, TRAMP-SIY, B6 and B6-SIY), ages 3-8 months old, were also maintained in the MIT facility. In some cases, B6 (C57BL/6) mice were purchased from the Jackson Laboratory (Bar Harbor, ME). Recombinant WSN (H1N1) influenza virus with SIYRYYGL peptide engineered onto the neuraminidase stalk originally constructed by plasmid-based reverse genetics [16] was grown on Madine-Darby Canine Kidney (MDCK) cells. Similar methods were used to produce WSN virus engineered with SIINFEKL (OVA) peptide sequence.

Antibodies & Reagents: Biotinylated 1B2 monoclonal antibody was produced in-house. 1B2 is a monoclonal antibody specific for the 2C TCR. Other anti-mouse monoclonal antibodies, CD16/32 (Fc blocker), Streptavidin-APC, CD8α-PerCP-Cy5.5 clone 53-6.7, CD8α-APC, CD8α-PE, CD8α-FITC, CD90.1(Thy1.1)-APC, CD90.1(Thy1.1)-FITC, vβ5-FITC, vα2-PE, CD127(IL-7Rα)-FITC Clone A7R34, PD-1-PE clone J43, CD62L-PE, CCR7-PE, CD184(CXCR4)-PE, Annexin-V-PE and CD95(Fas)-PE for flow cytometry studies were purchased from BioLegend (San Diego, CA), BD Biosciences (San Jose, CA) or eBioscience (San Diego, CA). 7-AAD was obtained from BD Biosciences BrdU Flow kit. Cleaved Caspase-3 antibody (#9661) was purchased from Cell Signaling Technology (Danvers, MA) and the secondary goat anti-rabbit IgG-PE antibody was obtained from Caltag. Pierce Chemical 4',6-

diamidino-2-phenylindole hydrochloride (DAPI) PI46190 was purchased from VWR (USA). Propidium iodide P4170 (PI) was purchased from Sigma-Aldrich (USA).

Lymphocyte Isolation (Lymph Nodes and Spleen): Lymph nodes (LN) and spleens from 2C RAG1$^{-/-}$ mice were extracted, one mouse at a time, after carbon dioxide (CO_2) inhalation. The sacrificed animal's fur was sterilized with 70% ethanol. Dissected LN and spleens were stored on ice in 4 ml of RPMI 1640 media supplemented with 5% fetal bovine serum and 10 mM HEPES buffer solution (RPMI complete). After dissection, the LN were gently mashed between rough surfaces of two microscope slides immersed in RPMI complete to release lymphocytes. Cell suspensions were filtered through an 80-μm nylon mesh (Sefar) and transferred into 15-ml BD Falcon tubes kept on ice. A similar procedure was followed for cell isolation from the spleen. Splenocytes used for flow cytometry analysis were further purified by a red blood cell (RBC) lysis step after grinding.

Cell Transfer & Influenza Infection: Cells isolated from 2C lymph nodes and spleens as described above were resuspended in Hank's Balanced Salt Solution (HBSS, serum-free media), filtered and kept on ice. Following approved animal care facility protocol, recipient mice were anesthetized with 2.5% Avertin and intranasally infected with 100 pfu of WSN-SIY or 100 pfu WSN-SIIN Influenza virus suspended in 50 μl. Still under anesthesia, infected mice were immediately injected retroorbitally with 1-2 x 10^6 total live cells suspended in 100 μl HBSS.

Memory Cell Transfer & Carboxyfluorescein Succinymidyl Ester (CFSE) Proliferation Studies: B6 mice received 2C Thy1.1$^+$ T cells retroorbitally and were intranasally infected with

WSN-SIY virus as described above. One-month after infection, the spleens of these mice were extracted and processed following the procedure above. The Miltenyi Biotec MACS CD8α^+ T cell isolation kit (Cat. #130-090-859) was used to enrich for $CD8^+$ T cells. For the CFSE proliferation studies, after enrichment, the cells were stained with 5 μM CFSE from Invitrogen CellTrace™ CFSE cell proliferation kit (Cat. #C34554) following the manufacturer's instructions. A portion of the enriched cell suspension (with or without CFSE) was analyzed by flow cytometry to determine the number of 2C Thy1.1$^+$ $CD8^+$ T cells obtained after enrichment. Then, the cells were resuspended in serum-free HBSS media such that each recipient mouse received approximately $0.5x10^6$ 2C Thy1.1$^+$ $CD8^+$ T cells in 100 μl of HBSS. Mice were anesthetized with 2.5% Avertin before performing any retroorbital cell transfer injections.

Lymphocyte Extraction (Prostate and Lungs): Prostate lobes were extracted by microdissection following procedures in Current Protocols in Immunology [1]. Briefly, the urogenital system from each mouse was extracted after CO_2 inhalation, and transferred into 15-ml of RPMI complete on ice. A dissecting microscope was used to identify prostate lobes in the urogenital system placed on cold 1x PBS. The prostate lobes were subsequently removed using tweezers and transferred into 2-ml of 1 mg/ml Collagenase A (from Roche) in RPMI complete solution. The tissue was digested for about 45 min in a 37°C water bath, vortexing at 15-20 min intervals. Then, digested tissues were gently mashed between rough surfaces of two microscope slides immersed in RPMI complete to release lymphocytes. Cell suspensions were filtered through an 80-μm nylon mesh (Sefar) and transferred into 15-ml Falcon tubes kept on ice.

To extract cells from the lungs, each specimen was ground through a cell strainer in 10 ml of RPMI complete. Then the suspension was centrifuged and resuspended in 2 ml of 2 mg/ml

Collagenase A (from Roche) in RPMI complete solution. The tissue was digested for 1 hr in a 37°C water bath, vortexing at 15-20 min intervals. An equal volume of 70% Percoll was added to the digest followed by centrifugation at ~2000 rpm for 20 min. Tissue debris and supernatant from lungs were gently aspirated, followed by RBC lysis.

Red Blood Cell (RBC) Lysis: Two milliliters of red blood cell lysis buffer (144 mM ammonium chloride and 17 mM Tris-HCl pH7.4 in distilled deionized water) was added to pellets from spleen and lungs specimens and kept on ice for 2-4 min, vortexing at 2 min intervals. Ten millimeters of RPMI complete was added to stop the lysis. Cell suspensions were centrifuged at ~1200 rpm, resuspended in an appropriate buffer for further analysis, and filtered through a nylon mesh (Sefar) into appropriately labeled tubes kept on ice.

Cell Counting: The total number of viable cells for each tissue specimen was counted using a hemacytometer and tryphan blue exclusion.

Flow Cytometry: Appropriate numbers of counted cells in suspension were transferred into labeled Falcon® round-bottom tubes (FACS tubes), and centrifuged at ~1200 rpm for 5 min. All procedures were performed on ice. Antibodies in FACS buffer (1% BSA and 0.1% sodium azide in 1x PBS) were used for staining following the manufacturer's recommended range. Purified anti-mouse CD16/32 (BioLegend), the Fc blocker, was added for 10 min prior to adding the primary antibody. Cells were incubated with the primary biotinylated antibody on ice for 30-45 min, washed and then incubated with the secondary and fluorophore-conjugated antibodies for 15-20 min while covered with foil paper. The cells were washed again, and resuspended in 50-

200 μl of DAPI or 1 μg/ml propidium iodide solution except where indicated. Note that cells stained with CCR7-PE (from eBioscience) were incubated in a 37°C water bath following optimized conditions recommended in the manufacturer's instructions. Samples were sorted using a BD™ LSRII or BD FACSCalibur™ flow cytometer (BD Biosciences). Further data analysis was carried out using FlowJo software (Tree Star, Inc., Ashland, OR).

Bromodeoxyuridine (BrdU) Proliferation: Mice received 2C T cells retroorbitally and were intranasally infected with WSN-SIY virus as described above. Thirty days later, they were fed 0.8 mg/ml BrdU in their drinking water kept in opaque bottles. Their BrdU water was changed daily for up to 16 days. Control mice received water without BrdU. BrdU administration was stopped after 16 days (46 dpi), and regular drinking water was resumed for all mice. For short-term pulse experiments, mice were injected intraperitoneally (i.p.) with 200 μl of a 10 mg/ml stock available from the BD Biosciences BrdU Flow kit (Cat. #559619). Therefore, each mouse received one injection of 2 mg BrdU i.p. Tissues from these mice were analyzed 36 hr after the injection. On the day of analyses, tissue harvest and processing procedures described above were followed. 2C T cells that incorporated BrdU was determined by flow cytometry using the BD Biosciences BrdU Flow kit (Cat. #559619). Antibody volumes suggested by the manufacturer were adjusted to 100 μl for each sample (1:100 dilutions). Further data analysis was carried out using FlowJo software and Microsoft Excel spreadsheet functions. The percentage of 2C T cells that incorporated BrdU in each tissues (% BrdU+ 2C T cells) was calculated as % BrdU+ 2C T cells = ($BrdU^+$ $Thy1.1^+$ $CD8^+$ cells/ Total $Thy1.1^+$ $CD8^+$ cells) x 100%.

7-aminoactinomycin D (7-AAD) Cell Cycle Analysis: Mice received 2C T cells retroorbitally and were intranasally infected with WSN-SIY virus as described above. Eighty-five days later, tissues from these mice were processed for extraction of lymphocytes as previously described. These cells were stained with Thy1.1-FITC and CD8α-APC antibodies, fixed and permeabilized using the BD Biosciences BrdU Flow kit (Cat. #559619). The steps for BrdU staining were omitted. Following the manufacturer's instructions, 100 µl of 7-AAD in BrdU kit staining buffer was added to each sample (i.e. 20 µl 7-AAD and 80 µl buffer per sample). Further data analysis was carried out using the Dean-Jett-Fox cell cycle model in the FlowJo software.

Caspase-3 intracellular staining: Freshly isolated cell suspensions were prepared as described above. The procedure for Caspase-3 staining was performed following the instructions from the manufacturer, Cell Signaling Technology which is briefly described here. Cells were stained with Fc blocker, Thy1.1-APC and CD8α-FITC antibodies. Then the cells were fixed with 1 ml of 3.7% of paraformaldehyde at 37°C for 10 min, washed with 1x PBS and then permeabilized with cold 90% methanol on ice for 30 min. Cells were washed with wash buffer (5g BSA in 1L of 1x PBS) and then stained with Caspase-3 following recommended instructions by the manufacturer. Controls did not receive Caspase-3. After incubation at room temperature (RT) for 1 hr, cells were washed and stained with the secondary goat anti-rabbit IgG-PE antibody for 30 min at RT. Again the cells were washed and resuspended in wash buffer ready for analysis by the BD FACSCalibur™ flow cytometer (BD Biosciences). Further data analysis was carried out using FlowJo software (Tree Star, Inc., Ashland, OR).

Statistical Analyses: All p-values are from unpaired two-tailed equal variance Student's t-Tests.

2.7. References

(1) Hurwitz, A. A.; Foster, B. A.; Allison, J. P.; Greenberg, N. M.; Kwon, E. D. In *The TRAMP Mouse as a Model for Prostate Cancer;* Current Protocols in Immunology; John Wiley & Sons, Inc.: 2001; pp 20.5.1-20.5.23.

(2) Shen, C. H.; Ge, Q.; Talay, O.; Eisen, H. N.; Garcia-Sastre, A.; Chen, J. Loss of IL-7R and IL-15R is Associated with Disappearance of Memory T Cells in Respiratory Tract Following Influenza Infection. *J. Immunol.* **2008**, *180*.

(3) Bai, A.; Higham, E.; Eisen, H. N.; Wittrup, K. D.; Chen, J. Rapid Tolerization of Virus-Activated Tumor-Specific CD8+ T Cells in Prostate Tumors of TRAMP Mice. *Proc. Natl. Acad. Sci. U. S. A.* **2008**, *105*, 13003-13008.

(4) Bromley, S. K.; Thomas, S. Y.; Luster, A. D. Chemokine Receptor CCR7 Guides T Cell Exit from Peripheral Tissues and Entry into Afferent Lymphatics. *Nat. Immunol.* **2005**, *6*, 895-901.

(5) Gallatin, W. M.; Weissman, I. L.; Butcher, E. C. A Cell-Surface Molecule Involved in Organ-Specific Homing of Lymphocytes. 1983. *J. Immunol.* **2006**, *177*, 5-9.

(6) Kaech, S. M.; Tan, J. T.; Wherry, E. J.; Konieczny, B. T.; Surh, C. D.; Ahmed, R. Selective Expression of the Interleukin 7 Receptor Identifies Effector CD8 T Cells that Give Rise to Long-Lived Memory Cells. *Nat. Immunol.* **2003**, *4*, 1191-1198.

(7) Tough, D. F.; Sprent, J.; Stephens, G. L. Measurement of T and B Cell Turnover with Bromodeoxyuridine. *Curr Prot Immunol* **2007**, *Unit 4.7*, 4.7.1.

(8) Tough, D. F.; Sprent, J. Turnover of Naive- and Memory-Phenotype T Cells. *J. Exp. Med.* **1994**, *179*, 1127-1135.

(9) O'Sullivan, G. C.; Corbett, A. R.; Shanahan, F.; Collins, J. K. Regional Immunosuppression in Esophageal Squamous Cancer: Evidence from Functional Studies with Matched Lymph Nodes. *J. Immunol.* **1996**, *157*, 4717-4720.

(10) Dubois, P. M.; Pihlgren, M.; Tomkowiak, M.; Van Mechelen, M.; Marvel, J. Tolerant CD8 T Cells Induced by Multiple Injections of Peptide Antigen show Impaired TCR Signaling and Altered Proliferative Responses in Vitro and in Vivo. *J. Immunol.* **1998**, *161*, 5260-5267.

(11) Krammer, P. H.; Arnold, R.; Lavrik, I. N. Life and Death in Peripheral T Cells. *Nat. Rev. Immunol.* **2007**, *7*, 532-542.

(12) Kerr, J. F.; Wyllie, A. H.; Currie, A. R. Apoptosis: A Basic Biological Phenomenon with Wide-Ranging Implications in Tissue Kinetics. *Br. J. Cancer* **1972**, *26*, 239-257.

(13) Hernandez, J.; Aung, S.; Redmond, W. L.; Sherman, L. A. Phenotypic and Functional Analysis of CD8(+) T Cells Undergoing Peripheral Deletion in Response to Cross-Presentation of Self-Antigen. *J. Exp. Med.* **2001**, *194*, 707-717.

(14) Wherry, E. J.; Blattman, J. N.; Murali-Krishna, K.; van der Most, R.; Ahmed, R. Viral Persistence Alters CD8 T-Cell Immunodominance and Tissue Distribution and Results in Distinct Stages of Functional Impairment. *J. Virol.* **2003**, *77*, 4911-4927.

(15) Zheng, X.; Gao, J. X.; Zhang, H.; Geiger, T. L.; Liu, Y.; Zheng, P. Clonal Deletion of Simian Virus 40 Large T Antigen-Specific T Cells in the Transgenic Adenocarcinoma of Mouse Prostate Mice: An Important Role for Clonal Deletion in Shaping the Repertoire of T Cells Specific for Antigens Overexpressed in Solid Tumors. *J. Immunol.* **2002**, *169*, 4761-4769.

(16) Fodor, E.; Devenish, L.; Engelhardt, O. G.; Palese, P.; Brownlee, G. G.; Garcia-Sastre, A. Rescue of Influenza A Virus from Recombinant DNA. *J. Virol.* **1999**, *73*, 9679-9682.

CHAPTER 3

THE EFFECT OF ANTIGEN IN T CELL PERSISTENCE

3.1. Summary

This chapter discusses the effect of antigen on T cell persistence. From the results described in the previous chapters, one sees that antigen induces extensive proliferation of antigen-specific T cells *in vivo* even when these cells are in a tolerizing environment. Interestingly the presence of antigen also leads to depletion of antigen-specific T cells from tissues with no or lower levels of antigen such as the spleen. This depletion correlates with low levels of IL-7Rα. These combined effects lead to the perceived preferential persistence of antigen-specific T cells in TRAMP-SIY prostate. Therefore, the presence of antigen is one of the molecular factors contributing to T cell persistence in a tolerizing tumor environment.

3.2. Introduction

The fate of T cells after antigen encounter is variable depending on the amount of antigen and the strength of costimulatory signal. The signal to T cells about the presence of foreign or aberrant levels of self-antigen in the periphery is 'signal 1'. 'Signal 2' is the costimulatory signals which usually involve B7 molecules signaling [1]. In the presence of both signals, T cells become activated. This activation process occurs in three phases in the draining lymph nodes and takes about 48 hr with multiple transient and stable encounters with antigen-presenting cells [2]. The activation process ends with proliferation i.e. clonal expansion of antigen-specific T cells [2]. Activated $CD8^+$ T cells differentiate into effector T cells that can secrete cytokines, granule proteins, and other molecules necessary for their continued expansion and lysis of target cells presenting the antigenic peptide sequence on the appropriate MHC molecule. Typically, a T cell contraction process follows. This contraction is a decline in antigen-specific T cell numbers due to apoptosis. Persisting T cells after this contraction stage are called memory T cells and are maintained by survival cytokines such as IL-7 and IL-15. Memory T cells can be restimulated and expand in response to the same type of antigen initially used to generate them. This narration above briefly describes the process that antigen plays in the generation of functional persisting T cells.

In other cases, inappropriate amounts of antigen stimulation or costimulation leads to T cell tolerance. There are three forms of tolerance in the periphery: (1) anergy, (2) deletion, and (3) suppression by regulatory T cells [1, 3]. Anergic T cells are those generated after antigen stimulation and inadequate costimulation. These cells are unable to secrete IL-2 needed for clonal expansion, and/or unable to perform their effector functions such as lysing target cells. In the second form of peripheral tolerance, T cells experience repeated antigen stimulation, for

example, due to large doses of antigen, and are deleted due to apoptosis. This process is known as activation-induced cell death (AICD), and may be Fas-mediated [1]. The third type of peripheral tolerance is induced by suppressive or regulatory T cells. In some cases, T cells that have encountered antigen suppress the response of other T cells to the same antigen [1].

Published research has mostly focused on the role of antigen in the generation of tolerant T cells but not on its role in maintenance of tolerant T cells. Several groups, including ours, have shown that $CD8^+$ T cells infiltrate tumor sites. The fate of these T cells range from being functional i.e. able to eradicate tumors, to the different forms of peripheral tolerance described. T cells in the TRAMP-SIY prostate appear to be anergic and persisting. This chapter discusses the role of antigen in the persistence of antigen-specific tolerant T cells.

3.3. Discussion

The effect of antigen on T cells is usually activation which leads to proliferation, differentiation, anergy and/or apoptosis [1]. Analysis of CFSE-labeled T cells show that tolerant 2C T cells proliferate extensively in the presence of antigen (Figs. 14 to 16). BrdU pulse-chase experiments analyzing persisting 2C T cells in the prostate showed rapid turnover of both tolerant and non-tolerant 2C T cells (Fig. 18).

Functionally impaired persistent T cells are also observed in chronic infection cases [4, 5], and studies in cancer models could aid understanding of what is occurring in chronic infections, and vice-versa. In both cancer and chronic infections, antigen that can be processed and presented to $CD8^+$ T cells, is always present in the tissue. Yet, antigen-specific $CD8^+$ T cells become ineffective against tumor cells and chronic virus-infected cells, but persist in the tissue [4-7]. Recent reports show that some antigen-specific $CD8^+$ memory T cells are dependent on antigen for their persistence [8-10]. For example, Tanchot *et al.* (1997) showed that in the presence of antigen and the correctly matched MHC class I molecules, memory $CD8^+$ T cells proliferate and survive better than experimental groups without antigen [8]. More recently, in cell transfer experiments similar to ours, Shin *et al.* (2007) reported that antigen-specific $CD8^+$ T cells in chronic lymphocytic choriomeningitis virus (LCMV) infected mice persist as a result of extensive proliferation in the presence of antigen [9]. These persisting $CD8^+$ T cells were previously reported to be 'exhausted' or non-functional [4]. Like the persisting non-functional antigen-specific T cells generated in response to chronic LCMV infection [9], persisting T cells in the tolerizing tumor environment are maintained by extensive proliferation in the presence of persistent antigen [9].

Another interesting aspect of the effect of antigen is its role in the depletion of antigen-specific T cells from peripheral tissues such as the spleen (Figs. 4 and 5). In chronic infection models, fully 'exhausted' T cells exposed to high antigen load are deleted [11] because they are more sensitive to death. Antigen-specific T cells in the TRAMP-SIY model are likely to be continuously exposed to SIY antigen because of the leakiness of the probasin promoter [12]. The presence of persistent antigen in the prostate creates a situation of persistent antigen-presentation, possibly by dendritic cells, in SIY antigen-expressing spleens. As a result, 2C T cells are trapped in an "effector" T cell state. In accordance with this state, 2C T cells from the spleens of SIY-expressing mice express low levels of IL-7Rα (Fig. 8). Only mice that lack persistent antigen are able to progress to a memory phenotype of high IL-7Rα levels (Fig. 8) needed for maintaining antigen-specific T cells in the spleen [13]. Kaech *et al.* (2003) showed that antigen-specific T cells with low IL-7Rα levels were more prone to apoptosis [14]. As a result, these cells did not persist [14]. An increased sensitivity to cell death in the presence of persistent antigen might therefore be able to explain the perceived impaired proliferation reported about tolerant T cells. It might also explain the deletion of cells seen in other tissues such as the spleen. Then one might ask "how are cells still persisting in the prostate of SIY antigen expressing mice?" The answer seems to lie in the effect of tumor-related factors that seem to be modulating the cell death effects of antigen. (See the next chapter for more details.)

The results so far show that the presence of antigen (1) drives extensive proliferation of tolerant T cells and (2) correlates with low levels of IL-7Rα in peripheral tissues which make these antigen-specific T cells sensitive to apoptosis. Therefore, persistence of tolerant T cells is driven by extensive proliferation but it is also limited by increased sensitivity of tolerant T cells to cell death in the presence of persistent antigen.

3.4. References

(1) Abbas, A. K.; Lichtman, A. H.; Pober, J. S. In *Cellular and molecular immunology;* W.B. Saunders: Philadelphia, 2000; , pp 553.

(2) Mempel, T. R.; Henrickson, S. E.; Von Andrian, U. H. T-Cell Priming by Dendritic Cells in Lymph Nodes Occurs in Three Distinct Phases. *Nature* **2004**, *427*, 154-159.

(3) Rocha, B.; Grandien, A.; Freitas, A. A. Anergy and Exhaustion are Independent Mechanisms of Peripheral T Cell Tolerance. *J. Exp. Med.* **1995**, *181*, 993-1003.

(4) Zajac, A. J.; Blattman, J. N.; Murali-Krishna, K.; Sourdive, D. J.; Suresh, M.; Altman, J. D.; Ahmed, R. Viral Immune Evasion due to Persistence of Activated T Cells without Effector Function. *J. Exp. Med.* **1998**, *188*, 2205-2213.

(5) Rehermann, B.; Nascimbeni, M. Immunology of Hepatitis B Virus and Hepatitis C Virus Infection. *Nat. Rev. Immunol.* **2005**, *5*, 215-229.

(6) O'Sullivan, G. C.; Corbett, A. R.; Shanahan, F.; Collins, J. K. Regional Immunosuppression in Esophageal Squamous Cancer: Evidence from Functional Studies with Matched Lymph Nodes. *J. Immunol.* **1996**, *157*, 4717-4720.

(7) Overwijk, W. W., et al Tumor Regression and Autoimmunity After Reversal of a Functionally Tolerant State of Self-Reactive CD8+ T Cells. *J. Exp. Med.* **2003**, *198*, 569-580.

(8) Tanchot, C.; Lemonnier, F. A.; Perarnau, B.; Freitas, A. A.; Rocha, B. Differential Requirements for Survival and Proliferation of CD8 Naive Or Memory T Cells. *Science* **1997**, *276*, 2057-2062.

(9) Shin, H.; Blackburn, S. D.; Blattman, J. N.; Wherry, E. J. Viral Antigen and Extensive Division Maintain Virus-Specific CD8 T Cells during Chronic Infection. *J. Exp. Med.* **2007**, *204*, 941-949.

(10) Swanson, P. A.,2nd; Hofstetter, A. R.; Wilson, J. J.; Lukacher, A. E. Cutting Edge: Shift in Antigen Dependence by an Antiviral MHC Class Ib-Restricted CD8 T Cell Response during Persistent Viral Infection. *J. Immunol.* **2009**, *182*, 5198-5202.

(11) Wherry, E. J.; Blattman, J. N.; Murali-Krishna, K.; van der Most, R.; Ahmed, R. Viral Persistence Alters CD8 T-Cell Immunodominance and Tissue Distribution and Results in Distinct Stages of Functional Impairment. *J. Virol.* **2003**, *77*, 4911-4927.

(12) Zheng, X.; Gao, J. X.; Zhang, H.; Geiger, T. L.; Liu, Y.; Zheng, P. Clonal Deletion of Simian Virus 40 Large T Antigen-Specific T Cells in the Transgenic Adenocarcinoma of Mouse Prostate Mice: An Important Role for Clonal Deletion in Shaping the Repertoire of T Cells Specific for Antigens Overexpressed in Solid Tumors. *J. Immunol.* **2002**, *169*, 4761-4769.

(13) Shen, C. H.; Ge, Q.; Talay, O.; Eisen, H. N.; Garcia-Sastre, A.; Chen, J. Loss of IL-7R and IL-15R is Associated with Disappearance of Memory T Cells in Respiratory Tract Following Influenza Infection. *J. Immunol.* **2008**, *180*.

(14) Kaech, S. M.; Tan, J. T.; Wherry, E. J.; Konieczny, B. T.; Surh, C. D.; Ahmed, R. Selective Expression of the Interleukin 7 Receptor Identifies Effector CD8 T Cells that Give Rise to Long-Lived Memory Cells. *Nat. Immunol.* **2003**, *4*, 1191-1198.

CHAPTER 4

THE ROLE OF TUMORIGENIC/TUMOR-RELATED FACTORS IN T CELL PERSISTENCE

4.1. Summary

Analyses of cell numbers per gram of prostate indicate that factors in the tumor environment, other than SIY antigen, contribute to T cell persistence. These factors are currently referred to as tumorigenic or tumor-related factors to reflect the fact that mice analyzed in this study are in their hyperplastic to neoplastic stages of prostate tumor progression before palpable visible tumors can be detected. This chapter shows that these tumor-related factors do not include IL-15 and IL-7 which are cytokines known to support functional memory T cells.

Further analysis is also performed to determine potential candidates supporting T cell persistence. From published microarray data comparing genes expressed in B6 and TRAMP prostates, I identified 12 potential candidates that may support T cell infiltration, proliferation and/or survival. Ten candidates were selected from genes differentially expressed that belong to cytokines, chemokines, growth factors, cadherins or integrins gene ontology classes. These classes were chosen because in general (1) cytokines and growth factors are known to promote cell proliferation, while (2) chemokines, cadherins, and integrins usually have roles in cell migration. The remaining candidates, Survivin and Racgap1, are two genes reported to be differentially expressed between B6 and TRAMP prostate microarray datasets from two different research groups. Further investigation is required to validate expression of these potential candidates and determine whether they have a role in supporting T cell persistence in TRAMP and TRAMP-SIY prostates.

4.2. Introduction

$CD8^+$ T cells infiltrate inflamed tissue and tumors. The presence of $CD8^+$ T cells at the tumor site is often correlated with regression or at least slow progression of tumors in both animal cancer models and human patients [1-3]. The previous chapters have shown that antigen-specific T cells infiltrate and persist in the TRAMP and TRAMP-SIY transgenic prostate cancer models. In addition to antigen, factors from the tumor environment seem to be contributing to T cell persistence. This chapter seeks to explore the role of these tumorigenic/tumor-related factors and to identify molecular candidates supporting persistence of T cells. Some of these candidates could include soluble factors such as IL-15 and IL-7.

Studies in naïve and memory $CD8^+$ T cells show that cytokines such as IL-15, IL-7, IL-2 and their receptors are important for $CD8^+$ T cells' survival and maintenance [4-9]. These cytokines belong to the common-γ chain (γ_c) family of cytokines. They all signal through γ_c but specificity of function is conferred by their unique receptor subunits. IL-15 deficient ($IL\text{-}15^{-/-}$) and $IL\text{-}15R\alpha^{-/-}$ mice have substantially lower numbers of naïve and memory $CD8^+$ T cells compared to wild-type ($IL\text{-}15^{+/+}$) mice [4-6, 10-13]. Marcondes *et al.* (2007) showed that simian immunodeficiency virus, (SIV)-specific $CD8^+$ T cells persisted for over 6 months in the brains of monkeys which had significantly increased levels of IL-15 after SIV, a chronic virus infection [14]. No IL-2 was detected in this virus-infected organ [14]. IL-15 levels did not change at other tissue sites, and lower levels of IL-15 corresponded to loss of SIV-specific T cells [14]. In benign prostatic hyperplasia (BPH) tissues from human patients, inflamed prostate epithelial and stroma cells were shown to express IL-15 and $IL\text{-}15R\alpha$ [15]. This high IL-15 level correlated with increased T cell numbers in the prostate [15]. The authors showed that T cells from BPH prostate showed a dose-dependent proliferative response to IL-15 but they did not assess the function of

the T cells present [15]. More recently however, in a different chronic infection model, Shin *et al.* (2007) demonstrated that persisting non-functional LCMV-specific $CD8^+$ T cells do not depend on IL-7 and IL-15 for their maintenance [16]. No one has revealed if tolerant T cells in a tumor environment persist due to the presence of IL-15, IL-7 or neither cytokine. IL-15 is secreted in a *trans* presentation model [17], that is both IL-15 and IL-15Rα are produced by the same cells [18]. In order for cells to respond to IL-15 signals, IL-15Rα forms a complex with IL-15Rβ and γ_c receptor subunits found on target cells [19]. Therefore signaling through IL-15 is a cell contact-mediated process which results in memory $CD8^+$ T cell proliferation and maintenance. Although current studies show that administering exogenous IL-15/IL-15Rα with T cells during immunotherapy enhances survival of T cells in the recipient [20, 21] and reverses tolerant T cells into functional cells [22, 23], the role of endogenous IL-15 on persistence of T cells in a tolerizing tumor environment has not been clearly defined.

IL-7 and IL-7R contribute to T cell survival by inducing proliferation and preventing apoptosis [6, 24, 25]. Naïve $CD8^+$ T cells proliferate in response to IL-7 both in *vitro* and *in vivo* [6]. In $IL\text{-}7R^{-/-}$ mice, B-cell lymphoma(Bcl)-2 expression is impaired, and correlates with diminished memory $CD8^+$ T cell numbers compared to $IL\text{-}7R^{+/+}$ mice [6]. Bcl-2 is a member of the Bcl-2 family of apoptosis regulatory molecules, which is found at high levels in surviving T cells [26-28]. Memory $CD8^+$ T cells are partially dependent on IL-7 for homeostatic proliferation [6]. In our lab, Dr. Ching-Hung Shen showed that loss of IL-7Rα and IL-15Rβ expression in memory 2C T cells generated in response to WSN-SIY influenza virus, correlated with rapid decline of memory 2C T cells from the lung airways [29]. However, memory 2C T cells were maintained in these mice's spleens where IL-7Rα and IL-15Rβ was still being expressed [29]. Like IL-15, the main source of IL-7 for T cell proliferation *in vivo* appears to be non-bone marrow-derived cells

[6]. Again, the role of IL-7 in persistence of tolerant 2C T cells is yet to be elucidated. In this study, we investigate the effect of tumor-related factors, and identify the role that IL-15 and IL-7 might play in supporting persistence of T cells in a tolerizing tumor environment.

4.3. Results

Tumor-related factors have a dominant effect on persistence of tolerant T cells

Factors in the prostate tumor environment, which we call tumorigenic or tumor-related factors, appear to support infiltration and persistence of T cells. Antigen-specific T cells infiltrate both SIY antigen-expressing and tumor transgenic prostates by 9 dpi (Fig. 4). As the time after infection progresses, there begins to be only statistically significant differences in 2C T cell numbers between non-tumor (B6/B6-SIY) and tumor (TRAMP/TRAMP-SIY) transgenic mice (Fig. 4). Observing that the tumor transgenic prostates appeared larger than normal mice, we analyzed the number of 2C T cells per gram of prostate to rule out the possibility that the increased cell numbers was simply due to larger tissue mass. Measurements of the dry weight of the urogenital system and the dry weight of prostates showed that all mouse models had prostates that were about ten percent of the urogenital system (Fig. 24). The urogenital system in this case consists of the drained bladder, seminal vesicles, urethra, ureters, ampullary glands and the prostate. The weight of the prostate was therefore calculated as 10% of the weight of the urogenital system excised. These results showed that tumor transgenic mice had prostates about thrice the size of non-tumor mice (Fig. 25). The analysis of the number of 2C T cells per gram of prostate revealed a significant effect from the presence of antigen in the prostate at early time points (9 dpi) while tumorigenic factors had a more dominant role on 2C T cell persistence (Fig. 26).

The effect of tumor-related factors on T cell persistence is also evident in experiments using non-antigen-specific OT-I T cells. Prostates from tumor and non-tumor mice that received OT-I T cells and WSN-SIIN virus were analyzed 2 mpi. The analysis of OT-I $CD8^+$ T cell numbers revealed statistically significant differences between B6 versus TRAMP and B6-SIY

versus TRAMP-SIY prostates (Fig. 6). A comparison of the number of cells per gram of prostate again showed that the tumor environment contributes to higher 'numbers' of T cells (Fig. 27). The PDLN also showed markedly higher numbers between corresponding tumor and non-tumor mice for both 2C (Fig. 4) and OT-I recipients (Fig. 6). These results suggest that in addition to antigen, there are tumor-related factors that play a dominant role in supporting persistence of T cells. Some of these factors may include cytokines such as IL-15 and IL-7 that are known to support functional memory T cell maintenance. The role of these cytokines in tolerant T cell persistence is still unknown.

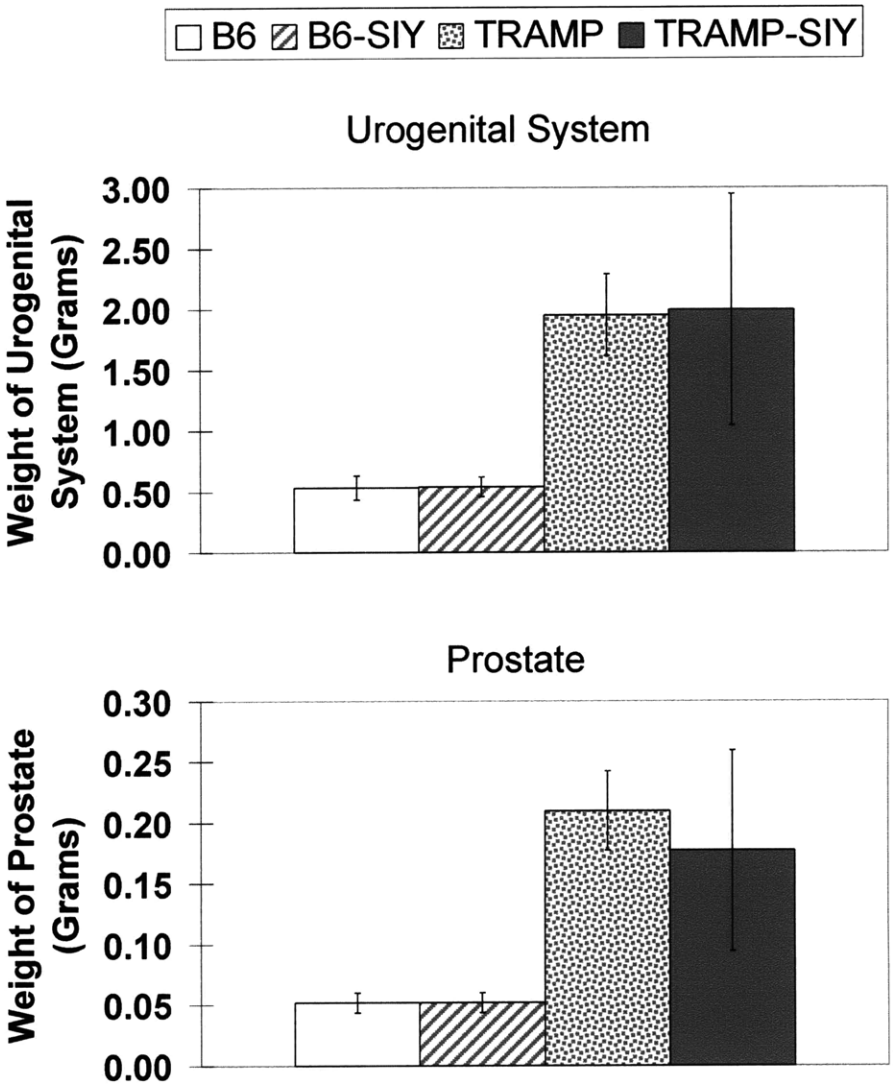

Figure 24. Reason for ten percent estimation of prostate weight based on the weight of the urogenital system.

The urogenital system and prostates of B6 (white), B6-SIY (stripes), TRAMP (dots) and TRAMP-SIY (gray) mice were measured immediately following tissue excision. None of these mice have ever been infected or received 2C T cells. The error bars indicate standard deviations for each group (n = 5 -7 per group).

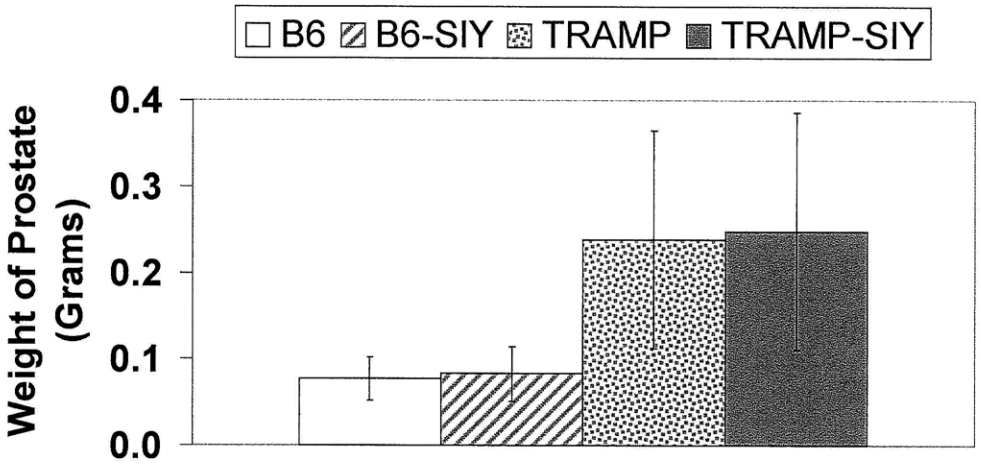

Figure 25. Tumor transgenic prostates are thrice the weight of non-tumor prostates. Chart shows average weights of B6 (white), B6-SIY (stripes), TRAMP (dots) and TRAMP-SIY (gray) prostates for mice ranging from 4-8 months old at the time of harvest. The error bars indicate standard deviations for each group ($n \geq 25$ per group).

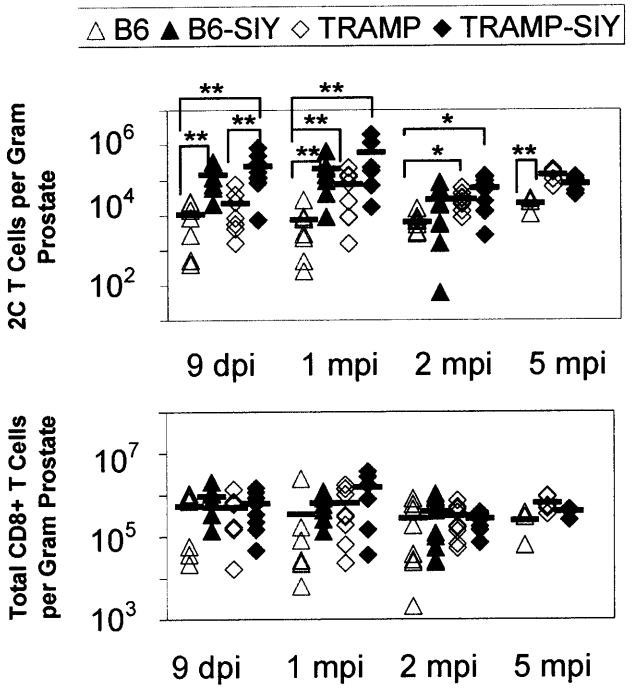

Figure 26. Tumor-related factors contribute to T cell persistence.
Prostates were harvested after 2C T cell transfer and WSN-SIY influenza infection as described in the methods section. 2C T cell numbers were determined as previously described. The number of cells per gram of prostate was calculated using the weight of each mouse's prostate determined at the time of tissue harvest. Each shape represents data for one mouse ($n \geq 5$ per group). Solid black bars indicate the average of the data for each mouse model. The p-values for cell numbers from student t-tests comparing B6 to TRAMP, B6-SIY to TRAMP-SIY, B6 to B6-SIY and TRAMP to TRAMP-SIY are given for $p<0.05$. Values $p<0.01$ are represented with an asterisk (*) and $p<0.05$ are represented with a double asterisk (**).

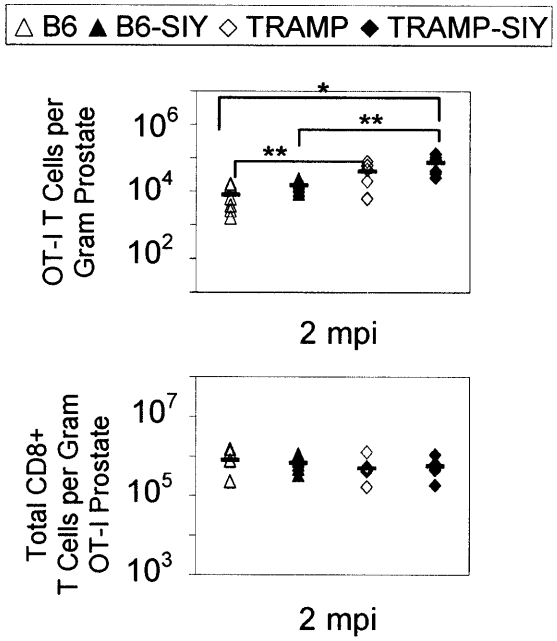

Figure 27. Tumor-related factors have a dominant role in the persistence of T cells in the prostate.

Prostates were harvested after OT-I T cell transfer and WSN-SIIN influenza infection as described in the methods section. 2C and OT-I T cell numbers were determined as previously described. The number of cells per gram of prostate was calculated using the weight of each mouse's prostate determined at the time of tissue harvest. Each shape represents data for one mouse ($n \geq 5$ per group). Solid black bars indicate the average of the data for each mouse model. The p-values for cell numbers from student t-tests comparing B6 to TRAMP, B6-SIY to TRAMP-SIY, B6 to B6-SIY and TRAMP to TRAMP-SIY are given for $p<0.05$. Values $p<0.01$ are represented with an asterisk (*) and $p<0.05$ are represented with a double asterisk (**).

IL-15Rβ, IL-7Rα, IL-2Rα and γ_c are expressed at similar levels in 2C T cells from the prostate

Upon comparison of the expression of the receptor subunits required for response to IL-15, IL-7 and IL-2, no significant differences are observed at the RNA (Fig. 28) or protein (Figs. 29 to 33) level between tolerant and non-tolerant 2C T cells in the prostate. These cytokines all belong to the γ_c family of cytokines. Flow cytometry analysis show similar levels of γ_c expression in tolerant and non-tolerant 2C T cells (Fig. 29). Functional memory 2C T cells from WSN-SIY infected B6 mice are known to express IL-15Rβ and IL-7Rα and to persist in the spleen, whereas 2C T cells in the lungs gradually lose these receptor subunits, which corresponds to a decline in 2C T cell numbers in the lungs [29]. Thus B6 spleen and lung specimens were used as positive and negative controls respectively. At all time points analyzed, 9 dpi, 1 mpi, 2 mpi, the IL-15Rβ and IL-7Rα expression levels for 2C T cells in the prostate do not differ significantly for all mice strains (Figs. 30 and 31). IL-2 shares the β and γ receptor subunits with IL-15. The two cytokines can exert their unique effects by the difference in their α receptor subunit. The expression level for IL-2Rα was also tested. No significant difference was observed at 2 mpi for IL-2Rα (Figs. 33). In the prostate, the protein expression levels of all the mouse strains overlap, and are slightly lower than those in naïve 2C T cells (Figs. 29 to 31, 33). Analysis of RNA levels of these receptor subunits in 2C T cells sorted from 1 mpi prostates also showed less than 2-fold difference between TRAMP and TRAMP-SIY prostates (Fig. 28). This data is in agreement with the protein expression assessed by flow cytometry. These results indicated that tolerant and non-tolerant 2C T cells do not show differences in their response to IL-15 or IL-7 at the receptor level.

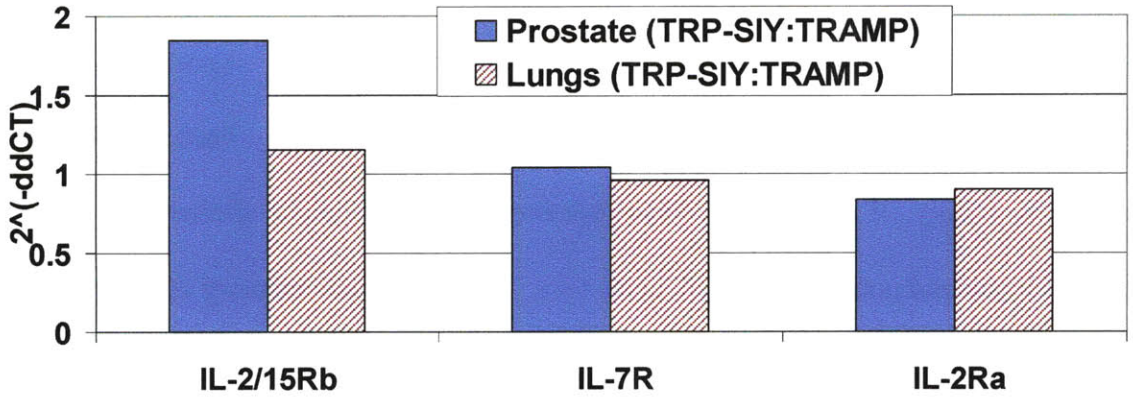

Figure 28. Antigen-specific 2C T cells express similar levels of IL-15Rβ and IL-7Rα in SIY and non-SIY mouse prostates.
Relative mRNA levels of receptor subunits expressed in 2C T cells sorted from TRAMP and TRAMP-SIY prostates and lungs 30 dpi (1 mpi). Data was extracted from a PCR superarray screen performed by Eileen Higham (Chen Lab).

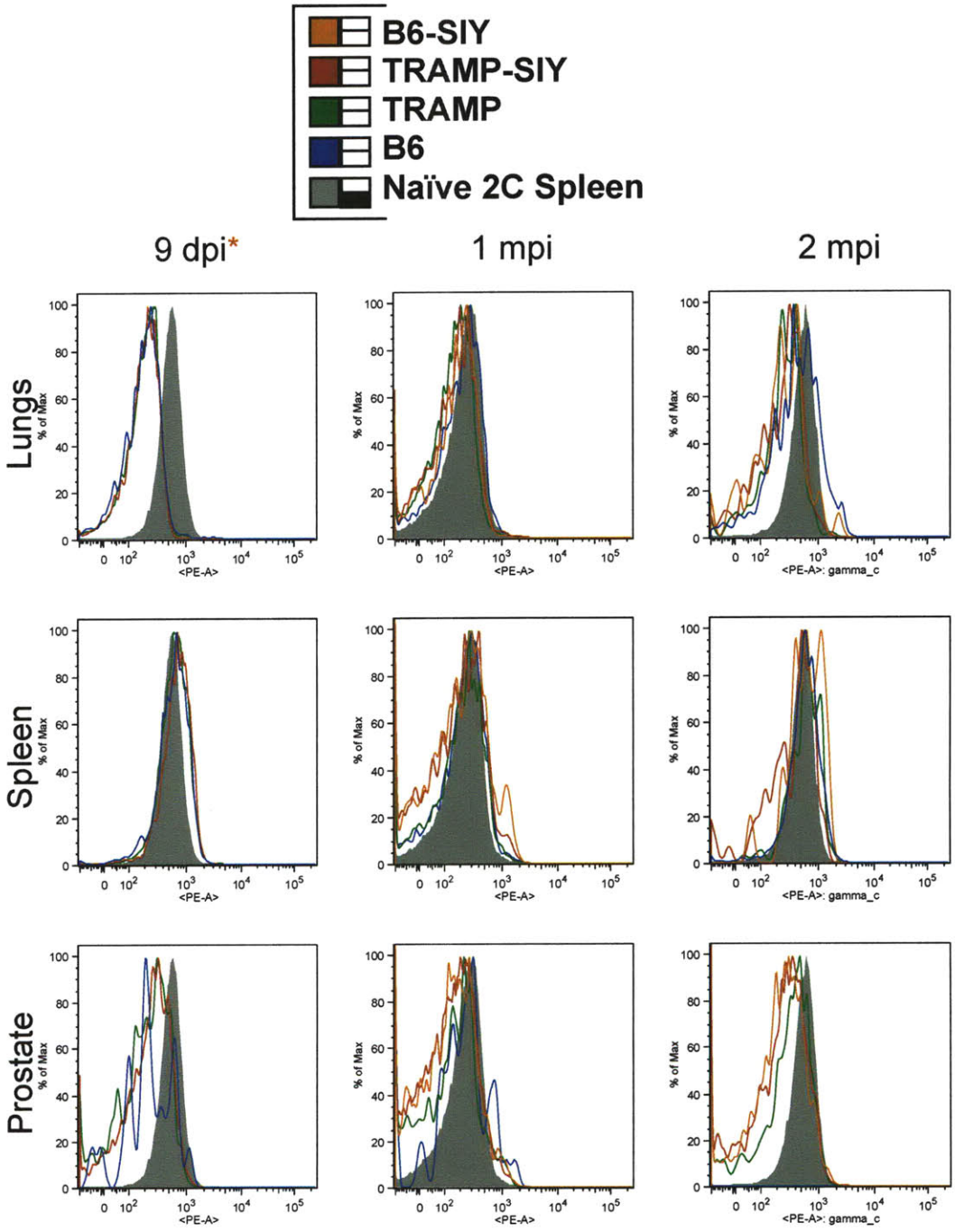

*No data for B6-SIY at 9 dpi

Figure 29. No significant difference in γ_c expression between 2C T cells in TRAMP-SIY and other mouse strains.

Lungs, spleens and prostates were harvested from TRAMP-SIY (red), TRAMP (green), B6-SIY (orange) and B6 (blue) mice at 9 days, 1 month and 2 months after 2C T cell transfer and WSN-SIY influenza infection. Cells were stained with 1B2, CD8α, and γ_c antibodies, as well as DAPI or PI to exclude dead cells, followed by flow cytometry analysis. Using FlowJo software, histograms were generated by gating on PI^{Neg} $CD8^+$ cells followed by FSC versus SSC lymphocyte gating, selecting $1B2^+$ $CD8^+$ cells, and finally, overlaying histogram plots of each receptor subunit as shown for the different mouse strains. Freshly isolated naïve 2C T cells were used to determine baseline level comparisons (gray shadow).

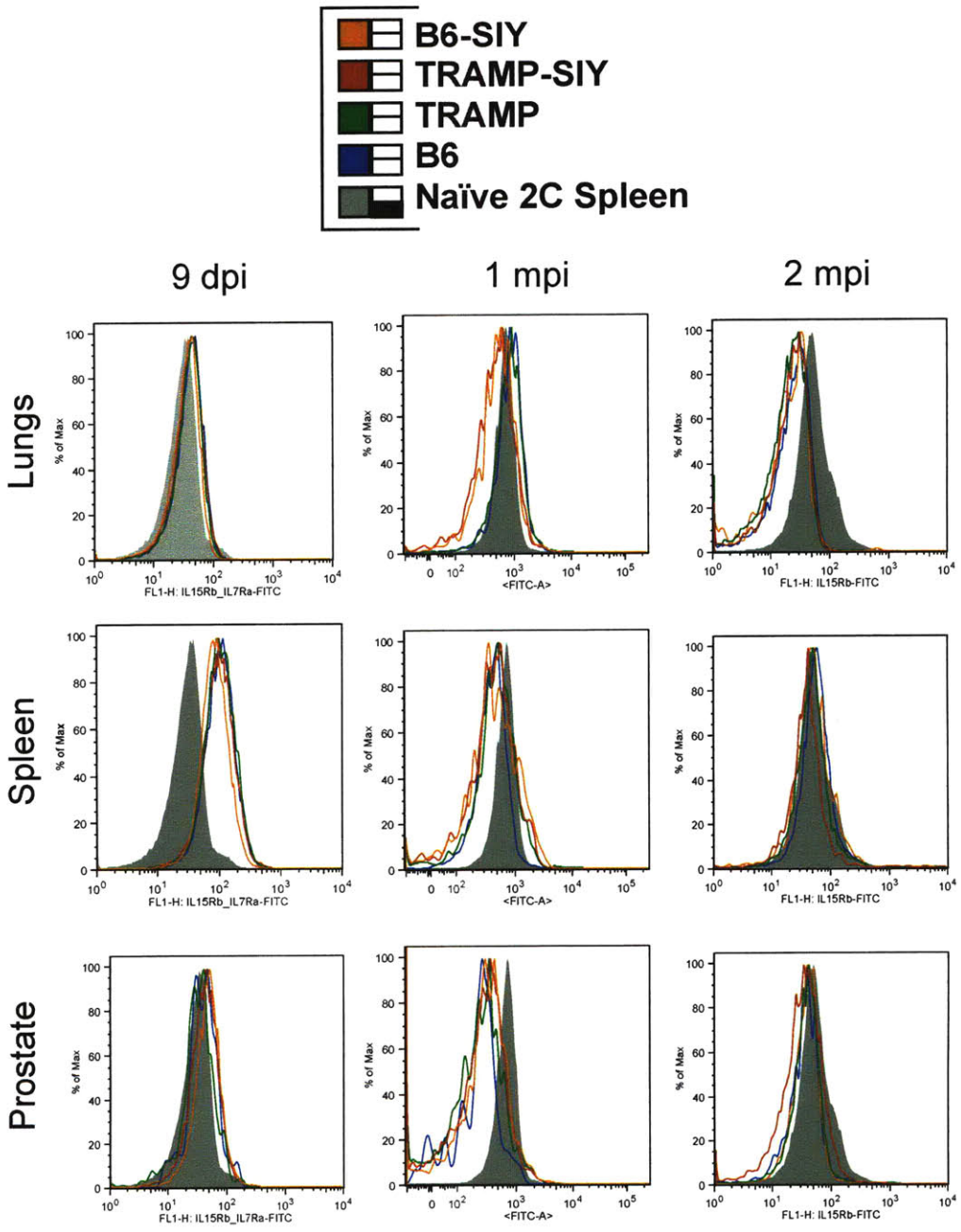

Figure 30. No significant difference in IL-15Rβ expression between 2C T cells in TRAMP-SIY and other mouse strains.

Lungs, spleens and prostates were harvested from TRAMP-SIY (red), TRAMP (green), B6-SIY (orange) and B6 (blue) mice at 9 days, 1 month and 2 months after 2C T cell transfer and WSN-SIY influenza infection. Cells were stained with 1B2, CD8α, and IL-15Rβ antibodies, as well as DAPI or PI to exclude dead cells, followed by flow cytometry analysis. The FlowJo analysis is similar to that described for γ_c. Freshly isolated naïve 2C T cells were used to determine baseline level comparisons (gray shadow).

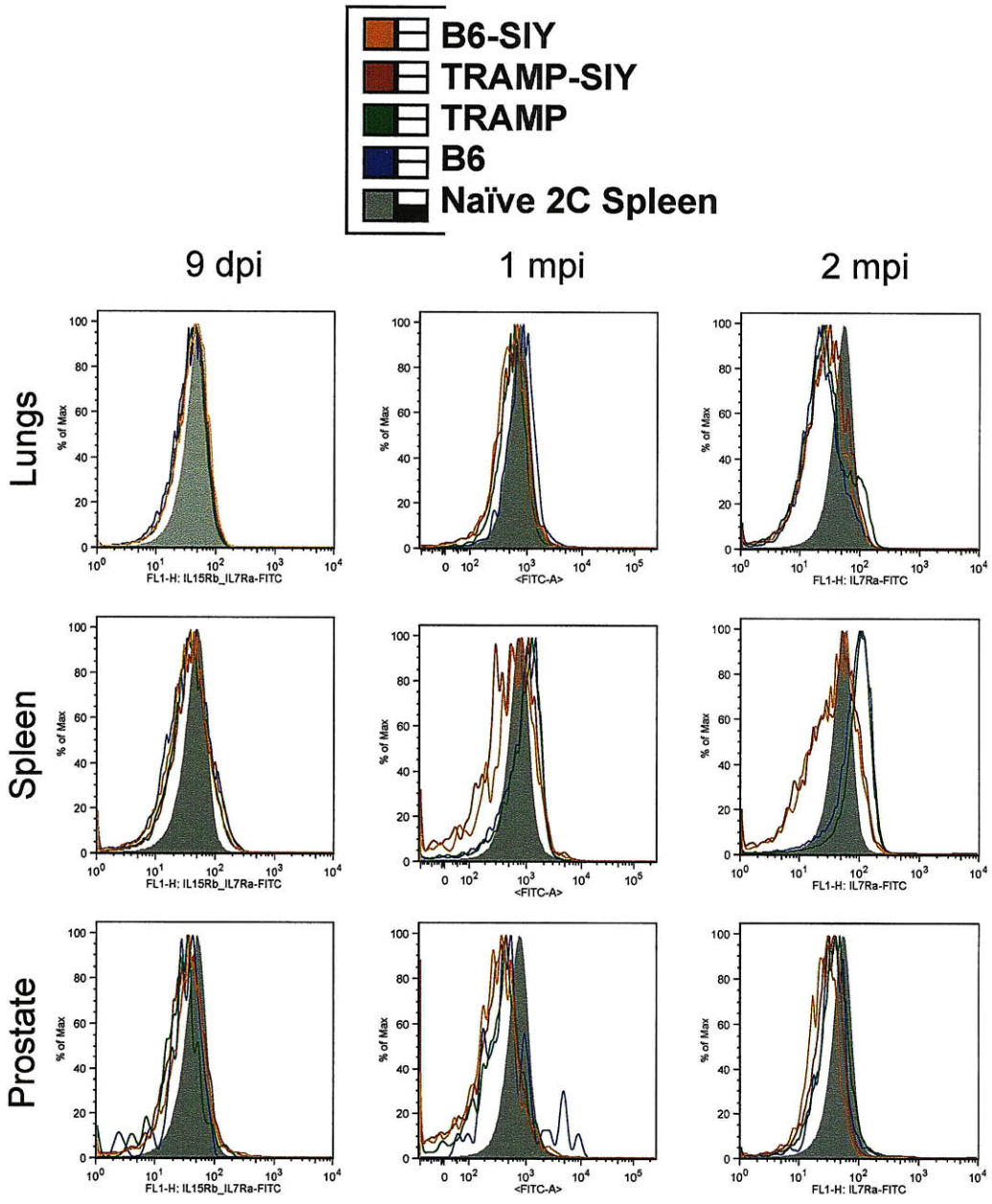

Figure 31. Difference in IL-7Rα expression between 2C T cells in SIY and non-SIY spleens but not in prostates and lungs.

Lungs, spleens and prostates were harvested from TRAMP-SIY (red), TRAMP (green), B6-SIY (orange) and B6 (blue) mice at 9 days, 1 month and 2 months after 2C T cell transfer and WSN-SIY influenza infection. Cells were stained with 1B2, CD8α, and IL-7Rα antibodies, as well as DAPI or PI to exclude dead cells, followed by flow cytometry analysis. The FlowJo analysis is similar to that described for γ_c. Freshly isolated naïve 2C T cells were used to determine baseline level comparisons (gray shadow).

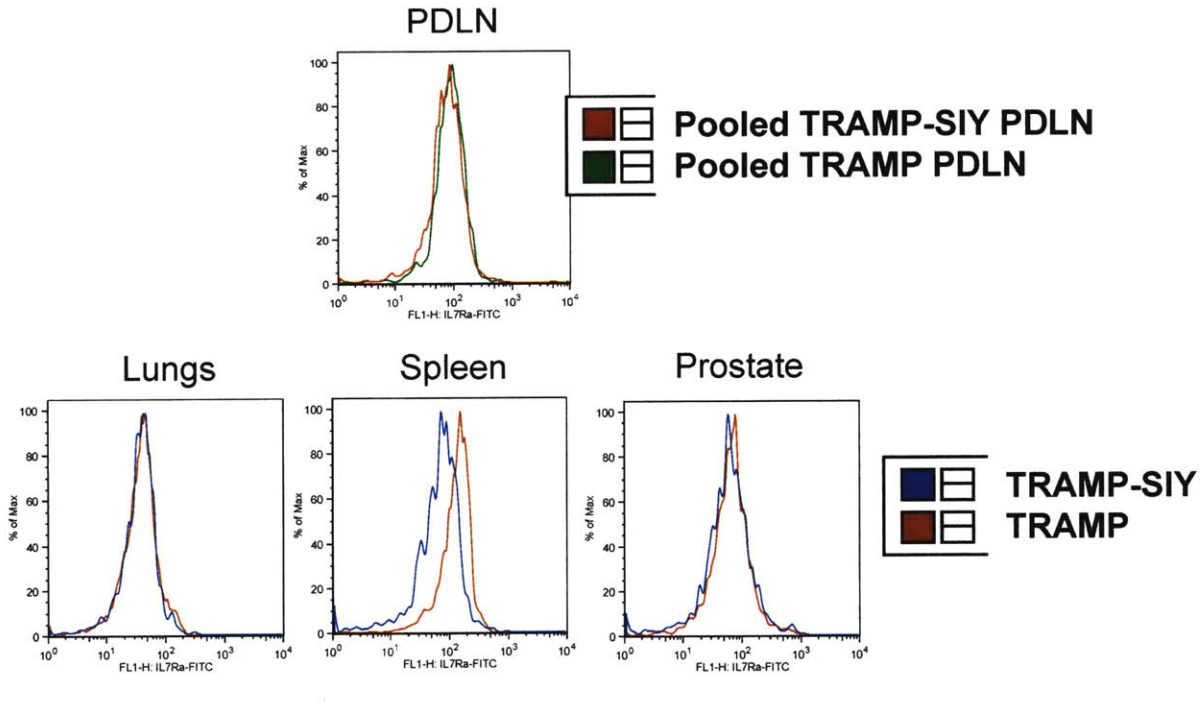

Figure 32. Similar levels of IL-7Rα in the PDLN.
PDLN from three TRAMP (green) and TRAMP-SIY (orange) mice 2 mpi were pooled and stained with 1B2, CD8α, and IL-7Rα antibodies, as well as PI to exclude dead cells, followed by flow cytometry analysis using FlowJo software. Lungs, spleens and prostates from a pair of TRAMP (red) and TRAMP-SIY (blue) mice were also analyzed. IL-7Rα expression histograms were generated by gating on PI^{Neg} $CD8^{+}$ cells followed by FSC versus SSC lymphocyte gating, selecting $1B2^{+}$ $CD8^{+}$ cells, and finally, overlaying histogram plots.

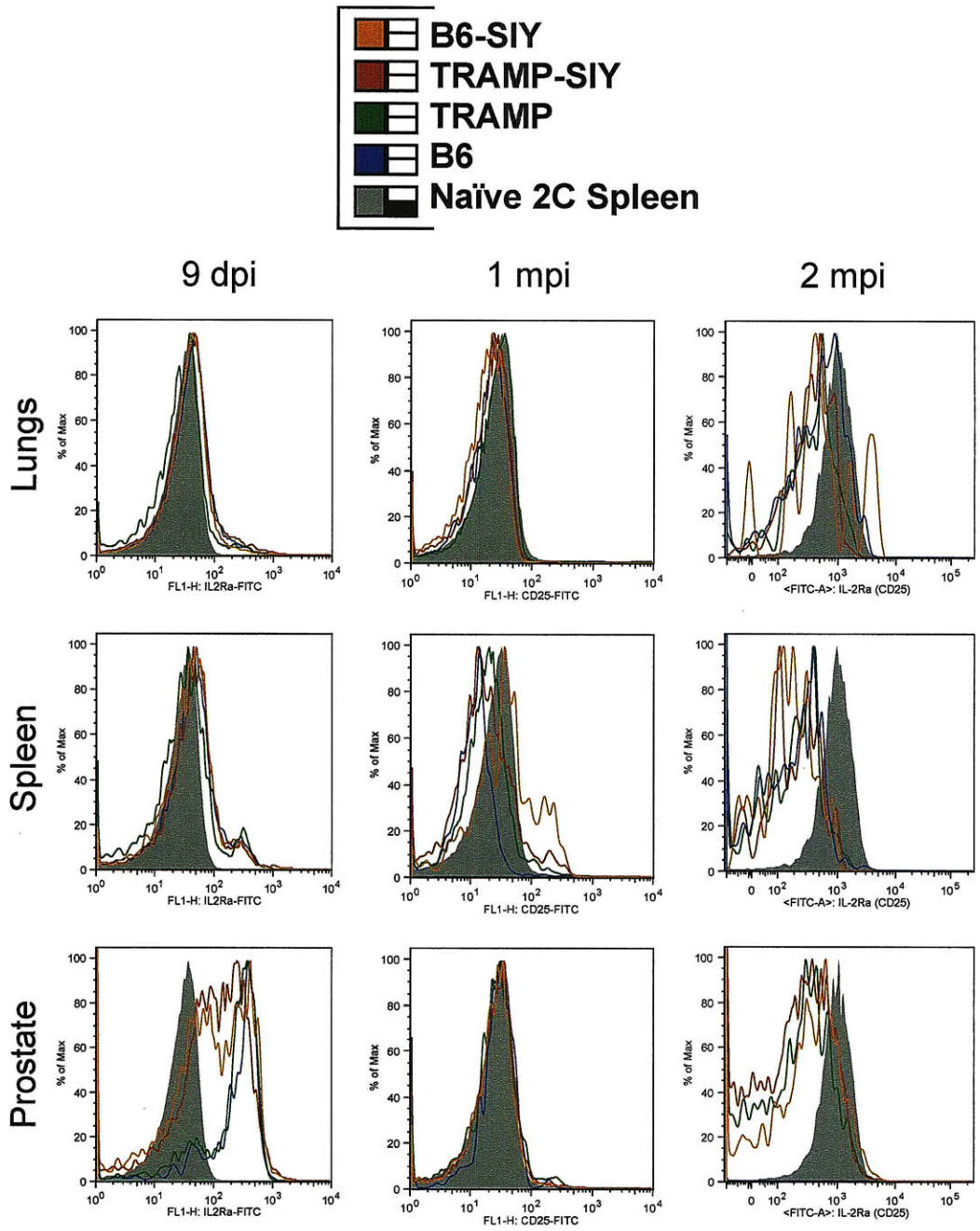

Figure 33. No significant difference in IL-2Rα expression between 2C T cells in TRAMP-SIY and other mouse strains.

Lungs, spleens and prostates were harvested from TRAMP-SIY (red), TRAMP (green), B6-SIY (orange) and B6 (blue) mice at 9 days, 1 month and 2 months after 2C T cell transfer and WSN-SIY influenza infection. Cells were stained with 1B2, CD8α, and IL-2Rα antibodies, as well as DAPI or PI to exclude dead cells, followed by flow cytometry analysis. The FlowJo analysis is similar to that described for γ_c. Freshly isolated naïve 2C T cells were used to determine baseline level comparisons (gray shadow).

2C T cells from tumor transgenic prostates respond similarly to IL-15 or IL-7 stimulation

The effects of these cytokines on 2C T cells may be in the cells' response to IL-15 and IL-7. In Fig. 31, we observed that IL-7Rα expression in the prostate is lower compared to naïve 2C T cells regardless of the presence or absence of SIY antigen. These results made us consider the possibility that 2C T cells in the prostate may be responding to IL-7 *in vivo*. Increased intracellular staining for phosphorylated Stat5 (pStat5) would indicate that tolerant T cells can respond to this cytokine. pStat5 experiments were carried out using freshly isolated 2C T cells from TRAMP and TRAMP-SIY prostates. Some cells were also stimulated with either IL-7 or IL-15 to determine whether tolerant 2C T cells could respond to these cytokines. Figures 34 to 36 show the results. Unstimulated 2C T cells freshly isolated from TRAMP-SIY 1-2 mpi (~47 dpi) have similar or lower levels of pStat5 expression compared to 2C T cells from TRAMP prostates (Fig. 34). When 2C T cells from TRAMP-SIY prostate are stimulated with IL-7 (20 ng/ml) or IL-15 (40ng/ml) for 30 min at 37°C, there is a slight increase (shift to the right, Figs. 35 and 36) in pStat5 levels. However, this is only 1-2 fold rise compared to 6-fold increase in naïve 2C T cells stimulated with IL-7 (Fig. 35). No appreciable difference was observed in 2C T cells from TRAMP prostate after short-term stimulation with either cytokine (Figs. 35 and 36). These results suggest that 2C T cells from TRAMP-SIY prostate do not respond differently to IL-7 or IL-15 compared to cells from TRAMP prostate. In fact, tolerant 2C T cells do not appear to respond to either IL-7 or IL-15.

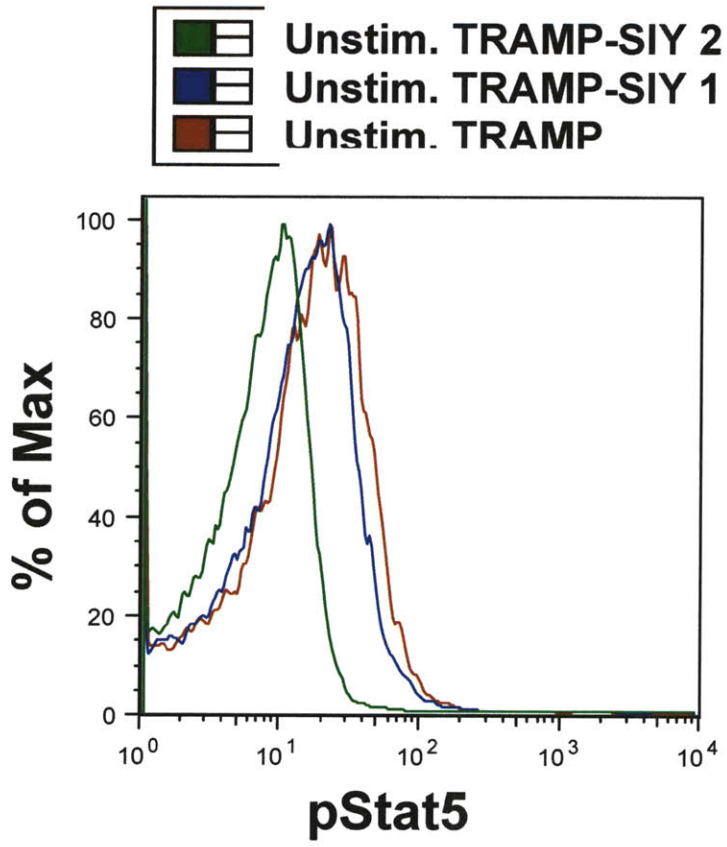

Figure 34. Phosphorylated Stat5 levels in 2C T cells from TRAMP-SIY prostate are lower or comparable to TRAMP prostate.

Prostates were harvested from TRAMP-SIY and TRAMP mice 1- 2 mpi (~47 dpi) after 2C T cell transfer and WSN-SIY influenza infection. Cells were stained with 1B2 and CD8α antibodies, fixed, permeabilized and stained with pStat5 antibody following the manufacturer's protocol (Cell Signaling Technology) for flow cytometry staining. Data was analyzed using FlowJo software. Histograms were generated by gating on FSC versus SSC to select lymphocyte-sized cells, gating on $1B2^+$ $CD8^+$ cells, and finally overlaying histogram plots of pStat5 expression for each mouse strain shown. "Unstim" is an abbreviation for unstimulated cells.

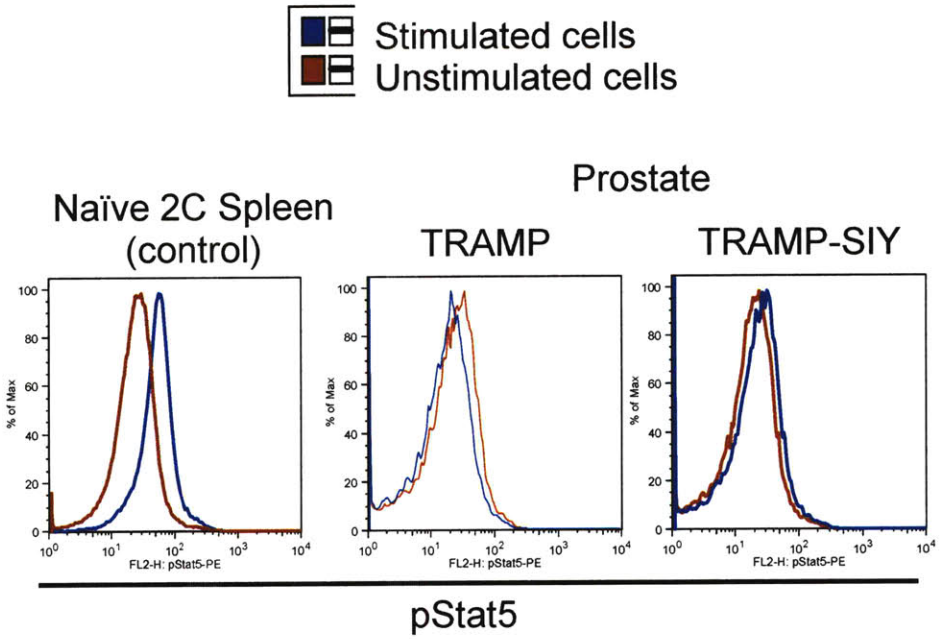

Figure 35. Tolerant 2C T cells do not respond to IL-7.
Cells from TRAMP-SIY prostates ~47 dpi were analyzed for pStat5 expression as described in the methods section. Using the FlowJo software, histograms showing pStat5 expression were generated by gating on FSC versus SSC to select lymphocyte-sized cells, followed by gating on Thy1.1^{+} CD8^{+} cells, and finally overlaying histogram plots of pStat5 expression. Unstimulated cells are in red and stimulated cells are shown in blue. pStat5 levels on freshly isolated naïve 2C T cells that respond to IL-7 stimulation (blue) are shown as a positive control.

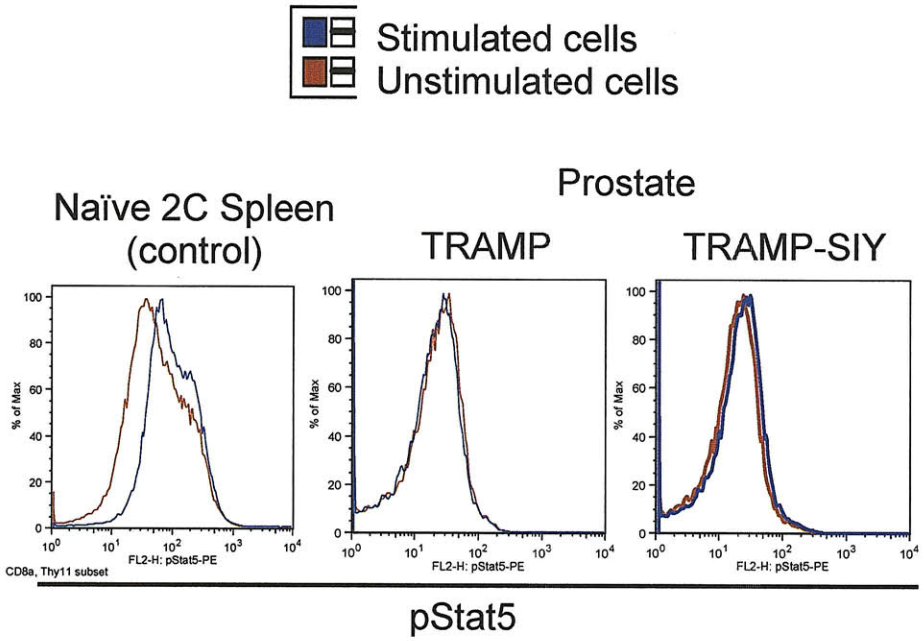

Figure 36. Tolerant 2C T cells do not respond to IL-15.
Cells from TRAMP-SIY prostates ~47 dpi were analyzed for pStat5 expression as described in the methods section. Using the FlowJo software, histograms showing pStat5 expression were generated by gating on FSC versus SSC to select lymphocyte-sized cells, followed by gating on Thy1.1^{+} CD8^{+} cells, and finally overlaying histogram plots of pStat5 expression. Unstimulated cells are in red and stimulated cells are shown in blue. pStat5 levels on freshly isolated naïve 2C T cells that respond to IL-15 stimulation (blue) are shown as a positive control.

IL-15 and IL-7 are not expressed at detectable levels in tumor transgenic prostates

Because the results above (Figs. 28 to 36) showed that there were no differences at the receptor level for tolerant 2C T cells that might explain their persistence in TRAMP-SIY prostate, we chose to investigate whether the difference lay in the availability of the cytokine in the prostate. RNA levels of IL-15 and IL-7 in TRAMP and TRAMP-SIY prostates were determined by real-time quantitative PCR (qPCR) experiments. Cell suspension from the bone marrow of B6 mice was chosen as a positive control since these cytokines are found in abundance in this tissue. Although IL-7 and IL-15 could be detected in the bone marrow of B6 mice, neither of these cytokines could be detected in the prostate (Figs. 37 and 38). GAPDH was used as the housekeeping gene, which served as an additional control. Since the GAPDH expression using the same cDNA for the prostates could be detected easily (Fig. 39), we confirmed that IL-15 and IL-7 are not produced in TRAMP and TRAMP-SIY prostates. Therefore, persistence of tolerant 2C T cells in the prostate does not depend on IL-15 or IL-7.

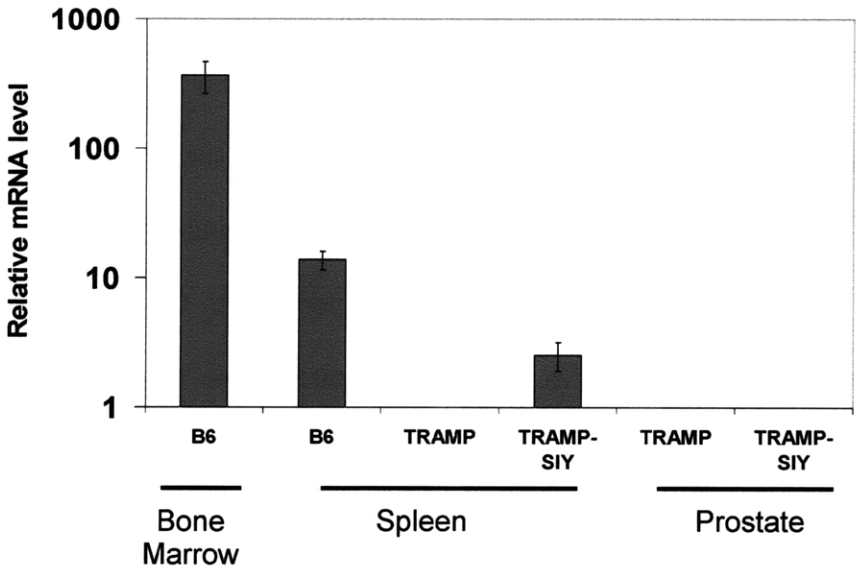

Figure 37. IL-15 is not detected in tumor transgenic prostates.
RNA was extracted from prostates of TRAMP-SIY and TRAMP mice and transcribed into cDNA (as described in the Methods section). The transcript levels of IL-15 and GAPDH were determined using quantitative real-time PCR. Transcripts from the bone marrow of B6 mice were used as controls. IL-15 levels were normalized to GAPDH levels of the same tissue. The chart shows relative expression levels of IL-15 in the different tissues indicated. Error bars represent the standard deviation from duplicate (B6) or triplicate (TRAMP and TRAMP-SIY) samples.

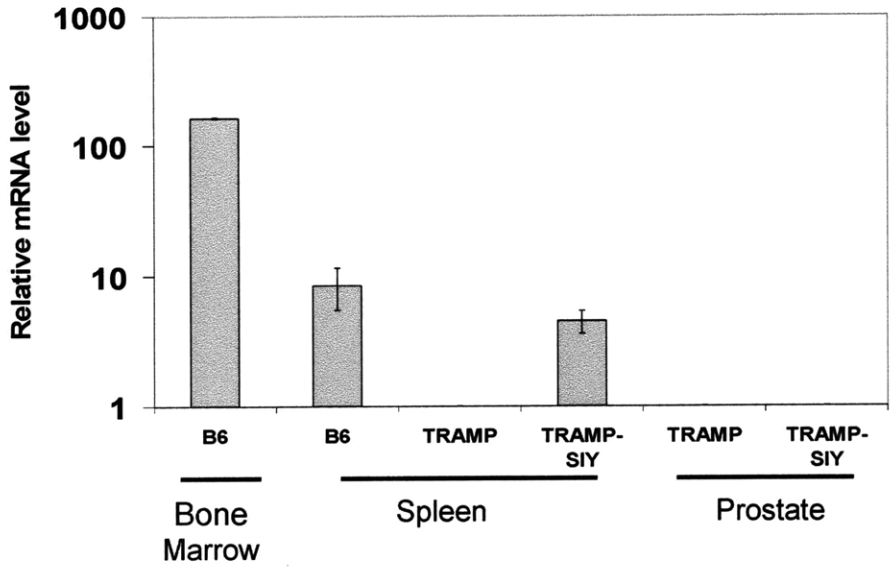

Figure 38. IL-7 is not detected in tumor transgenic prostates.
RNA was extracted from prostates of TRAMP-SIY and TRAMP mice and transcribed into cDNA (as described in the Methods section). The transcript levels of IL-7 and GAPDH were determined using quantitative real-time PCR. Transcripts from the bone marrow of B6 mice were used as controls. IL-7 levels were normalized to GAPDH levels of the same tissue. The chart shows relative expression levels of IL-7 in the different tissues indicated. Error bars represent the standard deviation from duplicate (B6) or triplicate (TRAMP and TRAMP-SIY) samples.

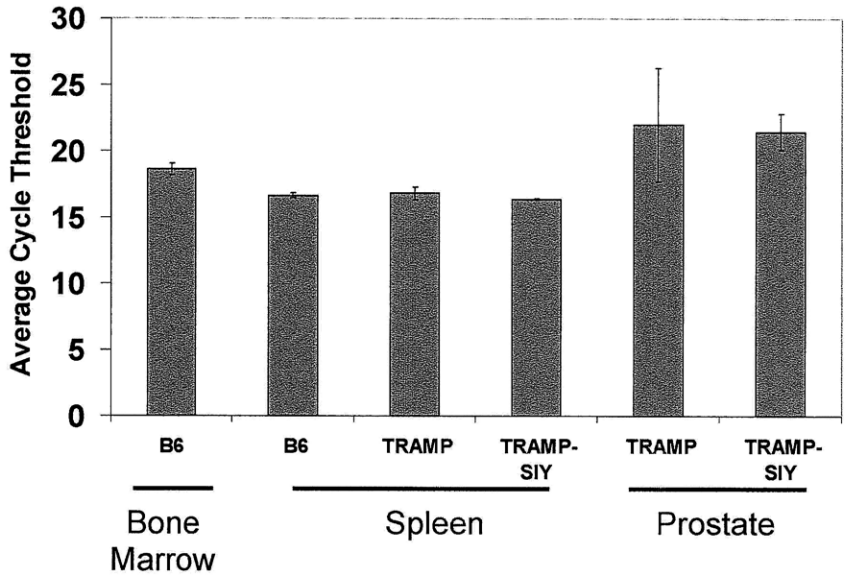

Figure 39. GAPDH cycle thresholds are similar for all tissues.
RNA was extracted from prostates of TRAMP-SIY and TRAMP mice and transcribed into cDNA. IL-15, IL-7 and GAPDH transcripts were run on the ABI7500 thermacycler as described in the methods section. This chart shows the average of the cycle threshold (Ct) values obtained for each sample. Each RT product for qPCR was set up in technical duplicates. Two B6, three TRAMP and three TRAMP-SIY mice were analyzed. Error bars represent the standard deviation from all replicates.

Potential candidates that support T cell persistence

Tumorigenic or tumor-related factors might enhance T cell infiltration and/or increase cell proliferation in the tumor environment. This deduction stems from the fact that tumor transgenic prostates have about 5-fold greater number of 2C or OT-I T cell infiltrates at 2 mpi than non-tumor mice (Figs. 4 and 6). Also, the number of 2C T cells increases at 5 mpi (Fig. 4). (It is important to note that the texture of the tissue at 5 mpi is denser than earlier timepoints analyzed and resembles that of solid tumors.) To identify potential molecules that support T cells in the prostate tumor environment, I mined through published microarray data. Two groups performed microarray analyses comparing gene expression in normal B6 prostates to TRAMP prostates [30, 31]. Of their top candidates differentially expressed in early stages of prostate tumor progression (4-6 months old mice), both groups identified Survivin (also known as Birc5) and Racgap1 as genes upregulated in TRAMP prostate relative to normal B6 prostate.

Survivin belongs to the family of Inhibitor of Apoptosis (IAP) genes [32] and has been shown to be expressed in human and TRAMP prostates [33]. Krajewska *et al.* (2003) evaluated tissue sections from TRAMP prostates by immunohistochemisty. The authors found 93% of the transformed foci in TRAMP mice with prostatic intraepithelial neoplasia expressing elevated levels of Survivin compared to 33% of normal controls [33]. Also, 47% of the transformed tissue examined from mice with prostate cancer was positively stained for Survivin. Normal controls did not have any cancer foci [33]. Similar results have been observed in immunostained tissue sections from prostate cancer patients [33]. This data also correlates well with published microarray results [30, 31]. Other groups have been able to generate $CD8^+$ T cell specific response to Survivin antigen in a variety of human cancers including patients with prostate cancer [34, 35]. Their results suggest Survivin could induce T cell infiltration into the prostate. Furthermore, this

molecule is important for proliferation of peripheral $CD8^+$ T cells [36]. Xing *et al.* (2004) discovered that Survivin-deficient mice had fewer $CD8^+$ T cells in the spleens and lymph nodes but similar numbers to wild-type in the thymus [36]. Additional studies showed that Survivin-deficient cells' proliferation was impaired [36]. $CD8^+$ T cells transduced with retroviral vectors expressing Survivin proliferated and survived longer than non-transduced controls [37]. Combining Survivin with Bcl-x_L (another anti-apoptotic molecule) provided an additive effect that resulted in functional persisting $CD8^+$ T cells that prevented tumor growth [37]. These results suggest that Survivin could contribute to T cell persistence by inducing T cell infiltration into the prostate tumor environment, as well as enhancing T cell proliferation and survival.

Racgap1 is the Rac guanosine triphosphatase (GTPase) activating protein 1, also known as the male germ cell Rac GTPase activating protein (MgcRacGAP). As a GTPase activating protein (GAP), Racgap1 acts as a catalyst by binding to activated Rho GTPases and thereby negatively regulates Rho-mediated signals [32]. Racgap1 is involved in cytokinesis [38] and hematopoietic stem differentiation including $CD8^+$ T cell development in the thymus [39], amongst other roles, for example, migration of endothelial cells [40]. In general these roles involve cell proliferation and cell migration; two processes that may lead to increased T cells in the TRAMP prostate. It is still unclear whether Racgap1 would play a role in supporting persistence of adoptively transferred T cells even though it is among the genes differentially expressed between B6 and TRAMP prostates.

Considering that the mechanism for T cell persistence might occur through enhanced proliferation, increased survival and/or through cell trafficking, I postulated that other candidates that support T cell persistence might include chemokines, cytokines, growth factors, cadherins and integrins. With the aid of a postdoctoral fellow, Dr. Guangan Hu, we identified genes in

these categories that are differentially expressed in normal B6 versus TRAMP prostates (using the public access dataset from the microarray analysis performed by Haram *et al.* (2008) [31]. Genes function that are classified in the gene ontology for chemokines and cytokines or growth factors or cadherins and integrins were selected. Expression profiles of these genes were extracted from the GEO dataset (GSE10525). Differentially expressed genes between B6 and TRAMP prostates were identified using a nonparametric Wilcoxon-Whitney test in MeV program (http://www.tm4.org/mev.html) with a false discovery rate FDR (<0.05) control. Diagrams of expression profiles of these genes are shown in Figs. 40 and 41. Table 2 is a summary of ten potential candidates obtained from this analysis.

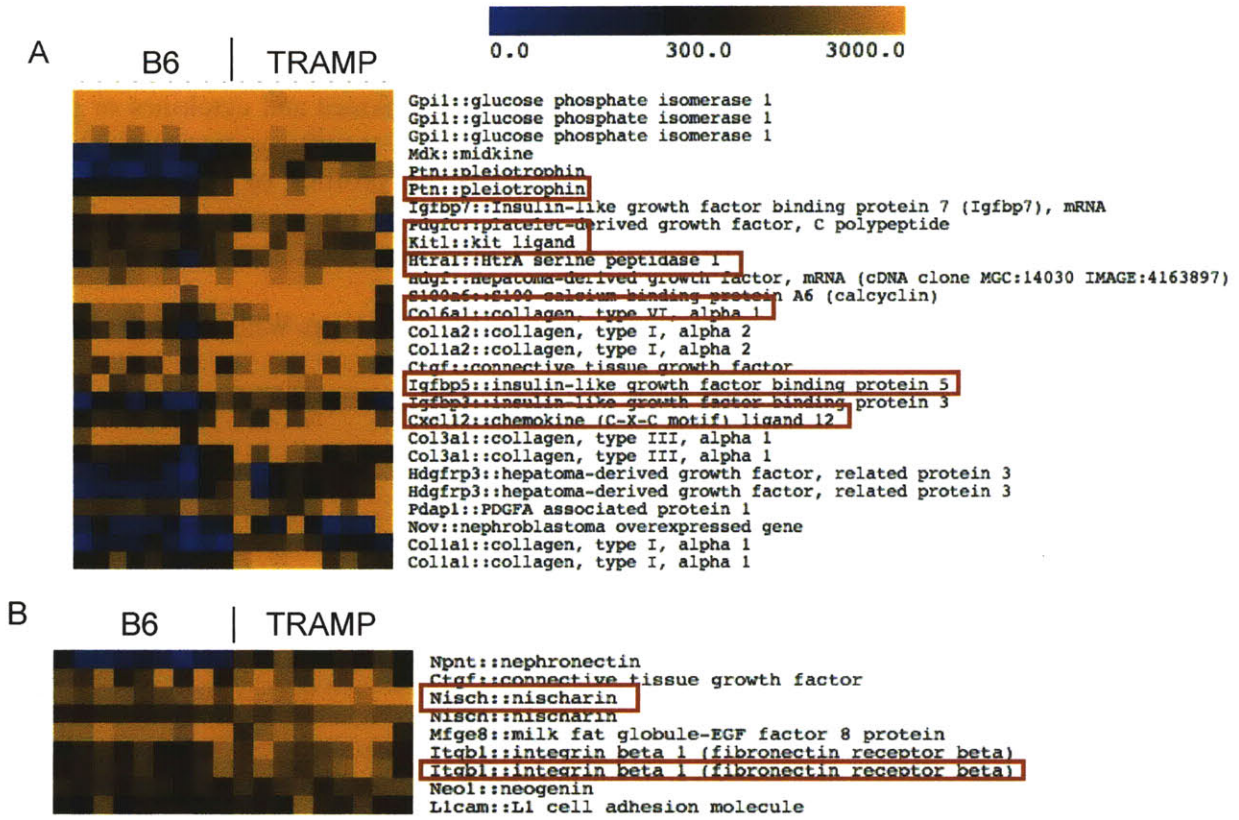

Figure 40. Genes upregulated in TRAMP prostate.
Genes differentially expressed between B6 and TRAMP prostates from mining GEO dataset (GSE10525) made available by Haram et al. (2008) [31] for genes classified as cytokines and chemokines or (A) growth factors or (B) cadherins and integrins in their gene ontology function. (Cxcl12 was the only visually different gene in cytokines and chemokines analysis.) Differentially expressed genes between B6 and TRAMP prostates were identified using a nonparametric Wilcoxon-Whitney test in MeV program (http://www.tm4.org/mev.html) with a False Discovery Rate FDR (<0.05) control (by Dr. Guangan Hu in Chen Lab).

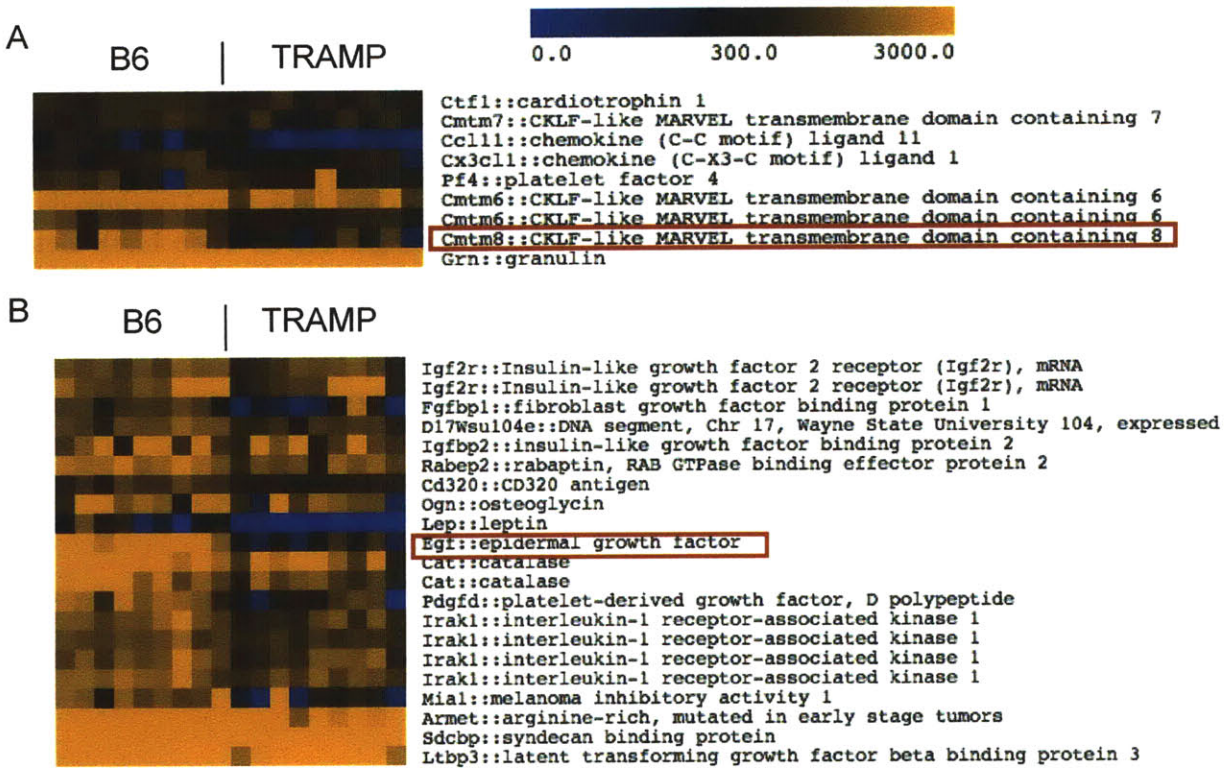

Figure 41. Genes downregulated in TRAMP prostate.
Genes differentially expressed between B6 and TRAMP prostates from mining GEO dataset (GSE10525) made available by Haram et al. (2008) [31] for genes classified as (A) cytokines and chemokines (A) or (B) growth factors in their gene ontology function. (Results from cadherins and integrins test did not appear different visually.) Differentially expressed genes between B6 and TRAMP prostates were identified using a nonparametric Wilcoxon-Whitney test in MeV program (http://www.tm4.org/mev.html) with a False Discovery Rate FDR (<0.05) control (by Dr. Guangan Hu in Chen Lab).

Table 2. Summary of candidates from Microarray analysis. List of genes differentially expressed between B6 and TRAMP prostates from mining GEO dataset (GSE10525) made available by Haram et al. (2008) [31]. These genes were selected from genes classified as cytokines and chemokines or growth factors or cadherins and integrins in their gene ontology function. Differentially expressed genes between B6 and TRAMP prostates were identified using a nonparametric Wilcoxon-Whitney test in MeV program (http://www.tm4.org/mev.html) with a False Discovery Rate FDR (<0.05) control (by Dr. Guangan Hu in Chen Lab). Details about known receptors on T cells, function, primer and antibody (abbreviated Ab) availability were found through further literature searches. "Y" stands for Yes and "N" means No. The blank spaces are for molecules where no reports were found.

Gene	Tumor Level	Receptor on T cells	Function	Primer Available	Receptor Ab Available	Soluble Factor	Neutralizing Ab
Cxcl12	Up	CXCR4, CXCR7	cell migration (CXCR4) and cell proliferation (CXCR7)	Y	Y	Y	Y
Ptn	Up	None found	cell proliferation (fibroblasts), neurites outgrowth, bone mineralization	N		Y	
Kitl	Up	CD117 (c-Kit receptor)	hematopoiesis, spermatogenesis	Y	Y	Y	Y
Htra1	Up	None found	inhibitor of Tgfbeta family proteins (Bmp4, Bmp2, Tgfbeta1) involved in embryonic development	Y			
Col6a1	Up	None found	stimulation of PBMC CD8 T cells by collagen VI peptides	Y			
Igfbp5	Up	None found	cell migration of lymphocytes, monocytes and fibroblasts via MAPK (abstract)	Y		Y	
Nisch	Up	None found	inhibitor of alpha5beta1 dependent cell migration	Y		Y	
Itgb1	Up	CD49a-d	forms VLA1-4, leukocyte adhesion to ECM (collagens, laminin, fibronectin)	Y (and CD29 Ab)	Y (CD49b, CD49d)	(membrane, not soluble)	
Cmtm8	Down	None found	clearance of EGFR and cell apoptosis	Y			
Egf	Down	None found	cell proliferation via EGFR signaling	Y		Y	

From this list of ten genes, two candidates, Cxcl12 and Itgb1 may be selected for further investigation because these molecules seem capable of supporting T cell persistence in the prostate through cell migration or enhanced proliferation mechanisms. Both of these genes have known receptors that are expressed on T cells. Furthermore, primers for these genes Cxcl12 and Itgb1 are readily available from commercial vendors to validate their expression in B6 and TRAMP models by qPCR analysis. Also, there are commercially available antibodies to the receptors on T cells. Having antibodies to these receptors make it feasible to determine any differences in the protein expression levels among 2C T cells from tumor versus non-tumor prostates.

4.4. Discussion

The persistence of adoptively transferred non-specific OT-I T cells also persisting in the prostate suggested that other tumor-related factors support T cell persistence (Fig. 6), and may even have a more dominating role than the presence of antigen. The analysis of T cell numbers per gram of prostate revealed that the difference in 2C and OT-I T cell numbers between non-tumor (B6/B6-SIY) and tumor (TRAMP/TRAMP-SIY) transgenic prostates (Figs. 26 and 27) is not a result of prostate-intrinsic factors since the number of cells per gram of tissue for each mouse model is not similar.

More recently, in a polyoma virus model, Swanson *et al.* (2009) also demonstrated that antigen-specific memory $CD8^+$ T cells are maintained through an early antigen-dependent proliferation phase and a later antigen-independent survival phase [41]. It is clear from the differences between non-tumor and tumor transgenic prostates that other antigen-independent tumor-related factors support T cell persistence particularly at later timepoints (Fig. 26). It appears that the presence of persistent antigen supports increased cell death. However, in the prostate, T cells may persist because there are tumor-related factors that counter this effect. The presence of these tumor-related factors may also explain why antigen-specific T cells persist in the tumor environment but are depleted from other tissues without tumor factors. The oncoprotein SV40 T antigen transgene in the TRAMP and TRAMP-SIY models are driven by a prostate-specific probasin promoter [42] which would concentrate the tumor effects largely to the prostate tissue. Interestingly, the total number of $CD8^+$ T cells when analyzed per gram of prostate tissue in 2C and OT-I recipient mice is generally similar for all the mouse models irrespective of whether they are tumor transgenic and/or express the SIY antigen in their

prostates (Figs. 26 and 27). These data suggest that the prostate has additional molecules regulating the number of T cells that persist in this tissue.

The results of this study revealed that tolerant 2C T cells do not depend on IL-15 and IL-7 for persistence *in vivo*. RNA and flow cytometry analyses of the receptor subunit expression (Figs. 28 to 33) showed that there were no differences in the response to these cytokines between tolerant and non-tolerant 2C T cells in the prostate. Signaling response of IL-15, IL-7 and IL-2 occurs through the Janus kinase - Signal transducer and activator of transcription (JAK-STAT) pathway [43, 44]. Phosphorylation of Stat5 in this pathway is an indicator that T cells are responding to stimulation by IL-15, IL-7 and IL-2 [43, 44]. IL-7Rα is downregulated in cells responding to IL-7 stimulation whereas all other receptor subunits (IL-15Rβ and IL-2Rα) are upregulated in cells responding to IL-15 and IL-2. Although the levels of IL-7Rα are low in antigen-specific 2C T cells, short-term IL-7 stimulation of freshly isolated T cells showed that there were no differences in pStat5 levels (Fig. 35). These results suggest that tolerant T cells have a similar response to IL-15 and IL-7 as non-tolerant 2C T cells in the prostate, and in fact, tolerant 2C T cells do not respond to either cytokine. Moreover, qPCR analyses revealed that IL-15 and IL-7 are not detected in the prostate of tumor transgenic mice (Figs. 37 and 38). Therefore, 2C T cell persistence cannot be dependent on the presence of these soluble factors, IL-15 and IL-7.

These results are in contrast to those observed in tissue specimens from human patients with BPH [15]. Inflamed prostate epithelial and stroma cells from tissue specimens of patients with BPH were shown to express IL-15 and IL-15Rα [15]. The authors correlated high levels of IL-15 with increased T cell numbers in the prostate, and showed that T cells from BPH prostate showed a dose-dependent proliferative response to IL-15 *in vitro*. However, they did not assess

the function of the T cells present [15]. Dr. Ailin Bai also showed that the number of 2C T cells from TRAMP and TRAMP-SIY prostates increase when cultured for four days in IL-2, IL-15 and IL-7 *in vitro* [23]. Results from IFN-γ and TNF-α secretion assays showed that these 2C T cells were becoming functional [23]. Therefore, it is possible that in the presence of these cytokines, antigen-specific T cells are not tolerant. The difference in the functional state of the T cells might explain the contrast between my results and those reported by Handisurya *et al.* (2001) [15]. In this study, with short-term (30 min at 37°C) IL-15 or IL-7 stimulation, freshly isolated tolerant 2C T cells did not show appreciable response to either cytokine (Figs. 35 and 36) suggesting that these cells do not depend on this cytokine *in vivo*. Furthermore, the results indicate that a short-time of stimulation is not enough to break tolerance. RNA transcripts of IL-15 and IL-7 cannot be detected in the prostate environment where we have tolerant antigen-specific T cells (Figs. 37 and 38). Therefore, persisting tolerant 2C T cells would not correlate with high IL-15 levels.

Decline in IL-7 is correlated with persistence of tolerant T cells. Recently, Di Carlo *et al.* (2009) reported loss of IL-7 in neoplastic glands from prostate cancer patients [45]. Samples from prostate cancer patients expressed approximately 60-fold less IL-7 mRNA compared to normal prostates [45]. Di Carlo *et al.* (2009) correlated this loss with a decline in functional $CD8^+$ T cells that could infiltrate tumors; the remaining $CD8^+$ T cells were not terminally differentiated into effector cells and were confined to the stroma, outside the glandular epithelial tumor regions [45]. Therefore, it appears that this is an example of non-functional $CD8^+$ T cells that might be able to persist without IL-7 *in vivo*. This is in agreement with results in this thesis that tolerant 2C T cells persist in TRAMP-SIY prostate without IL-7.

This lack of dependence on IL-15 and IL-7 has been observed in persisting non-functional antigen-specific T cells generated in response to chronic LCMV infection [16]. In this article, persisting "exhausted" or tolerant T cells which expressed low levels of IL-15Rβ and IL-7Rα were maintained by extensive proliferation in the presence of persistent antigen [16]. The presence of antigen may explain the only difference observed in IL-7Rα expression in the spleens (Figs. 31 and 32), and has been discussed in the previous chapter (about the effect of antigen in T cell persistence). Gene expression profile analysis showed that exhausted T cells in the LCMV model expressed higher levels of Jak3, and lower levels of both Jak1 and Stat5b transcripts compared to functional memory cells [46]. These gene expression differences would suggest that there are signaling deficiencies occurring in tolerant T cells [46]. Therefore, like the persisting non-functional antigen-specific T cells generated in response to chronic LCMV infection [16], persisting T cells in the tolerizing tumor environment appear to be independent of IL-15 and IL-7, and maintained by extensive proliferation in the presence of persistent antigen.

The availability of published microarray data comparing gene expression between B6 and TRAMP prostates prompted me to identify potential candidates that support T cell persistence from this dataset. I postulated that the effects on infiltration, proliferation and/or survival could be modulated through cytokines, chemokines, growth factors, cadherins and integrins. From the published microarray data, a total of 12 candidates were identified (Table 2 including Survivin and Racgap1). Of this list, Cxcl12 and Itgb1 seem feasible to investigate further since they have known receptors on T cells and have readily available commercial reagents. Real-time qPCR and flow cytometry results would be expected to show increased RNA and protein expression levels in TRAMP prostates compared to normal B6 prostates. Also, small molecule inhibitors to

the soluble factors may be used to assess the effect of these soluble molecules to T cell persistence.

4.5. Materials and Methods

Mice & Viruses: 2C TCR and OT-I TCR transgenic mice on $RAG1^{-/-}$ and B6 backgrounds were maintained at the Massachusetts Institute of Technology (MIT) Animal Care Facility. Congenic 2C TCR Thy1.1 mice were also bred in our facility. OT-I TCR CD45.1 transgenic mice on a $RAG2^{-/-}$ background were a kind donation from Tyler Jacks lab at MIT. Recipient mouse strains (TRAMP, TRAMP-SIY, B6 and B6-SIY), ages 3-8 months old, were also maintained in the MIT facility. In some cases, B6 (C57BL/6) mice were purchased from the Jackson Laboratory (Bar Harbor, ME). Recombinant WSN (H1N1) influenza virus with SIYRYYGL peptide engineered onto the neuraminidase stalk originally constructed by plasmid-based reverse genetics [47] was grown on Madine-Darby Canine Kidney (MDCK) cells. Similar methods were used to produce WSN virus engineered with SIINFEKL (OVA) peptide sequence.

Antibodies & Reagents: Biotinylated 1B2 monoclonal antibody was produced in-house. 1B2 is a monoclonal antibody specific for the 2C TCR. Other anti-mouse monoclonal antibodies, CD16/32 (Fc blocker), Streptavidin-APC, CD8α-PerCP-Cy5.5 Clone 53-6.7, CD8α-APC, CD8α-PE, CD8α-FITC, CD90.1(Thy1.1)-APC, CD90.1(Thy1.1)-FITC, vβ5-FITC, vα2-PE, CD122(IL-2/15Rβ)-FITC Clone TM-β1, CD127(IL-7Rα)-FITC Clone A7R34, CD127(IL-7Rα)-Alexa Fluor® 488, CD25(IL-2Rα)-FITC Clone PC-61.5, and CD132(γ_c)-PE for flow cytometry studies were purchased from either BioLegend (San Diego, CA) or BD Biosciences (San Jose, CA). Phospho-Stat5 (Tyr694) antibody (Cat. #9351S) was purchased from Cell Signaling Technology, the secondary goat anti-rabbit IgG-PE antibody came from Caltag, and the isotype IgG1-PE (A85-1) control antibody was purchased from BD Biosciences. Pierce Chemical 4',6-diamidino-2-phenylindole hydrochloride (DAPI) PI46190 was purchased from VWR (USA).

Propidium iodide P4170 (PI) was purchased from Sigma-Aldrich (USA). RNeasy Plus Mini (Cat. #74134) and RNeasy Fibrous Tissue Mini (Cat. #74704) kits were from QIAGEN (USA). Taqman® Universal PCR master mix (Cat. #4364340), Taqman® Reverse Transcription reagents kit (Cat. #N8080234), as well as IL-15 (Cat. #M00689964_m1), IL-7 (Cat. #Mm00434291-m1) and GAPDH (Cat. #Mm99999915_g1) primers were bought from Applied Biosytems (Foster City, CA).

Lymphocyte Isolation (Lymph Nodes and Spleen): Lymph nodes (LN) and spleens from 2C $RAG1^{-/-}$ mice were extracted, one mouse at a time, after carbon dioxide (CO_2) inhalation. The sacrificed animal's fur was sterilized with 70% ethanol. Dissected LN and spleens were stored on ice in 4 ml of RPMI 1640 media supplemented with 5% fetal bovine serum and 10 mM HEPES buffer solution (RPMI complete). After dissection, the LN were gently mashed between rough surfaces of two microscope slides immersed in RPMI complete to release lymphocytes. Cell suspensions were filtered through an 80-μm nylon mesh (Sefar) and transferred into 15-ml BD Falcon tubes kept on ice. A similar procedure was followed for cell isolation from the spleen. Splenocytes used for flow cytometry analysis were further purified by a red blood cell (RBC) lysis step after grinding.

Cell Transfer & Influenza Infection: Cells isolated from 2C lymph nodes and spleens as described above were resuspended in Hank's Balanced Salt Solution (HBSS, serum-free media), filtered and kept on ice. Following approved animal care facility protocol, recipient mice were anesthetized with 2.5% Avertin and intranasally infected with 100 pfu of WSN-SIY or 100 pfu

WSN-SIIN Influenza virus suspended in 50 µl. Still under anesthesia, infected mice were immediately injected retroorbitally with 1-2 x 10^6 total live cells suspended in 100 µl HBSS.

Lymphocyte Extraction (Prostate and Lungs): Prostate lobes were extracted by microdissection following procedures in Current Protocols in Immunology [48]. Briefly, the urogenital system from each mouse was extracted after CO_2 inhalation, and transferred into 15-ml of RPMI complete on ice. A dissecting microscope was used to identify prostate lobes in the urogenital system placed on cold 1x PBS. The prostate lobes were subsequently removed using tweezers and transferred into 2-ml of 1 mg/ml Collagenase A (from Roche) in RPMI complete solution. The tissue was digested for about 45 min in a 37°C water bath, vortexing at 15-20 min intervals. Then, digested tissues were gently mashed between rough surfaces of two microscope slides immersed in RPMI complete to release lymphocytes. Cell suspensions were filtered through an 80-µm nylon mesh (Sefar) and transferred into 15-ml Falcon tubes kept on ice.

To extract cells from the lungs, each specimen was ground through a cell strainer in 10 ml of RPMI complete. Then the suspension was centrifuged and resuspended in 2 ml of 2 mg/ml Collagenase A (from Roche) in RPMI complete solution. The tissue was digested for 1 hr in a 37°C water bath, vortexing at 15-20 min intervals. An equal volume of 70% Percoll was added to the digest followed by centrifugation at ~2000 rpm for 20 min. Tissue debris and supernatant from lungs were gently aspirated, followed by RBC lysis.

Estimation of Prostate Weight: To estimate the weight of the prostate, immediately following extraction, the urogenital system was weighed before being placed inside media, and then the prostate weight was estimated as 10% of the weight of the urogenital system excised. The

urogenital system in this case consists of the drained bladder, seminal vesicles, urethra, ureters, ampullary glands and the prostate. Ten percent was selected after performing experiments measuring the dry weight of the urogenital system and the dry weight of prostates, and showing that all mouse models had prostates that were about ten percent of the urogenital system (Fig. 24).

Red Blood Cell (RBC) Lysis: Two milliliters of red blood cell lysis buffer (144 mM ammonium chloride and 17 mM Tris-HCl pH7.4 in distilled deionized water) was added to pellets from spleen and lungs specimens and kept on ice for 2-4 min, vortexing at 2 min intervals. Ten millimeters of RPMI complete was added to stop the lysis. Cell suspensions were centrifuged at ~1200 rpm, resuspended in an appropriate buffer for further analysis, and filtered through a nylon mesh (Sefar) into appropriately labeled tubes kept on ice.

Cell Counting: The total number of viable cells for each tissue specimen was counted using a hemacytometer and tryphan blue exclusion.

Flow Cytometry: Appropriate numbers of counted cells in suspension were transferred into labeled Falcon® round-bottom tubes (FACS tubes), and centrifuged at ~1200 rpm for 5 min. All procedures were performed on ice. Antibodies in FACS buffer (1% BSA and 0.1% sodium azide in 1x PBS) were used for staining following the manufacturer's recommended range. Purified anti-mouse CD16/32 (BioLegend), the Fc blocker, was added for 10 min prior to adding the primary antibody. Cells were incubated with the primary biotinylated antibody on ice for 30-45 min, washed and then incubated with the secondary and fluorophore-conjugated antibodies for

15-20 min while covered with foil paper. The cells were washed again, and resuspended in 50-200 µl of DAPI or 1 µg/ml propidium iodide solution except where indicated. Samples were sorted using a BD™ LSRII or BD FACSCalibur™ flow cytometer (BD Biosciences). Further data analysis was carried out using FlowJo software (Tree Star, Inc., Ashland, OR).

pStat5 intracellular staining: Freshly isolated cell suspensions were prepared as described above for prostate tissue samples. Cells were stained with Fc blocker, Thy1.1-APC (or Biotinylated 1B2 followed by Streptavidin-APC) and CD8α-FITC antibodies. Then cells were stimulated with IL-7 (20ng/ml) or IL-15 (40 ng/ml) prepared in prewarmed RPMI complete. Unstimulated controls did not receive cytokine. All cells were incubated in a 37°C waterbath for 30 min. After stimulation, the cells were fixed with 1 ml of 0.37% of paraformaldehyde at 37°C for 10 min, washed with 1x PBS and then permeabilized with cold 90% methanol on ice for 30 min. Cells were washed with pStat5 wash buffer (5g BSA in 1L of 1x PBS) and then stained with pStat5 following recommended instructions by the manufacturer. After incubation at room temperature (RT) for 30 min, cells were washed and stained with either the secondary goat anti-rabbit IgG-PE or the isotype control antibody for 30 min at RT. Again the cells were washed and resuspended in pStat5 wash buffer ready for analysis by the BD FACSCalibur™ flow cytometer (BD Biosciences). Further data analysis was carried out using FlowJo software (Tree Star, Inc., Ashland, OR).

RNA Extraction and quantitative real-time PCR (qPCR)*:* Femurs from B6 mice were extracted and the bone marrows were infused with phenol red free HBSS (from GIBCO) to remove cells. Prostate and spleens were also harvested directly into 4ml of HBSS in petridishes. Then freshly

opened slides were used to grind these samples. After grinding, cell suspensions were transferred into appropriately labeled 15-ml Falcon tubes. The cells were centrifuged and resuspended in 1-1.5 ml of 1x PBS in order to transfer them into 1.5 ml eppendorf tubes. All subsequent procedures were carefully carried out to prevent any RNase contamination. RNA extraction for the bone marrow and spleens were performed using the RNeasy Plus Mini kit while that for the prostates were done using the RNeasy Fibrous Tissue Mini kit. Appropriate volumes of β-mercaptoethanol (β-ME) RLT buffer was added to each sample. Then a 23G1 needle followed by mixing with a 28½G needle were used to create finer cell suspensions. To eliminate the bubbles generated in this process, cells were frozen at -70°C for about 30 min. Then they were warmed in a 37°C waterbath for about 2 min. Defrosted cell suspensions in β-ME RLT buffer were transferred into QIAGEN QIAshredder columns. Remaining steps for RNA extraction followed the protocol from the manufacturer's kit handbook. Final volumes of extracted RNA were 50 µl. A Nanodrop spectrophometer was used to determine the RNA concentration of each sample. On the same day, reverse transcription (RT) reactions for each sample were performed to convert RNA into cDNA (RT product). This step used the Taqman® Reverse Transcription Reagents kit (from Applied Biosystems) following volumes and Thermacycler settings recommended by the manufacturer. Samples were stored at -20°C until the day of qPCR analysis. To prepare qPCR samples, the RT product was transferred into wells of optical plates. Each well contained 100 ng (based on original RNA concentration) of the sample. A cocktail of 1 µl of primer (IL-7 or IL-15 or GAPDH), DNase-RNase-free water, and 2x Taqman® Universal PCR Master Mix was added to each well. Total volume of qPCR premix was 20 µl. Each tissue sample was prepared in duplicates. The plate was sealed with optical caps and centrifuged for about 3 min to remove any bubbles. Then the plate was incubated at

50°C for 2 min, 95°C for 10 min, 95°C for 15 sec repeated 40 times, and finally cooled to 60°C for 1 min using an ABI 7500 real-time PCR system (Applied Biosytems, Foster City, CA). Relative expression levels were calculated using Microsoft Excel.

Statistical Analyses: All p-values are from unpaired two-tailed equal variance Student's t-Tests.

4.6. References

(1) Otahal, P.; Schell, T. D.; Hutchinson, S. C.; Knowles, B. B.; Tevethia, S. S. Early Immunization Induces Persistent Tumor-Infiltrating CD8+ T Cells Against an Immunodominant Epitope and Promotes Lifelong Control of Pancreatic Tumor Progression in SV40 Tumor Antigen Transgenic Mice. *J. Immunol.* **2006**, *177*, 3089-3099.

(2) Dudley, M. E., et al Adoptive Cell Transfer Therapy Following Non-Myeloablative but Lymphodepleting Chemotherapy for the Treatment of Patients with Refractory Metastatic Melanoma. *J. Clin. Oncol.* **2005**, *23*, 2346-2357.

(3) Morgan, R. A., et al Cancer Regression in Patients After Transfer of Genetically Engineered Lymphocytes. *Science* **2006**, *314*, 126-129.

(4) Lodolce, J. P.; Boone, D. L.; Chai, S.; Swain, R. E.; Dassopoulos, T.; Trettin, S.; Ma, A. IL-15 Receptor Maintains Lymphoid Homeostasis by Supporting Lymphocyte Homing and Proliferation. *Immunity* **1998**, *9*, 669-676.

(5) Kennedy, M. K., et al Reversible Defects in Natural Killer and Memory CD8 T Cell Lineages in Interleukin 15-Deficient Mice. *J. Exp. Med.* **2000**, *191*, 771-780.

(6) Schluns, K. S.; Kieper, W. C.; Jameson, S. C.; Lefrancois, L. Interleukin-7 Mediates the Homeostasis of Naive and Memory CD8 T Cells in Vivo. *Nat. Immunol.* **2000**, *1*, 426-432.

(7) Geginat, J.; Lanzavecchia, A.; Sallusto, F. Proliferation and Differentiation Potential of Human CD8+ Memory T-Cell Subsets in Response to Antigen Or Homeostatic Cytokines. *Blood* **2003**, *101*, 4260-4266.

(8) Morgan, D. A.; Ruscetti, F. W.; Gallo, R. Selective in Vitro Growth of T Lymphocytes from Normal Human Bone Marrows. *Science* **1976**, *193*, 1007-1008.

(9) Gillis, S.; Smith, K. A. Long Term Culture of Tumour-Specific Cytotoxic T Cells. *Nature* **1977**, *268*, 154-156.

(10) Becker, T. C.; Wherry, E. J.; Boone, D.; Murali-Krishna, K.; Antia, R.; Ma, A.; Ahmed, R. Interleukin 15 is Required for Proliferative Renewal of Virus-Specific Memory CD8 T Cells. *J. Exp. Med.* **2002**, *195*, 1541-1548.

(11) Schluns, K. S.; Williams, K.; Ma, A.; Zheng, X. X.; Lefrancois, L. Cutting Edge: Requirement for IL-15 in the Generation of Primary and Memory Antigen-Specific CD8 T Cells. *J. Immunol.* **2002**, *168*, 4827-4831.

(12) Judge, A. D.; Zhang, X.; Fujii, H.; Surh, C. D.; Sprent, J. Interleukin 15 Controls both Proliferation and Survival of a Subset of Memory-Phenotype CD8(+) T Cells. *J. Exp. Med.* **2002**, *196*, 935-946.

(13) Wu, T. S.; Lee, J. M.; Lai, Y. G.; Hsu, J. C.; Tsai, C. Y.; Lee, Y. H.; Liao, N. S. Reduced Expression of Bcl-2 in CD8+ T Cells Deficient in the IL-15 Receptor Alpha-Chain. *J. Immunol.* **2002**, *168*, 705-712.

(14) Marcondes, M. C.; Burdo, T. H.; Sopper, S.; Huitron-Resendiz, S.; Lanigan, C.; Watry, D.; Flynn, C.; Zandonatti, M.; Fox, H. S. Enrichment and Persistence of Virus-Specific CTL in the Brain of Simian Immunodeficiency Virus-Infected Monkeys is Associated with a Unique Cytokine Environment. *J. Immunol.* **2007**, *178*, 5812-5819.

(15) Handisurya, A.; Steiner, G. E.; Stix, U.; Ecker, R. C.; Pfaffeneder-Mantai, S.; Langer, D.; Kramer, G.; Memaran-Dadgar, N.; Marberger, M. Differential Expression of Interleukin-15, a Pro-Inflammatory Cytokine and T-Cell Growth Factor, and its Receptor in Human Prostate. *Prostate* **2001**, *49*, 251-262.

(16) Shin, H.; Blackburn, S. D.; Blattman, J. N.; Wherry, E. J. Viral Antigen and Extensive Division Maintain Virus-Specific CD8 T Cells during Chronic Infection. *J. Exp. Med.* **2007**, *204*, 941-949.

(17) Dubois, S.; Mariner, J.; Waldmann, T. A.; Tagaya, Y. IL-15Ralpha Recycles and Presents IL-15 in Trans to Neighboring Cells. *Immunity* **2002**, *17*, 537-547.

(18) Sandau, M. M.; Schluns, K. S.; Lefrancois, L.; Jameson, S. C. Cutting Edge: Transpresentation of IL-15 by Bone Marrow-Derived Cells Necessitates Expression of IL-15 and IL-15R Alpha by the Same Cells. *J. Immunol.* **2004**, *173*, 6537-6541.

(19) Schluns, K. S.; Stoklasek, T.; Lefrancois, L. The Roles of Interleukin-15 Receptor Alpha: Trans-Presentation, Receptor Component, Or both? *Int. J. Biochem. Cell Biol.* **2005**, *37*, 1567-1571.

(20) Klebanoff, C. A.; Finkelstein, S. E.; Surman, D. R.; Lichtman, M. K.; Gattinoni, L.; Theoret, M. R.; Grewal, N.; Spiess, P. J.; Antony, P. A.; Palmer, D. C.; Tagaya, Y.; Rosenberg, S. A.; Waldmann, T. A.; Restifo, N. P. IL-15 Enhances the in Vivo Antitumor Activity of Tumor-Reactive CD8+ T Cells. *Proc. Natl. Acad. Sci. U. S. A.* **2004**, *101*, 1969-1974.

(21) Roychowdhury, S.; May, K. F.,Jr; Tzou, K. S.; Lin, T.; Bhatt, D.; Freud, A. G.; Guimond, M.; Ferketich, A. K.; Liu, Y.; Caligiuri, M. A. Failed Adoptive Immunotherapy with Tumor-Specific T Cells: Reversal with Low-Dose Interleukin 15 but Not Low-Dose Interleukin 2. *Cancer Res.* **2004**, *64*, 8062-8067.

(22) Teague, R. M.; Sather, B. D.; Sacks, J. A.; Huang, M. Z.; Dossett, M. L.; Morimoto, J.; Tan, X.; Sutton, S. E.; Cooke, M. P.; Ohlen, C.; Greenberg, P. D. Interleukin-15 Rescues Tolerant

CD8+ T Cells for use in Adoptive Immunotherapy of Established Tumors. *Nat. Med.* **2006**, *12*, 335-341.

(23) Bai, A.; Higham, E.; Eisen, H. N.; Wittrup, K. D.; Chen, J. Rapid Tolerization of Virus-Activated Tumor-Specific CD8+ T Cells in Prostate Tumors of TRAMP Mice. *Proc. Natl. Acad. Sci. U. S. A.* **2008**, *105*, 13003-13008.

(24) Grabstein, K. H.; Namen, A. E.; Shanebeck, K.; Voice, R. F.; Reed, S. G.; Widmer, M. B. Regulation of T Cell Proliferation by IL-7. *J. Immunol.* **1990**, *144*, 3015-3020.

(25) Maraskovsky, E.; Teepe, M.; Morrissey, P. J.; Braddy, S.; Miller, R. E.; Lynch, D. H.; Peschon, J. J. Impaired Survival and Proliferation in IL-7 Receptor-Deficient Peripheral T Cells. *J. Immunol.* **1996**, *157*, 5315-5323.

(26) Grayson, J. M.; Zajac, A. J.; Altman, J. D.; Ahmed, R. Cutting Edge: Increased Expression of Bcl-2 in Antigen-Specific Memory CD8+ T Cells. *J. Immunol.* **2000**, *164*, 3950-3954.

(27) Dai, Z.; Arakelov, A.; Wagener, M.; Konieczny, B. T.; Lakkis, F. G. The Role of the Common Cytokine Receptor Gamma-Chain in Regulating IL-2-Dependent, Activation-Induced CD8+ T Cell Death. *J. Immunol.* **1999**, *163*, 3131-3137.

(28) Andrews, N. P.; Pack, C. D.; Vezys, V.; Barber, G. N.; Lukacher, A. E. Early Virus-Associated Bystander Events Affect the Fitness of the CD8 T Cell Response to Persistent Virus Infection. *J. Immunol.* **2007**, *178*, 7267-7275.

(29) Shen, C. H.; Ge, Q.; Talay, O.; Eisen, H. N.; Garcia-Sastre, A.; Chen, J. Loss of IL-7R and IL-15R is Associated with Disappearance of Memory T Cells in Respiratory Tract Following Influenza Infection. *J. Immunol.* **2008**, *180*.

(30) Morgenbesser, S. D., et al Identification of Genes Potentially Involved in the Acquisition of Androgen-Independent and Metastatic Tumor Growth in an Autochthonous Genetically Engineered Mouse Prostate Cancer Model. *Prostate* **2007**, *67*, 83-106.

(31) Haram, K. M.; Peltier, H. J.; Lu, B.; Bhasin, M.; Otu, H. H.; Choy, B.; Regan, M.; Libermann, T. A.; Latham, G. J.; Sanda, M. G.; Arredouani, M. S. Gene Expression Profile of Mouse Prostate Tumors Reveals Dysregulations in Major Biological Processes and Identifies Potential Murine Targets for Preclinical Development of Human Prostate Cancer Therapy. *Prostate* **2008**, *68*, 1517-1530.

(32) NCBI Entrez Gene http://www.ncbi.nlm.nih.gov/sites/entrez (accessed June, 2009).

(33) Krajewska, M.; Krajewski, S.; Banares, S.; Huang, X.; Turner, B.; Bubendorf, L.; Kallioniemi, O. P.; Shabaik, A.; Vitiello, A.; Peehl, D.; Gao, G. J.; Reed, J. C. Elevated Expression of Inhibitor of Apoptosis Proteins in Prostate Cancer. *Clin. Cancer Res.* **2003**, 9, 4914-4925.

(34) Andersen, M. H.; Pedersen, L. O.; Capeller, B.; Brocker, E. B.; Becker, J. C.; thor Straten, P. Spontaneous Cytotoxic T-Cell Responses Against Survivin-Derived MHC Class I-Restricted T-Cell Epitopes in Situ as Well as Ex Vivo in Cancer Patients. *Cancer Res.* **2001**, *61*, 5964-5968.

(35) Schaue, D.; Comin-Anduix, B.; Ribas, A.; Zhang, L.; Goodglick, L.; Sayre, J. W.; Debucquoy, A.; Haustermans, K.; McBride, W. H. T-Cell Responses to Survivin in Cancer Patients Undergoing Radiation Therapy. *Clin. Cancer Res.* **2008**, *14*, 4883-4890.

(36) Xing, Z.; Conway, E. M.; Kang, C.; Winoto, A. Essential Role of Survivin, an Inhibitor of Apoptosis Protein, in T Cell Development, Maturation, and Homeostasis. *J. Exp. Med.* **2004**, *199*, 69-80.

(37) Zhao, B.; Song, A.; Haque, R.; Lei, F.; Weiler, L.; Xiong, X.; Wu, Y.; Croft, M.; Song, J. Cooperation between Molecular Targets of Costimulation in Promoting T Cell Persistence and Tumor Regression. *J. Immunol.* **2009**, *182*, 6744-6752.

(38) Hirose, K.; Kawashima, T.; Iwamoto, I.; Nosaka, T.; Kitamura, T. MgcRacGAP is Involved in Cytokinesis through Associating with Mitotic Spindle and Midbody. *J. Biol. Chem.* **2001**, *276*, 5821-5828.

(39) Yamada, T.; Kurosaki, T.; Hikida, M. Essential Roles of mgcRacGAP in Multilineage Differentiation and Survival of Murine Hematopoietic Cells. *Biochem. Biophys. Res. Commun.* **2008**, *372*, 941-946.

(40) Soga, N.; Connolly, J. O.; Chellaiah, M.; Kawamura, J.; Hruska, K. A. Rac Regulates Vascular Endothelial Growth Factor Stimulated Motility. *Cell. Commun. Adhes.* **2001**, 8, 1-13.

(41) Swanson, P. A.,2nd; Hofstetter, A. R.; Wilson, J. J.; Lukacher, A. E. Cutting Edge: Shift in Antigen Dependence by an Antiviral MHC Class Ib-Restricted CD8 T Cell Response during Persistent Viral Infection. *J. Immunol.* **2009**, *182*, 5198-5202.

(42) Greenberg, N. M.; DeMayo, F.; Finegold, M. J.; Medina, D.; Tilley, W. D.; Aspinall, J. O.; Cunha, G. R.; Donjacour, A. A.; Matusik, R. J.; Rosen, J. M. Prostate Cancer in a Transgenic Mouse. *Proc. Natl. Acad. Sci. U. S. A.* **1995**, *92*, 3439-3443.

(43) Jiang, Q.; Li, W. Q.; Aiello, F. B.; Mazzucchelli, R.; Asefa, B.; Khaled, A. R.; Durum, S. K. Cell Biology of IL-7, a Key Lymphotrophin. *Cytokine Growth Factor Rev.* **2005**, *16*, 513-533.

(44) Waldmann, T. A. The Biology of Interleukin-2 and Interleukin-15: Implications for Cancer Therapy and Vaccine Design. *Nat. Rev. Immunol.* **2006**, 6, 595-601.

(45) Di Carlo, E.; D'Antuono, T.; Pompa, P.; Giuliani, R.; Rosini, S.; Stuppia, L.; Musiani, P.; Sorrentino, C. The Lack of Epithelial Interleukin-7 and BAFF/BLyS Gene Expression in Prostate Cancer as a Possible Mechanism of Tumor Escape from Immunosurveillance. *Clin. Cancer Res.* **2009**, *15*, 2979-2987.

(46) Wherry, E. J.; Ha, S. J.; Kaech, S. M.; Haining, W. N.; Sarkar, S.; Kalia, V.; Subramaniam, S.; Blattman, J. N.; Barber, D. L.; Ahmed, R. Molecular Signature of CD8+ T Cell Exhaustion during Chronic Viral Infection. *Immunity* **2007**, *27*, 670-684.

(47) Fodor, E.; Devenish, L.; Engelhardt, O. G.; Palese, P.; Brownlee, G. G.; Garcia-Sastre, A. Rescue of Influenza A Virus from Recombinant DNA. *J. Virol.* **1999**, *73*, 9679-9682.

(48) Hurwitz, A. A.; Foster, B. A.; Allison, J. P.; Greenberg, N. M.; Kwon, E. D. In *The TRAMP Mouse as a Model for Prostate Cancer;* Current Protocols in Immunology; John Wiley & Sons, Inc.: 2001; pp 20.5.1-20.5.23.

CHAPTER 5

FURTHER DISCUSSION AND FUTURE DIRECTIONS

5.1. Discussion

This thesis elucidates the mechanism for persistence of antigen-specific T cells in a tolerizing tumor environment using a spontaneous prostate cancer model referred to as the TRAMP-SIY model. The results described in previous chapters show that 2C T cells do not depend on IL-7 or IL-15 for persistence *in vivo*. Rather, a combination of antigen and tumor-related factors contribute to infiltration and persistence of T cells in the prostate tumor environment. In fact, the presence of antigen in the prostate correlates with depletion of antigen-specific cells from the spleens and draining lymph nodes, thereby, contributing to perceived persistence of antigen-specific T cells in the tolerizing TRAMP-SIY tumor environment. An additional effect of antigen is inducing extensive proliferation of antigen-specific T cells in TRAMP-SIY prostate, as well as increasing the sensitivity of antigen-specific T cells to cell death. However the effects of antigen appear to be dampened by the dominant effect of tumor-related factors on T cell persistence.

Validating potential tumor-related factors

Twelve candidates were identified as potential molecules that support T cell infiltration, proliferation and/or survival in the prostate of tumor transgenic mice. Ten of these molecules are upregulated in TRAMP prostates, while two are downregulated compared to B6 prostates analyzed by microarray [1, 2]. Six of these candidates are soluble factors while one of them is membrane-bound (Table 2). Cxcl12 and Kitl have commercially available neutralizing antibodies that may be used to determine whether these molecules have an effect on T cell persistence. The presence or absence of other molecules without readily available neutralizing antibodies or small molecule inhibitors may be verified using real-time qPCR. Primers are

commercially available (from Applied Biosystems Taqman gene expression assays) for all these candidates except Survivin. Similar to the analyses performed in previous chapters, one may compare B6 to TRAMP as well as B6-SIY prostates to TRAMP-SIY to validate that the differences in gene expression are really due to the effect of tumor. Comparison of B6 to B6-SIY and TRAMP to TRAMP-SIY would also help to elucidate any effect the presence of antigen has on expression of this molecule. While real-time qPCR could serve as a first screen, it may be more informative to also analyze the protein expression levels of these candidates. The correlation between gene and protein expression results may not always hold because of post-transcriptional and post-translational modification of these molecules. As a result, protein expression from candidates from the first qPCR screen should be evaluated by flow cytometry and/or western blotting, where antibodies are available. Itgb1, also known as CD29, is one example of these candidates that has a commercially available antibody.

Identifying the role of potential tumorigenic factors

Ultimately the goal is to determine the effect of these molecules on T cells *in vivo*. Some of these molecules such as Cxcl12, Kitl, and Itgb1 have known receptors on T cells [3, 4]. To assess their role on T cell persistence, since antibodies to these receptors are available, flow cytometry may be used to determine whether there are differences in receptor expression levels between T cells from tumor and non-tumor prostates. Further investigation could also be carried out by using siRNA to knockdown genes or using retroviral constructs to express genes in 2C or OT-I $CD8^+$ T cells. These genetically modified cells may be adoptively transferred into B6 and TRAMP recipient mice as described in previous chapters of this thesis. By using either 2C or OT-I cells, one can monitor the T cell numbers in different tissues by flow cytometry to

determine whether there are differences in T cell infiltration and persistence. In addition, mice deficient in any of these genes that are upregulated may be crossed onto the TRAMP mouse to generate TRAMP gene X-deficient mice. A set of experiments would be to transfer 2C or OT-I cells into TRAMP and TRAMP gene X-deficient mice, and determine the difference in T cell numbers, proliferation and survival/apoptotic death rate upon loss of this gene.

Monitoring the effect on tumor progression

Of particular importance is the effect any of these factors could have on tumor progression. Experiments to assess the function of T cells infiltrating the prostate should also be carried out. One can assess function by measuring IFN-γ and TNF-α secretion. Also, the level of PD-1 expression can also serve as a marker of tolerance because tolerant cells often express high levels of PD-1. If loss of a gene results in persisting functional T cells, then one may conclude that this tumorigenic or tumor-related factor induces tolerance and limits T cell persistence (possibly by inducing cell death or preventing proliferation).

Persisting functional T cells can limit tumor progression or prevent tumor growth altogether. However, we have not monitored the growth of prostate tumors in the TRAMP-SIY model yet. Magnetic resonance imaging (MRI) is a useful imaging modality for distinguishing soft tissues with different fluid (water) densities. The first proof that nuclear magnetic resonance imaging could be applied in biology came from experiments published in 1971 that compared cancerous tissue from rats to healthy tissue [5]. The author noted that cancerous tissue had longer relaxation times [5]. Depending on the acquisition settings, MRI can be used to differentiate between normal and prostate tissue with tumors since the texture and water content of these tissues should differ. This imaging modality does not require sacrificing mice at the time of

imaging. Therefore, one can acquire MRI images of the prostate from the same TRAMP and TRAMP-SIY mice starting from post-puberty (with tumor) stages to development of palpable prostate masses. Age-matched normal B6 mice may be used as controls. There are two constants in the magnetization equations, T1 and T2, that describe the property of the tissue being imaged [5, 6]. An image is described as T1-weighted or T1-dependent if its relative signal intensity is highly dependent on the T1 value of the tissue [5]. Similarly, the image is called T2-weighted or T2-dependent when it is sensitive to the tissue's T2 value [5]. The MRI scanner can be set to produce T1- or T2-weighted images by adjusting the pulse sequence of the magnetic field [5]. The result is that in T1 images, fluid and air appear black, and are indistinguishable from one another, whereas in T2 images, the brightest signal comes from fluid-filled areas [5] such as the bladder. By quantifying signal intensity, one would be able to correlate changes in tissue signal to development of tumor. These studies using mice that have not received 2C T cells would help to establish baseline tumor progression in the tumor transgenic mouse models.

The effect of an identified tumorigenic factor on tumor progression may also be evaluated through MRI studies. TRAMP gene-X deficient mice may be compared to TRAMP mice. Also, mice that have received genetically modified 2C T cells may also be compared to those controls without them. Tissue samples from these mice may also be analyzed by immunohistochemistry to validate MRI results. By immunohistochemistry, one can determine the neoplastic stages of the mouse and the extent of T cell infiltration into the prostate tissue. An example of the use of MRI to monitor effectiveness of T cell immunotherapy was recently published by Lazovic *et al.* (2008) [7]. The authors used an orthotopic xenograft murine model to demonstrate that genetically engineered glioblastoma-specific IL-13Rα2 T cells are effective in lysing glioblastoma cells. Interestingly in their studies, by quantifying signal intensity of T2-

and T1-weighted images, they showed that (1) T2 relaxation times, correlated with water content in tumor and tumor edema, increased within 24-hr after T cell transfer, (2) a corresponding enhancement occurred in T1-weighted postcontrast images after 24-hr, (3) apparent diffusion coefficient (ADC) levels, a measure of the diffusivity of water molecules, increased 2-3 days after treatment, and (4) T1-weighted postcontrast signal intensity decreased in glioblastoma sites that received IL-13Rα2 T cells 3-days after cell transfer, although ADC levels remained elevated [7]. The loss of this T1 signal corresponded to significantly decreased tumor volume and glioblastoma cell lysis evaluated by MRI and immunohistochemistry respectively, compared to non-treated and nonspecific T cells recipient mice [7]. This article demonstrates the potential use of MRI to monitor early stages of T cell immunotherapy. Applying these techniques to studies with the TRAMP-SIY model might help to evaluate therapeutic use of the novel candidates identified.

5.2. References

(1) Morgenbesser, S. D., et al Identification of Genes Potentially Involved in the Acquisition of Androgen-Independent and Metastatic Tumor Growth in an Autochthonous Genetically Engineered Mouse Prostate Cancer Model. *Prostate* **2007**, *67*, 83-106.

(2) Haram, K. M.; Peltier, H. J.; Lu, B.; Bhasin, M.; Otu, H. H.; Choy, B.; Regan, M.; Libermann, T. A.; Latham, G. J.; Sanda, M. G.; Arredouani, M. S. Gene Expression Profile of Mouse Prostate Tumors Reveals Dysregulations in Major Biological Processes and Identifies Potential Murine Targets for Preclinical Development of Human Prostate Cancer Therapy. *Prostate* **2008**, *68*, 1517-1530.

(3) Kitayama, J.; Nagawa, H.; Nakayama, H.; Tuno, N.; Shibata, Y.; Muto, T. Functional Expression of beta1 and beta2 Integrins on Tumor Infiltrating Lymphocytes (TILs) in Colorectal Cancer. *J. Gastroenterol.* **1999**, *34*, 327-333.

(4) Abbas, A. K.; Lichtman, A. H.; Pober, J. S. In *Cellular and molecular immunology;* W.B. Saunders: Philadelphia, 2000; , pp 553.

(5) Huettel, S. A.; Song, A. W.; McCarthy, G. In *Functional magnetic resonance imaging;* Sinauer Associates: Sunderland, Mass., 2004; , pp 492.

(6) Bushberg, J. T. In *The essential physics of medical imaging;* Lippincott Williams & Wilkins: Philadelphia, 2002; , pp 933.

(7) Lazovic, J.; Jensen, M. C.; Ferkassian, E.; Aguilar, B.; Raubitschek, A.; Jacobs, R. E. Imaging Immune Response in Vivo: Cytolytic Action of Genetically Altered T Cells Directed to Glioblastoma Multiforme. *Clin. Cancer Res.* **2008**, *14*, 3832-3839.